CAPITAL UNIVERSITY OF SCIENCE AND
TECHNOLOGY, ISLAMABAD

TM_{m0} Mode Rectangular Patch Antennas with Improved Radiation Characteristics

by

Zubair Ahmed

A thesis submitted in partial fulfillment for the
degree of Doctor of Philosophy

in the

Faculty of Engineering
Department of Electrical Engineering

2021

TM_{m0} Mode Rectangular Patch Antennas with Improved Radiation Characteristics

By

Zubair Ahmed

(DEE143004)

Dr. Diego Masotti, Associate Professor

University of Bologna, Bologna, Italy

(Foreign Evaluator 1)

Dr. Muhammad Arif Khan, Senior Lecturer

Charles Sturt University, Australia

(Foreign Evaluator 2)

Dr. Muhammad Mansoor Ahmed

(Thesis Supervisor)

Dr. Noor Muhammad Khan

(Head, Department of Electrical Engineering)

Dr. Imtiaz Ahmad Taj

(Dean, Faculty of Engineering)

DEPARTMENT OF ELECTRICAL ENGINEERING

CAPITAL UNIVERSITY OF SCIENCE AND TECHNOLOGY

ISLAMABAD

2021

Dedicated to my family for their support and encouragement throughout the thesis. To my parents, my wife, my son, and my daughter.

CAPITAL UNIVERSITY OF SCIENCE & TECHNOLOGY ISLAMABAD

Expressway, Kahuta Road, Zone-V, Islamabad
Phone:+92-51-111-555-666 Fax: +92-51-4486705
Email: info@cust.edu.pk Website: https://www.cust.edu.pk

CERTIFICATE OF APPROVAL

This is to certify that the research work presented in the thesis, entitled "**TMm0 Mode Rectangular Patch Antennas with Improved Radiation Characteristics**" was conducted under the supervision of **Dr. Muhammad Mansoor Ahmed**. No part of this thesis has been submitted anywhere else for any other degree. This thesis is submitted to the **Department of Electrical Engineering, Capital University of Science and Technology** in partial fulfillment of the requirements for the degree of Doctor in Philosophy in the field of **Electrical Engineering.** The open defence of the thesis was conducted on **January 01, 2021.**

Student Name : Zubair Ahmed (DEE-143004)

The Examination Committee unanimously agrees to award PhD degree in the mentioned field.

Examination Committee :

(a) External Examiner 1: Dr. Arbab Abdur Rahim
Assistant Professor
GIK Institute, Topi, Swabi

(b) External Examiner 2: Dr. Moazzam Maqsood
Assistant Professor
IST, Islamabad

(c) Internal Examiner : Dr. Noor Muhammad Khan
Professor
CUST, Islamabad

Supervisor Name : Dr. Muhammad Mansoor Ahmed
Professor
CUST, Islamabad

Name of HoD : Dr. Noor Muhammad Khan
Professor
CUST, Islamabad

Name of Dean : Dr. Imtiaz Ahmad Taj
Professor
CUST, Islamabad

AUTHOR'S DECLARATION

I, **Zubair Ahmed (Registration No. DEE-143004)**, hereby state that my PhD thesis titled, "**TMm0 Mode Rectangular Patch Antennas with Improved Radiation Characteristics**" is my own work and has not been submitted previously by me for taking any degree from Capital University of Science and Technology, Islamabad or anywhere else in the country/ world.

At any time, if my statement is found to be incorrect even after my graduation, the University has the right to withdraw my PhD Degree.

(Zubair Ahmed)

Dated: 01 January, 2021

Registration No : DEE-143004

PLAGIARISM UNDERTAKING

I solemnly declare that research work presented in the thesis titled "**TMm0 Mode Rectangular Patch Antennas with Improved Radiation Characteristics**" is solely my research work with no significant contribution from any other person. Small contribution/ help wherever taken has been duly acknowledged and that complete thesis has been written by me.

I understand the zero tolerance policy of the HEC and Capital University of Science and Technology towards plagiarism. Therefore, I as an author of the above titled thesis declare that no portion of my thesis has been plagiarized and any material used as reference is properly referred/ cited.

I undertake that if I am found guilty of any formal plagiarism in the above titled thesis even after award of PhD Degree, the University reserves the right to withdraw/ revoke my PhD degree and that HEC and the University have the right to publish my name on the HEC/ University Website on which names of students are placed who submitted plagiarized thesis.

(**Zubair Ahmed**)

Dated: 01 January, 2021

Registration No : DEE-143004

List of Publications

It is certified that following publication(s) have been made out of the research work that has been carried out for this thesis:-

1. **Z. Ahmed**, M. M. Ahmed, and M. B. Ihsan, "A Novel Differential Fed High Gain Patch Antenna Using Resonant Slot Loading," *Radioengineering*, vol. 27, pp. 662-670, 2018.

2. **Z. Ahmed**, M. M. Ahmed, M. B. Ihsan, A. A. Chaudhary and J. K. Arif, "Novel Dual Band Patch Antenna With Gap Coupled Composite Right/Left-Handed Transmission Line," *International Journal of Microwave and Wireless Technologies*, vol. 11, no. 1, pp. 87-93, 2019.

3. **Z. Ahmed** and M. M. Ahmed, "Sidelobe Reduction and Gain Enhancement in Higher Order TM_{30} and TM_{70} Mode Rectangular Patch Antennas Via Partial Notch Loading," *IET Microwaves, Antennas and Propagation*, vol. 13, no. 12, pp. 1955-1962, 2019.

(Zubair Ahmed)

Registration No: DEE143004

Acknowledgement

All praise be to almighty ALLAH who has been bestowing me with his great bounties and enabled me to complete my dissertation.

First of all, I would like to thank my advisor **Prof. Dr. Muhammad Mansoor Ahmed** for his guidance, invaluable time and encouragement throughout the course of this thesis. He is a great source of knowledge and working with him was a real privilege. His advice and guidance during various meetings at Capital University of Science and Technology (CUST) was a constant source of motivation.

I also want to thank my friends at NESCOM to provide support for antenna radiation pattern measurements. I would like to thank my family especially my wife and children, for the sacrifice and support during last six years of my PhD thesis.

(Zubair Ahmed)

Abstract

High gain, low-cost planar antennas are desired in many point to point wireless communication applications. The fundamental TM_{10} mode of rectangular patch antenna has a drawback of low gain in broadside direction. Higher-order TM_{m0} ($m = 3, 5, \cdots$) modes can provide large broadside gain but suffers from high E-plane sidelobe levels (SLL) and non-optimum gain. In this thesis, two techniques namely slot-loading and partial notch-loading techniques for improving the radiation characteristics of higher-order TM_{m0} ($m = 3, 5, \cdots$) modes in rectangular patch antennas are presented. Different single-layer high gain TM_{m0} mode patch antennas having high gain (12-16 dBi) and reduced SLLs ($<$ -12 dB) suitable for broadside medium-range applications are demonstrated.

In 1st part of the thesis, a slot-loading technique inspired by slotted waveguide antennas is proposed. In this technique, a pair of resonant slots is placed in the center out-of-phase region of TM_{30} mode rectangular patch antenna, which acts as a new radiating edge. Superposition of radiated fields of TM_{30} mode patch and fundamental mode of slots results in high directivity with reduced SLL. The placement of resonant slots also has a slight adverse effect on the in-phase current distribution resulting in an asymmetric radiation pattern. It is shown that a differential feeding scheme can be employed to achieve symmetric radiation pattern and gain enhancement by keeping the desired in-phase current distribution intact. The proposed antenna shows a measured gain of 12.8 dBi and SLL of -12 dB, and it can be used as a substitute for 2×2 array of patch antennas operating in fundamental mode. Furthermore, since some applications require single-fed patch antennas; therefore, a method for designing single-fed high gain TM_{30} mode patch with symmetric radiation pattern using a planar 2×2 slot array etched at the center of the patch is also presented.

In the 2nd part, a novel notch-loading technique for gain enhancement and E-plane SLL reduction in TM_{m0} ($m = 3, 5, \cdots$) mode patch antennas is presented. In this method, undesired out-of-phase surface current distribution regions of higher-order mode TM_{m0} ($m = 3, 5, \cdots$) patch are partially removed (notch-loaded) to

create additional radiating edges. It is demonstrated using an analytical model that the superposition of radiated fields due to these new radiating edges and unperturbed TM_{m0} ($m = 3, 5, \cdots$) mode results in gain enhancement and E-plane SLL reduction. Moreover, the proposed antennas are easy to fabricate due to their single-layer configuration. To verify the design, two notch-loaded higher mode patch antennas operating in TM_{30} and TM_{70} mode are fabricated and tested. Notch-loaded TM_{30} mode patch shows a measured E-plane SLL of -10.5 dB and gain of 12.9 dBi whereas, notch-loaded TM_{70} mode patch shows a measured E-plane SLL of -12.8 dB and gain of 16 dBi which is the highest reported antenna gain for single-layer TM_{70} mode rectangular patch antenna so far. In some applications, further reduction in SLL is desired. A method for designing low SLL TM_{30} mode patch with improved return loss using a combined notch and fractal slot loading is also presented. The new antenna shows a 5 dB reduction in SLL and 7 dB improvement in return loss compared to notch loaded TM_{30} mode patch.

Finally, in the 3^{rd} part of the thesis, high gain frequency reconfigurable dual-band patch antennas are investigated. A new technique based on metamaterial loaded patch antennas is developed. In this technique, a composite right/left-handed transmission line (CRLH TL) unit cell is gap-coupled with the radiating edge of a rectangular patch antenna. The dual-band behavior is achieved due to the coupling of zeroth-order resonance mode of CRLH TL and TM_{10} mode of the patch antenna. It is shown that the frequency ratio can be changed by varying the gap between the patch and CRLH TL unit cell. The proposed configuration enables frequency reconfigurability by changing the CRLH TL unit cell using a switch. A prototype of the antenna having frequency ratio $f_2/f_1 = 1.08$ is designed and fabricated. The proposed antenna shows measured $S_{11} \leq -10$ dB bandwidth of 100 MHz and 50 MHz at resonance frequencies of $f_1 = 4.84$ GHz and $f_2 = 5.22$ GHz, respectively. A 2×2 dual-band CRLH TL coupled patch array is also presented, showing more than 12.7 dBi gain at both resonant frequencies.

Contents

List of Figures

List of Tables

Abbreviations

AF	Array Factor
AMS	Artificial Magnetic Conductor
CMPA, RMPA	Circular and Rectangular Microstrip Patch Antennas
Copol	Co-polarization
Crosspol	Cross-polarization
CRLH	Composite Right Left Handed
LH, RH	Left and Right Handed
PEC	Perfect Electric Conductor
PMC	Perfect Magnetic Conductor
PRS	Partially Reflective Surfaces
SLL	Sidelobe Level
TL	Transmission Line
TM	Transverse Magnetic
ZOR	Zeroth Order Resonance

Symbols

c	Speed of light
C_R, L_R	Shunt capacitance and series inductance of RH part of CRLH
C_L, L_L	Series capacitance and shunt inductance of LH part of CRLH
d	Distance between centers of slots
D	Directivity of antenna
d_x, d_y	Distance between patch along x and y directions
f_{mn}	Resonant frequencies of TM_{mn} modes
h	Substrate height
L, W	Patch length and width
L_1, W_1	Length and width of ground plane
L_s	Probe inductance
ℓ	Length of slot (or length of notch)
ℓ_c, W_c	Interdigital capacitor length and width
ℓ_s, W_s	Stub length and width
p	Physical size of CRLH unit cell
P_{rad}	Radiated power
R_{in}	Input resistance of patch
s	Coupling gap between patch and CRLH TL unit cell
t	Width of slot
U	Radiation intensity
U_{max}	Maximum radiation intensity
w	Width of notch
Y	Admittance for shunt resonator of CRLH

Z	Impedance for series resonator of CRLH
β	Phase constant
$\epsilon_r, \epsilon_{eff}$	Relative and effective dielectric constant
λ	Wavelength in material
λ_g, λ_0	Guided and free space wavelength
μ	Permeability
ω	Radian frequency

Chapter 1

Introduction

Microstrip patch antennas are popular due to their several attractive features such as low profile, light-weight, ease of fabrication, and conformability with planar and non-planar surfaces. With the advent in wireless communication technology, small size and low profile antennas are sought and patch antenna is a good candidate for these applications. Unlike other antennas, patch antenna can easily be designed to achieve multiband operation, polarization diversity, and different pattern shapes. In fact, the variety in the design of patch antenna exceeds any other antenna type. Thousands of research papers have been published so far in this area and still continue to come in abundance.

Most of the work done in patch antenna is for fundamental mode and little attention have been paid to higher mode operation due to undesirable features such as null in broadside direction and high E-plane SLL. With the exception of a few early references [1, 2], the work on higher order mode patch antennas lay dormant till now, especially in the area of radiation pattern shaping of higher order mode patch antennas. Recently, there is a renewed interest in higher order mode patch antennas for broadside medium range applications, having gain of 10-16 dBi. However, high E-plane SLL and low gain limits their use for practical applications. Thus, there is need to develop techniques for E-plane SLL suppression and gain enhancement in higher order mode patch antennas. The first part of the research focuses on the improvements in radiation characteristics of higher order

mode rectangular patch antennas. Several novel techniques such as slot loading and partial notch loading are proposed for gain enhancement and SLL reduction of higher order mode rectangular patch antennas.

Metamaterials, which are artificial materials exhibiting unique properties not found naturally, have started new paradigm in microwave engineering. They have made possible the realization of many novel microwave devices and antennas. Metamaterial based antennas can be divided into two types: leaky wave antennas and resonant type small antennas [3]. Leaky wave antennas based on metamaterials can achieve forward and backward beam scanning, which is not possible in conventional antennas. Resonant type small antennas based on composite right/left handed (CRLH) transmission line (TL) metamaterials make use of unique dispersion characteristics. The phase constant, β of CRLH TL can have positive, zero and negative values, corresponding to positive order, zeroth order and negative order modes (resonances).

The multiple resonances of CRLH TL can be used for multi-band antenna operation. In addition, zeroth order mode having infinite wave length ($\beta = 0$) has drawn huge interest. The resonant frequency of zeroth order mode is independent of resonator length, which is very useful for realizing small antennas [4]. In most cases, miniaturized antenna based on zeroth order resonance have ominidirectional (monopole like) patterns. Multiband antennas based on metamaterial loaded patch antennas are also reported in literature by utilizing $\pm 1^{st}$ order and zeroth order mode. However, these antennas have several drawbacks such as design difficulty, fixed frequency ratio, monopole like pattern at zeroth order resonance and low efficiency.

With recent advancement in wireless communication technology, reconfigurable systems are gaining popularity and have spurred research interest for reconfigurable antennas. The second part of the research focuses on the development of new methods for designing multiband reconfigurable patch antennas [5, 6]. Novel high gain reconfigurable patch antennas based on the concept of zeroth order CRLH TL resonator and patch antenna coupling are presented.

1.1 Microstrip Patch Antenna

The basic geometry of microstrip antenna is shown in Fig. 1.1. It consists of a metallic radiating patch on top of a dielectric substrate with metalization or ground plane on the bottom side. Radiating patch can have variety of different shapes like rectangular, circular, triangular, and annular ring. In this thesis, we will focus on rectangular patch radiator which is the most commonly used shape. The geometry of rectangular patch antenna is shown in Fig. 1.2. It is characterized by two parameters namely: patch length L and patch width W. The patch is printed on a substrate having dielectric constant ϵ_r and substrate thickness h.

Microstrip antenna can be considered as discontinuity in the microstrip transmission line. A microstrip line terminated on an open boundary causes radiation due to fringing electric field at the open end. The radiation can be enhanced by increasing the width of microstrip line. A microstrip antenna is basically a $\lambda/2$ open end transmission line resonator whose width has been increased to achieve good radiation efficiency. It behaves like a parallel RLC resonator. For the fundamental mode, length L of patch antenna is about 0.5λ. The exact length is slightly less than $\lambda/2$ due to fringing effect at both sides of length L [7]. The patch width W affects the input impedance and gain of patch antenna. The larger value of W results in lower input impedance and higher gain. The width of patch usually lies between $0.5L \leq W \leq 2L$. A common choice which ensures good radiation efficiency is to select W equal to half wavelength corresponding to average of two dielectric mediums i.e. air and patch substrate.

The substrate parameters affect the radiation efficiency and bandwidth of patch antenna. The radiation efficiency is directly proportional to substrate height h and inversely proportional to dielectric constant ϵ_r. In order to achieve good radiation efficiency thick substrate with low ϵ_r must be chosen [8]. Different type feeding methods can be used to excite the patch antenna. Four most common feeding mechanisms are microstrip line feed, coaxial probe feed, proximity coupled feed and aperture coupled feed.

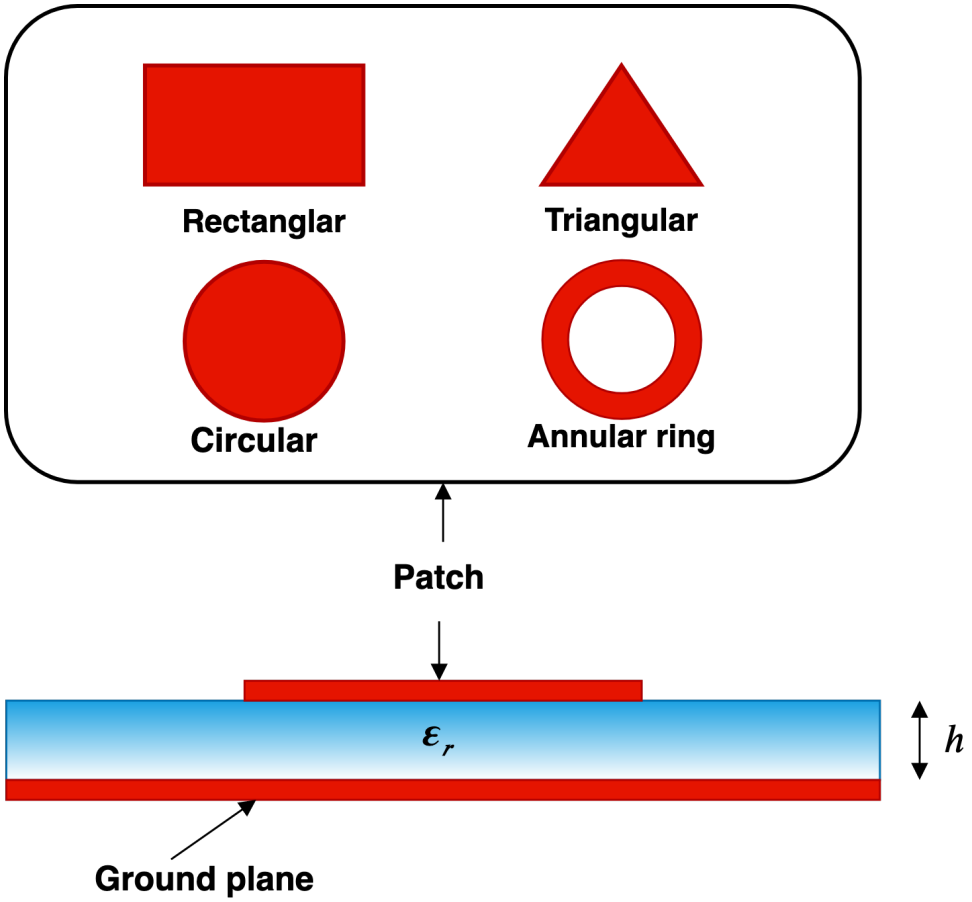

FIGURE 1.1: Basic geometry of patch antenna.

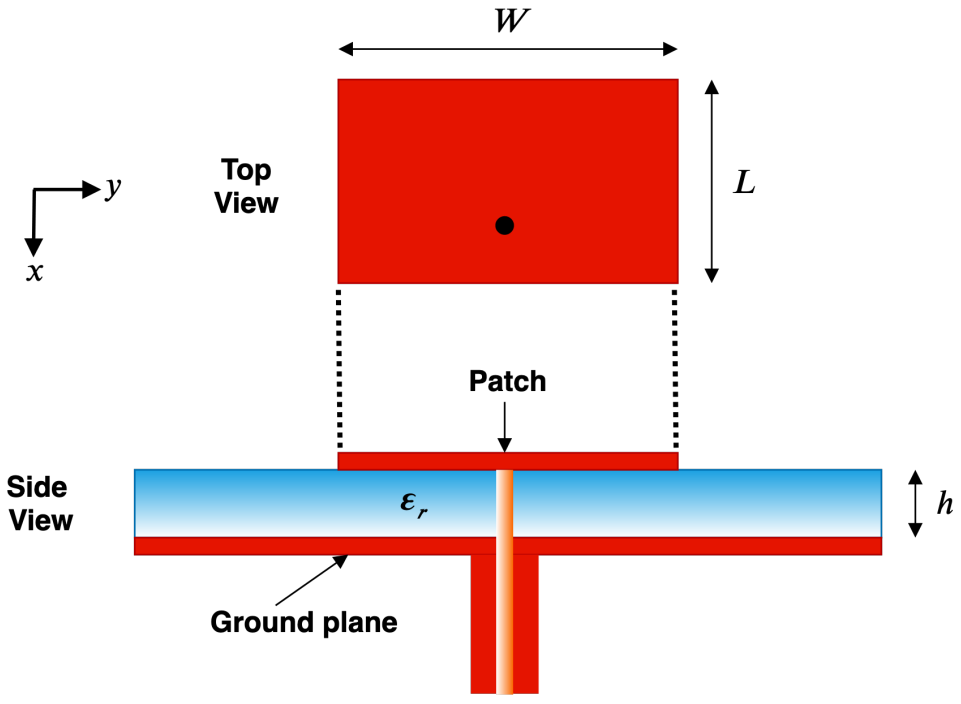

FIGURE 1.2: Geometry of rectangular patch antenna.

Microstrip antennas have several advantages which make them suitable for a variety of commercial and military applications. The have low profile, light weight, conformability to shaped surfaces and can be easily integrated with microwave circuits. In addition, they are easy to fabricate using low cost photo lithography technique. However, like any technology they also have some drawbacks. They have narrow bandwidth (typically 2-5%) [8], low gain (typically 5-8 dBi) [9] and low power handling capability. Over the years different techniques have been developed to overcome some of these disadvantages, e.g., impedance bandwidth can be improved by using proximity coupled patches [10] and stacked patches [9] . Similarly directivity can be enhanced using array of patch antenna [11, 12] and other techniques presented in Chapter 2.

It is worthwhile to comment on ease of fabrication for patch antennas which is also directly related to cost of fabrication. In general, patch antennas are easy to fabricate compared to other antennas. However, in case of patch antennas fabrication difficulty depends on two main factors. 1) single-layer or multilayer configuration and 2) need for plated through hole (PTH). Single-layer patch is more preferable because unlike multilayer configurations such as aperture coupled patch antennas it doesn't require alignments of different layers which is critical for RF performance. This issue become more severe for high frequency designs. In addition, high frequency substrate are costly and multilayer patch design will be more expensive. Simlarly, patch antennas which don't require PTH are less costly and easy to fabricate.

1.2 Higher Order Modes in Rectangular Patch Antenna

Rectangular patch antenna is commonly operated in the fundamental or dominant mode which has broadside radiation pattern. However, patch antenna also exhibit higher order resonances which can be found using the cavity model. In this model, patch is treated as a cavity with perfect electric conductor (PEC) or short circuit

TABLE 1.1: Calculated resonance frequencies of TM_{mn} modes.

Mode	TM_{01}	TM_{10}	TM_{11}	TM_{02}	TM_{20}	TM_{12}	TM_{21}	TM_{22}	TM_{03}	TM_{30}
Frequency (GHz)	1.04	1.14	1.52	2.03	2.27	2.32	2.48	3.04	3.04	3.4

boundary at the top and bottom, and perfect magnetic conductor (PMC) or open circuit boundary along the periphery. The resonance frequencies for TM_{mn} modes of rectangular patch antenna can be obtained using the following formula [7]:

$$f_{mn} = \frac{c}{2\sqrt{\epsilon_e}}\sqrt{\left(\frac{m}{L}\right)^2 + \left(\frac{n}{W}\right)^2} \tag{1.1}$$

where

m = No. of E-field variations along x-direction (along L)

n = No. of E-field variations along y-direction (along W)

c = Speed of light

ϵ_e = Effective dieletric constant

The effective dielectric conatant can be found using the following formula:

$$\epsilon_e = \frac{\epsilon_r + 1}{2} + \frac{\epsilon_r - 1}{2}\frac{1}{\sqrt{1 + \frac{10h}{W}}} \tag{1.2}$$

The calculation of resonance frequencies can be improved by taking into account the fringing fields. Resonance frequencies for first 10 modes of rectangular patch antenna ($L = 9$ cm, $W = 10$ cm, $\epsilon_r = 2.2$, $h = 0.15$ cm) are given in Table 1.1.

Among different resonant modes, TM_{10}, TM_{01} and TM_{30} modes have broadside radiation patterns [1]. For a given resonance frequency and substrate TM_{10} modes has largest bandwidth [13]. The TM_{10} and TM_{01} modes have orthogonal linear polarization which can be utilized in polarization diversity applications or to achieve circular polarization using appropriate feeding mechanism. TM_{10} and TM_{30} modes

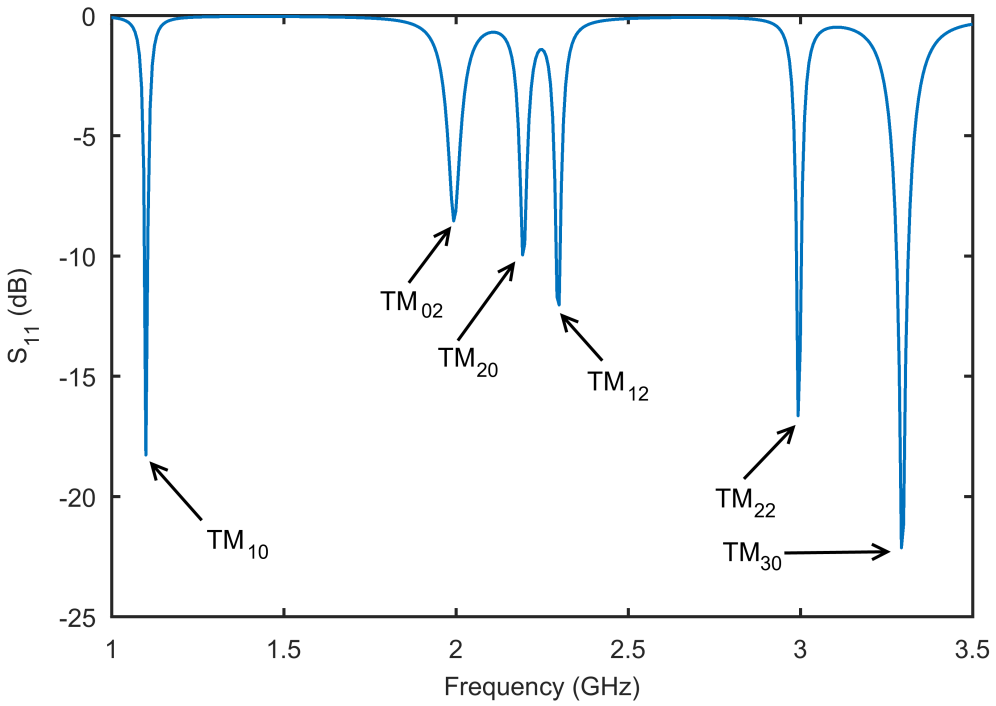

FIGURE 1.3: Resonance frequencies of excited TM_{mn} modes for rectangular patch antenna.

have same linear polarization and they can be used to achieve dual frequency operation. The directivity of higher order TM_{30} mode is larger than the TM_{10} mode but at the expense of larger size (about three time larger). In addition, it suffers from high E-plane SLL. The excitation of different mode depends on feed point location. For a coaxial probe located along x-axis ($-L/2 \leq x \leq L/2, y = W/2$) six modes namely TM_{10}, TM_{02}, TM_{20}, TM_{12}, TM_{22}, and TM_{30} will be excited as shown in Fig. 1.3. For $W > L$ and probe located along x-axis, dominant (lowest frequency) mode is TM_{01} but it is not well matched (therefore not visible in Fig. 1.3). Hence, the dominant excited mode of patch is TM_{10}.

A rectangular patch antenna having $L = 9$ cm, $W = 10$ cm, $\epsilon_r = 2.2$ has been simulated using full wave EM simulation software HFSS. A coaxial probe is used to feed the antenna. The resonance frequencies of different TM_{mn} modes can be observed in Fig. 1.3. The simulated electric field magnitudes and surface current distributions for six excited modes i.e. TM_{10}, TM_{02}, TM_{20}, TM_{12}, TM_{22} and TM_{30} are shown in Figs. 1.4 and 1.5. It can be seen from the surface current distribution or electric field plots that radiated field will not add constructively in broadside

direction except for TM_{10} and TM_{30} modes. In general, all TM_{m0} modes (with odd m) of rectangular patch antenna have broadside radiation patterns.

To summarize, rectangular patch antennas are usually operated in the fundamental TM_{10} mode. Higher order modes namely TM_{20}, TM_{02}, TM_{12} and TM_{22} have end fire radiation. Higher order TM_{m0} modes (with odd m) such as TM_{30} mode has broadside radiation pattern and can provide high directivity due to increase in antenna size but is avoided due to higher E-plane SLL. Thus, there is a need to improve the radiation characteristics of higher order TM_{m0} modes (with odd m) of rectangular patch antennas.

1.3 CRLH TL Metamaterials

Left handed (LH) metamaterials are artificial materials having negative permittivity (ϵ) and permeability (μ). They were first predicted theoretically by Vaselago in 1967 [14]. LH metamaterial have negative refractive index ($n = -\sqrt{|\epsilon_r||\mu_r|}$) and antiparallel phase and group velocities (backward waves). LH metamaterials were experimentally verified in 2000 using thin wires and split ring resonators structure [15]. Since then many applications of LH metamaterials have emerged including novel microwave guided wave devices and antennas [4, 16]. Metamaterials can be described using transmission line theory. An equivalent circuit supporting backward wave is given in [17] which consists of a series capacitance and shunt inductance. The circuit is dual of conventional right handed (RH) lossless transmission line. However, due to parasitic effects practical realization of pure LH metamaterial is difficult. To circumvent this issue concept of composite right/left handed (CRLH) TL was proposed [18, 19].

The equivalent circuit models of conventional RH TL, LH TL and CRLH TL are shown in Fig. 1.6. It can be seen that CRLH TL includes a RH part in the form of a series inductance (L_R) and shunt capacitance (C_R), beside the required LH part which is composed of series capacitance (C_L) and shunt inductance (L_L). CRLH TL consists of two resonant circuits, a series resonator having impedance Z and

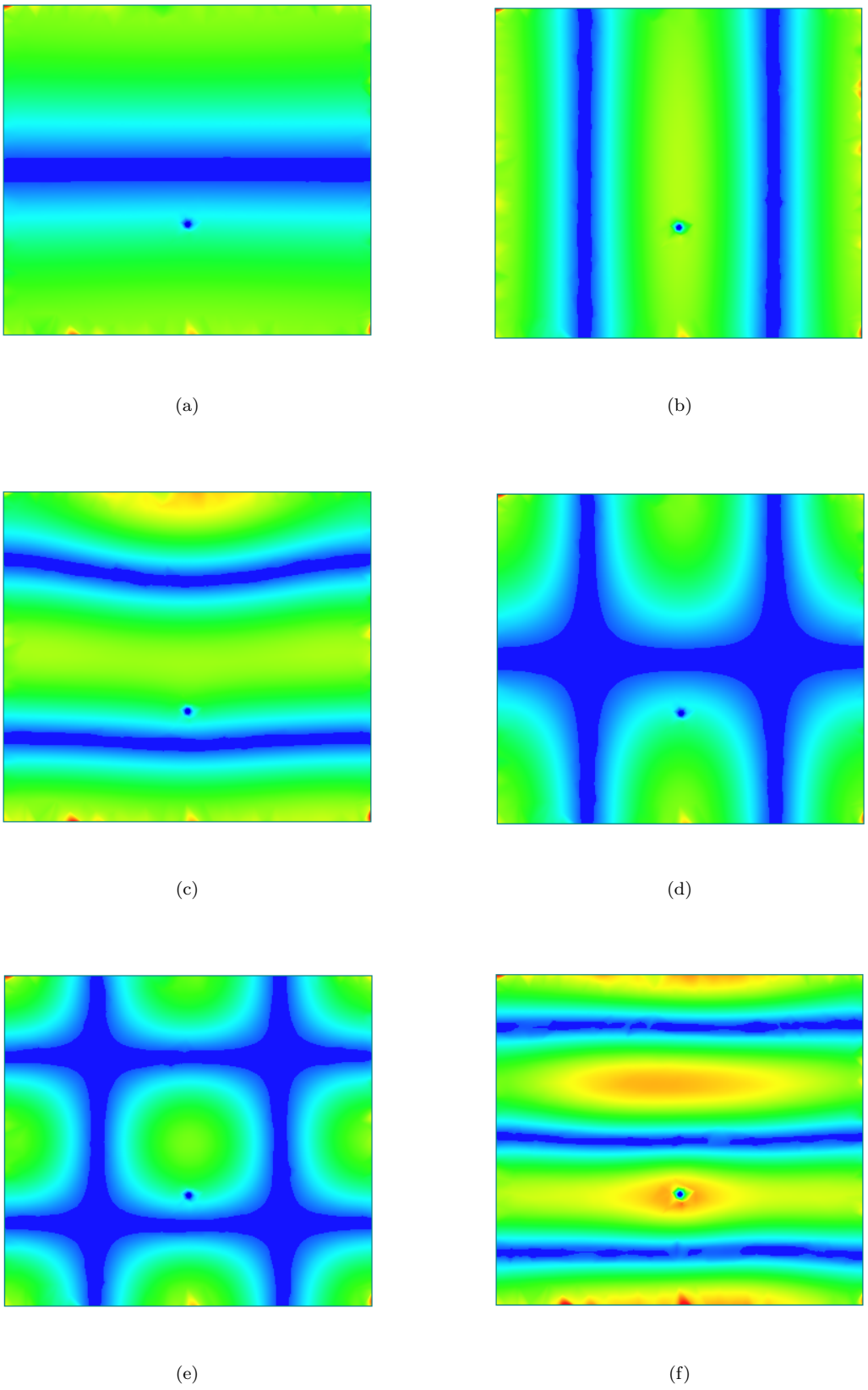

(a) (b)

(c) (d)

(e) (f)

FIGURE 1.4: Electric field magnitude for TM_{mn} modes of rectangular patch antenna. (*a*) TM_{10}, (*b*) TM_{02}, (*c*) TM_{20}, (*d*) TM_{12}, (*e*) TM_{22}, and (*f*) TM_{30}.

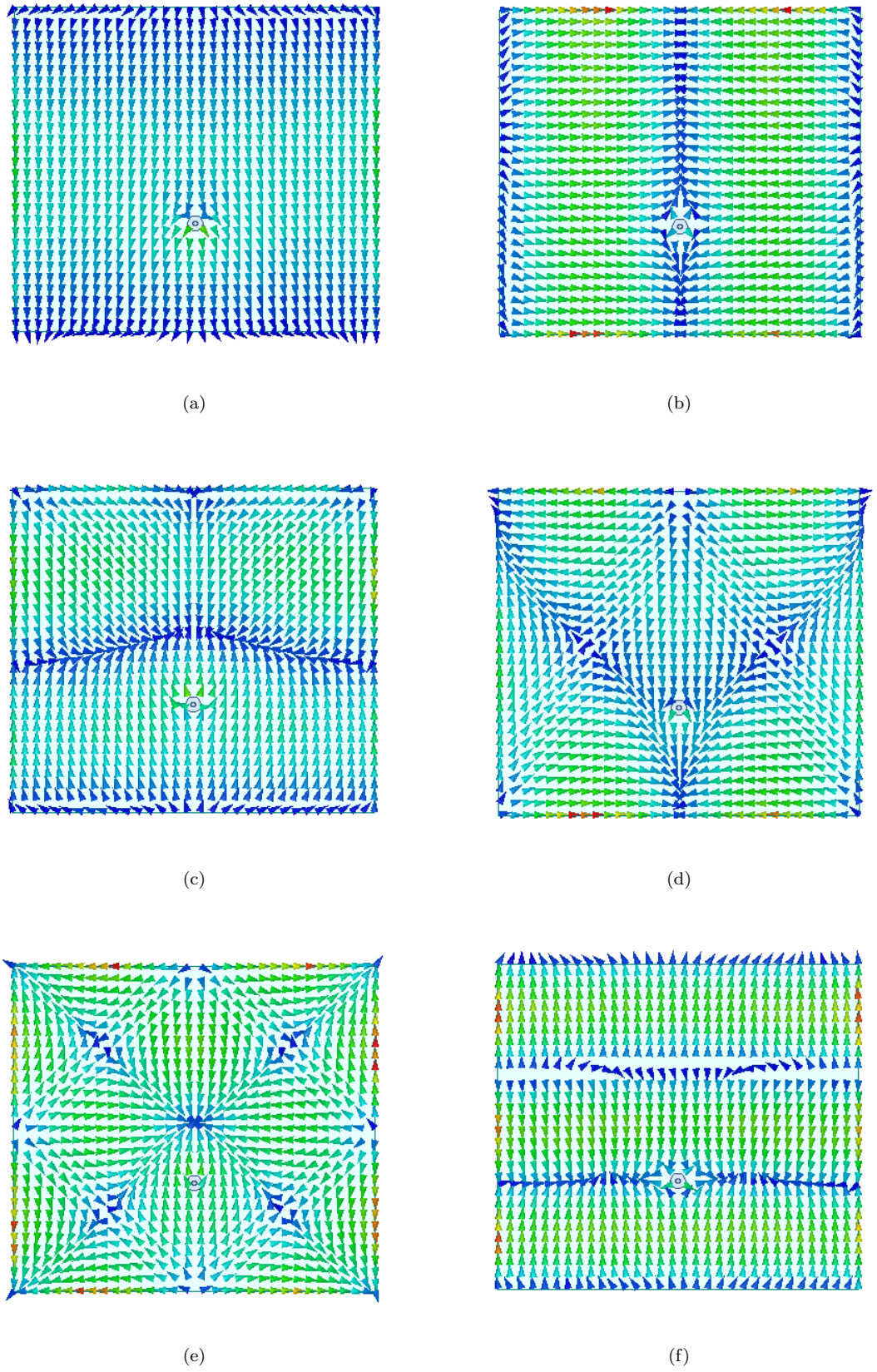

(a) (b)

(c) (d)

(e) (f)

FIGURE 1.5: Surface current distribution for TM_{mn} modes of rectangular patch antenna. (*a*) TM_{10}, (*b*) TM_{02}, (*c*) TM_{20}, (*d*) TM_{12}, (*e*) TM_{22}, and (*f*) TM_{30}.

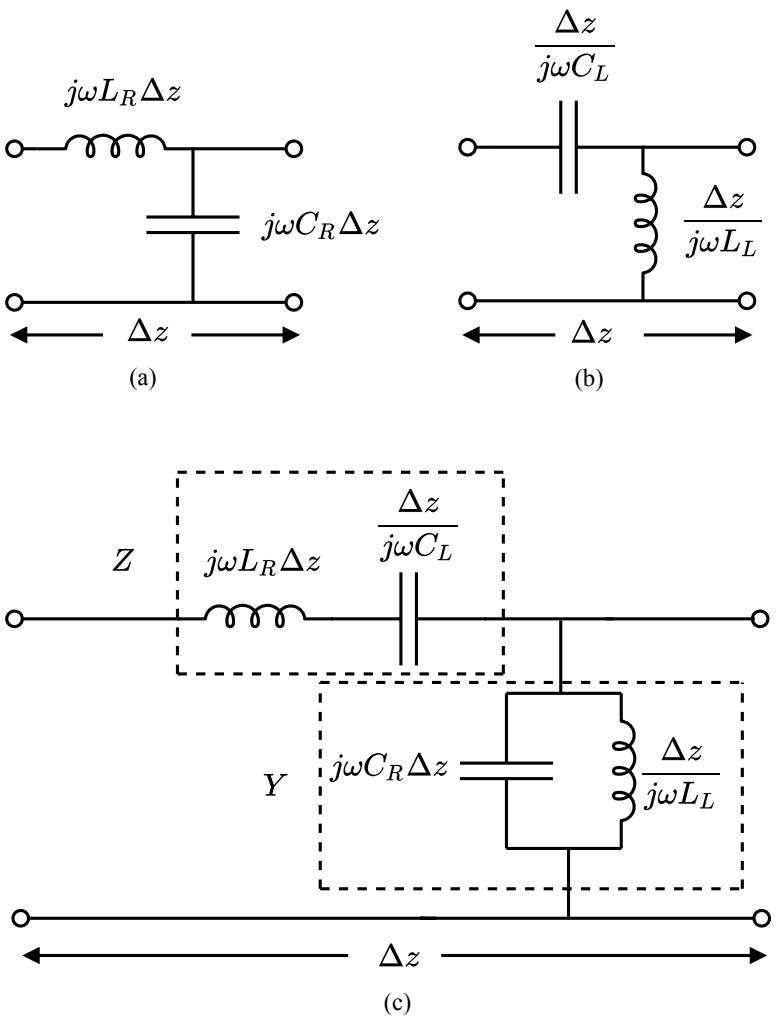

FIGURE 1.6: Equivalent circuit models for homogeneous lines (a) RH TL (b) LH TL (c) CRLH TL.

a shunt resonator having admittance Y. CRLH TL is known as balanced when series and shunt resonances are equal ($\omega_{se} = \omega_{sh}$). The characteristic impedance of balanced CRLH TL is independent of frequency which means that broadband impedance matching is possible. The phase constant β for balanced CRLH TL is given by $\beta = \sqrt{ZY} = \omega\sqrt{L_R C_R} - \dfrac{1}{\omega\sqrt{L_L C_L}}$ [20]. The dispersion characteristics of CRLH TL can be understood using $\omega - \beta$ diagram as shown in Fig. 1.7. Depending on frequency CRLH TL behave like LH or RH, the transition between two regions occurs at transition frequency ω_0. The phase constant is zero at ω_0 which means that phase shift ($\theta = \beta\ell$) for a TL of length ℓ is zero. However, propagation of wave will occurs because of non zero phase velocity at ω_0. The corresponding guided wavelength $\lambda_g = \dfrac{2\pi}{\beta}$ is infinite.

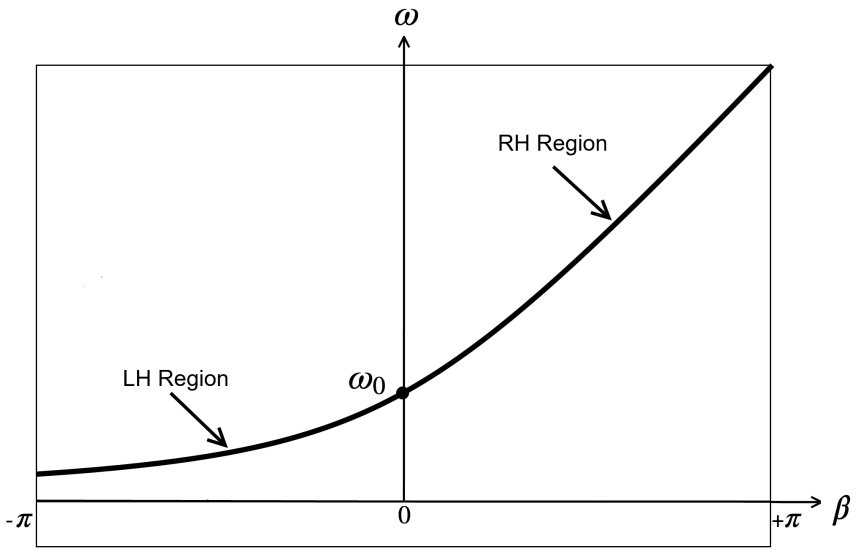

FIGURE 1.7: Dispersion diagram of balanced CRLH TL.

Although ideal homogeneous ($\Delta z \rightarrow 0$) case provides a good insight about the fundamental properties of CRLH TL, it cannot be realized practically. However, an effective homogeneous case can be achieved using a cascade of LC based CRLH TL unit cells as shown in Fig. 1.8. In order to ensure effective homogeneity, physical size of CRLH TL unit cell p must be less than $\frac{\lambda_g}{4}$ or equivalently its electrical length must be less than $\frac{\pi}{4}$ [16]. LC based CRLH TL can be implemented either using discrete surface mount components or distributed components in the form of transmission line e.g. microstrip TL. Physical size p of CRLH TL unit cell depends on the technology used for implementation of CRLH TL. For antenna applications, distributed CRLH TL is used along with open or short circuit termination. A CRLH TL implemented using microstrip technology is shown in Fig. 1.9. It consist of an interdigital capacitor and a short circuited shunt stub.

1.4 Positive, Negative and Zeroth Order Modes In CRLH TL

For CRLH TL, phase constant β can take positive, negative and zero value which corresponds to positive, negative and zeroth order resonant modes of CRLH TL.

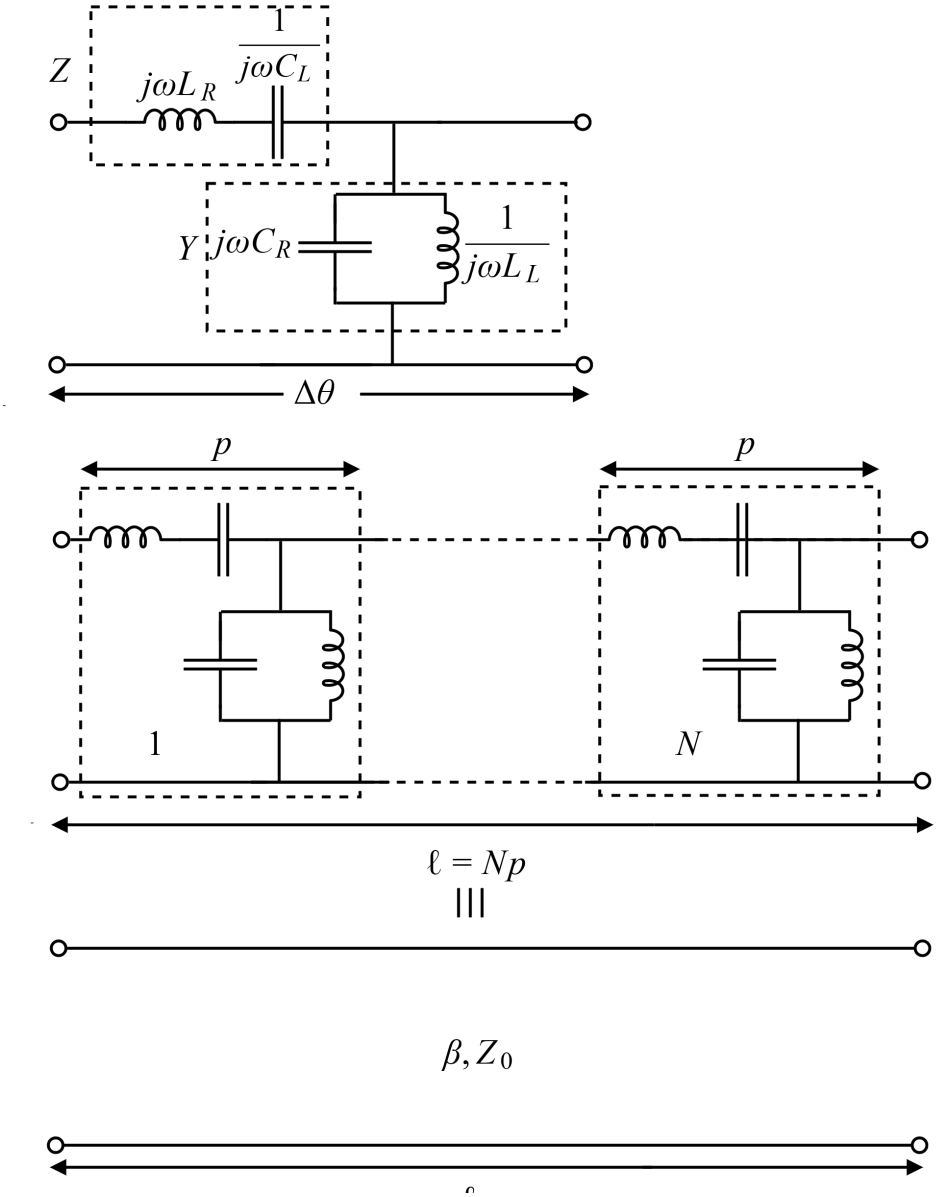

FIGURE 1.8: LC based CRLH TL.

The resonance frequencies of a short or open circuit CRLH TL resonator, composed of cascade of N unit cell occurs when length $\ell = \frac{n\lambda_g}{2}$ $(n = 0, \pm1, \pm2, ..., , \pm N-1)$ or equivalently $\beta = \frac{n\pi}{\ell}$ $(n = 0, \pm1, \pm2, ..., \pm N-1)$. Depending on the value of n different resonances (modes) are generated including positive order, zeroth order and negative order resonances. The total number of resonances depends on the number of unit cells in the CRLH TL. Figure 1.10 shows the resonance frequencies of a 3-stage ($N = 3$) CRLH TL. The resonance frequencies are calculated by sampling the dispersion curve at $\frac{n\pi}{\ell}$ intervals. It can be seen that due

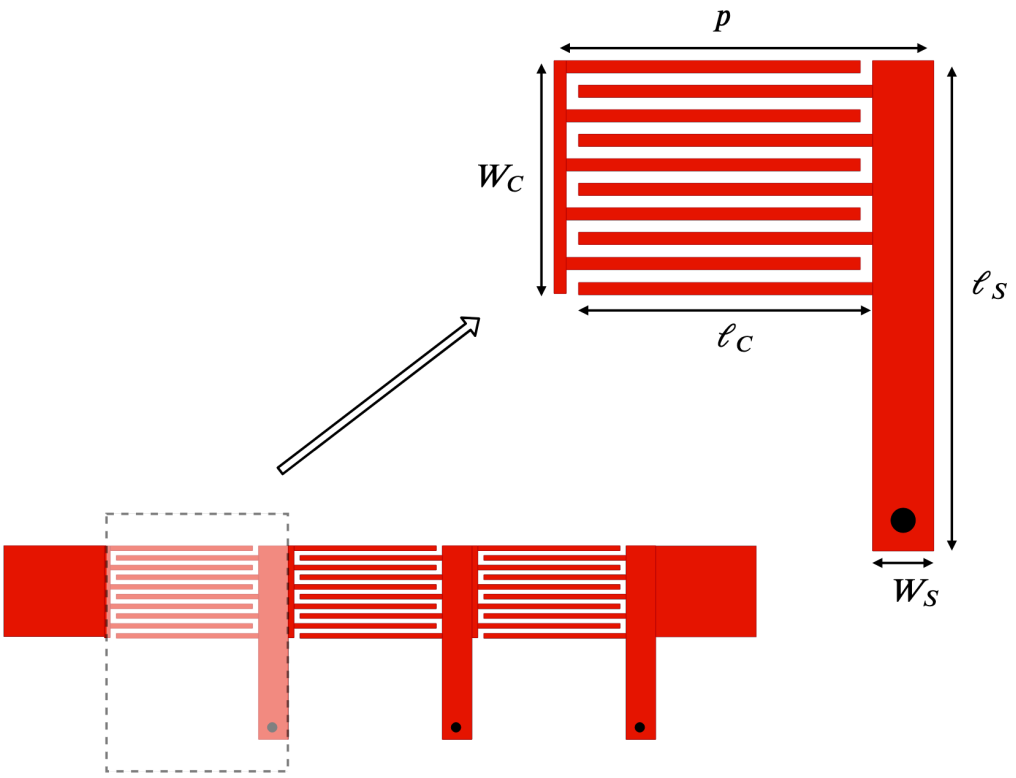

FIGURE 1.9: Microstrip TL implementation of CRLH TL.

to non-linear nature of phase constant $\beta(\omega)$, the resonance frequencies are not an integer multiple. The voltage of open circuited CRLH TL resonator for different resonant modes is plotted in Fig. 1.11. The field distribution for $(\pm n)$ modes are identical. This property is useful for designing dual band components [16]. For zeroth order mode $n = 0$, field distribution is constant which means that resonance frequency is independent of length. The zeroth order mode is useful for realization of miniaturized resonators.

1.5 Thesis Contributions

As mentioned previously, the thesis focuses on two main research topics namely gain enhancement and SLL suppression of higher order TM_{m0} mode (with odd m) of rectangular patch antennas, and high gain CRLH TL based frequency reconfigurable patch antennas. The main contributions of the research are summarized below:

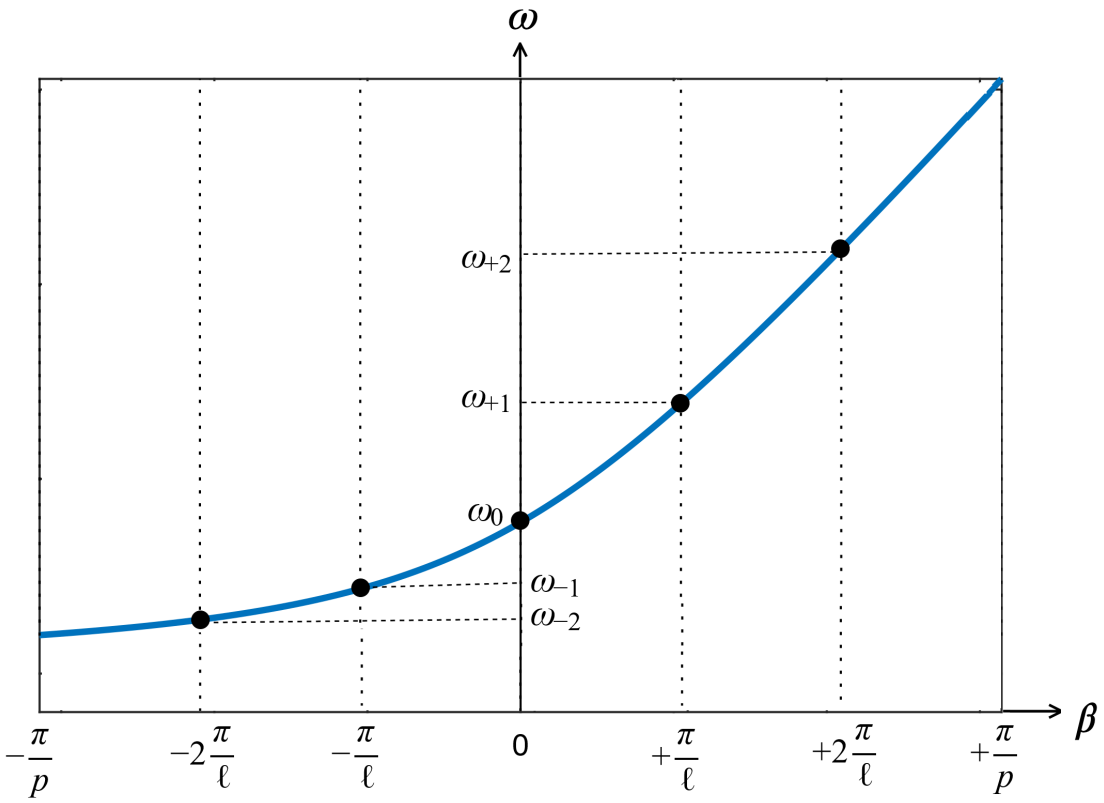

FIGURE 1.10: Resonance frequencies of 3-stage CRLH TL.

1.5.1 High Gain Low SLL TM_{m0} Mode Rectangular Patch Antennas

The main causes of low gain and high E-plane SLL in conventional TM_{m0} mode rectangular patch antennas are investigated. Two approaches are proposed for improving the radiation characteristics of higher order TM_{m0} mode rectangular patch antennas i.e. slot loading and partial notch loading. Both methods use superpositions of radiated fields of conventional TM_{m0} mode patch and some new radiators present in the out of phase current distribution regions of higher order mode patch antenna. The main advantage of these techniques is that gain enhancement and SLL reduction is achieved without increasing the size of antenna. Moreover, due to single layer configuration they provide ease of fabrication. The proposed TM_{m0} mode rectangular patch antennas are very suitable for medium range broadside applications having gain requirements in the range of 12-16 dBi. It is worthwhile to point out that proposed antennas achieve the high gain performance as a single

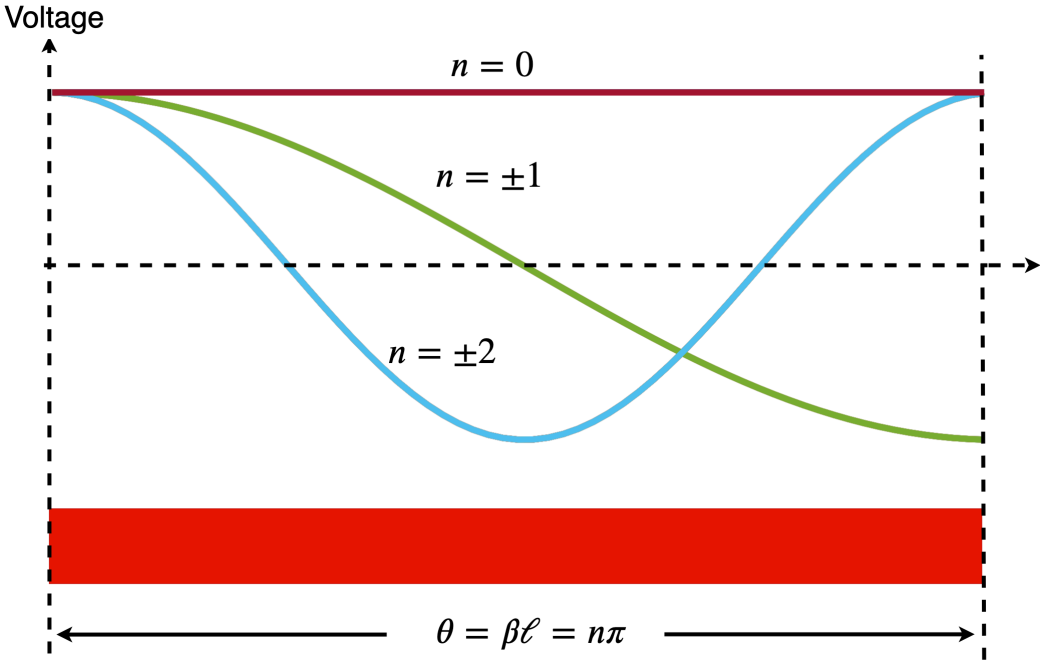

FIGURE 1.11: Voltage distribution for open circuited CRLH TL resonator.

radiator and can be use as a subsitute for equivalent array antennas. A summary of contributions are listed below.

1.5.2 Slot Loading Technique

1. A slot loading technique which uses superposition of radiated fields of conventional TM_{30} mode and new in-phase radiators created using an array of 1×2 slots in the out-of-phase surface current distribution region of higher mode patch is proposed and demonstrated.

2. Analysis of proposed slot loaded TM_{30} mode patch antenna using cavity model and superposition principle.

3. A differential feeding scheme is proposed to circumvent asymmetric radiation pattern and high cross polarization of slot loaded TM_{30} mode patch antenna. In addition, it simplifies integration with differential circuits.

4. It is shown that compared to conventional TM_{30} mode patch 2.4 dB improvement in gain and about 10 dB improvement in SLL is possible using proposed slot loading technique while size remains same.

5. In many practical applications, single-fed antennas are more desired. A single-fed, high gain TM_{30} mode patch using a planar 2×2 slot array etched at the center of patch is presented.

1.5.3 Notch Loading Technique

1. A partial notch loading technique which uses superposition of radiated fields of conventional TM_{m0} mode and new in-phase radiators created by partially removing the out-of-phase surface current distribution region of higher mode patch is proposed.

2. Two novel single layer higher mode patch antennas, namely, notch loaded TM_{30} mode rectangular patch antenna and TM_{70} mode rectangular patch antenna are designed and demonstrated.

3. Analysis of proposed notch loaded TM_{30} mode and TM_{70} patch antennas using cavity model and superposition principle.

4. It is shown that compared to conventional TM_{30} mode patch 3 dB improvement in gain and about 8 dB reduction in SLL is possible using proposed notch technique while size remains same.

5. A method for further reduction in SLL and improvement in return loss of TM_{30} mode patch using a combined notch and fractal slot loading is also presented. The proposed notch and fractal slot loaded TM_{30} mode patch can achieve more than 5 dB reduction in SLL and about 7 dB improvement in return loss compared to notch loaded TM_{30} mode patch antenna.

6. It is demonstrated that proposed TM_{70} mode patch has peak gain of 16 dBi, which is the highest reported gain for single layer TM_{70} mode patch antenna reported so far.

7. It is shown that proposed notch loaded TM_{70} mode patch can achieve more than 5 dB improvement in gain and about 15 dB reduction in SLL compared to conventional TM_{70} mode antenna while size remains same.

1.5.4 High Gain CRLH TL Coupled Reconfigurable Patch Antennas

1. A method for realizing dual band antenna for broadside applications is proposed using gap-coupled TM_{10} mode patch and ZOR mode of CRLH TL unit cell.

2. A CRLH TL coupled patch having resonance frequency ratio of 1.08 is designed and demonstrated.

3. It is shown that proposed scheme enables frequency reconfigurability by changing the resonance frequency of ZOR mode CRLH TL unit cell.

4. High gain dual band CRLH TL coupled patch array having more than 12.7 dBi gain at both resonance frequencies is demonstrated.

1.6 Thesis Organization

The outline of thesis is as follows: **Chapter 1** provides an introduction of two research problems investigated in this thesis namely, methods for improving the high E-plane SLL and low gain in TM_{m0} mode rectangular patch antennas and possibility of using ZOR mode of CRLH TL for achieving multiband reconfigureable patch antennas. A brief background of microstrip antenna technology, microstrip rectangular patch antenna, higher order mode in rectangular patch antennas, CRLH TL based metamaterials and their unique modal behavior supporting positive, zeroth and negative order resonances is discussed. The main contributions of the research and an outline of thesis is also presented.

Chapter 2 presents detail literature review about gain enhancement techniques for microstrip patch antennas. The existing methods for SLL suppression and gain enhancement of higher order mode patch antennas are also investigated. Moreover, a brief overview for multiband techniques in CRLH TL loaded patch antennas is presented. Motivation of thesis and its main objectives are stated.

In **Chapter 3**, slot loading technique for SLL reduction and gain enhancement in TM_{30} mode rectangular patch antenna is presented. In this method, new in-phase radiators are created by cutting slots in the center of patch. Theoretical analysis based on cavity method and superposition principle is presented. The results were verified using full wave EM simulations. Parametric analysis describing effect of different slot parameters on antenna performance is presented. The problem of asymmetric radiation pattern in slot loaded TM_{30} mode patch antenna is investigated. A differential loading technique was proposed to overcome this issue. A detailed comparison of conventional and proposed slot loaded TM_{30} mode patch is also presented.

Chapter 4 describes another technique for gain enhancement and SLL suppression of TM_{m0} mode rectangular patch antennas. In this technique, out-of-phase surface current distribution regions are partially removed to create new radiating edges between the radiating edges of conventional TM_{m0} mode rectangular patch antennas. Theoretical far field expressions for proposed notch loaded higher mode patch antennas are presented. Two novel single layer designs based on TM_{30} mode and TM_{70} mode patch antennas are proposed. Effect of notch loading on performance of both antennas is investigated using full wave simulations. Comparison of proposed and conventional TM_{m0} mode rectangular patch antenna is presented.

Chapter 5 describe two methods for improving the performance of TM_{30} mode patch antennas. The first method is applicable to slot loaded TM_{30} mode patch presented in Chapter 3. In this method, a 2×2 slot array is etched at the center of TM_{30} mode patch to achieve single-fed, high gain and low SLL antenna with symmetric radiation pattern. The second method is applicable to notch loaded TM_{30} mode patch as presented in Chapter 4. It is demonstrated that SLL reduction and return loss improvement can be achieved by etching a fractal slot in the center of TM_{30} mode patch.

Chapter 6 presents a method for designing multiband reconfigurable patch antennas. In this method, a CRLH TL unit cell is gap-coupled with the patch antenna. The working principle of proposed antenna is investigated. Parametric analysis

using full wave EM simulations is presented. As a design example a dual band CRLH TL coupled patch is proposed and investigated. A high gain 2x2 dual band CRLH TL coupled patch array is also presented .

In **Chapter 7**, conclusion of this research work is presented along with some future recommendations.

Chapter 2

Literature Review

2.1 Gain Enhancement Techniques for Patch Antennas

High gain planar antennas with low SLL are desired in various wireless communication applications. Microstrip patch antenna due to its low cost, ease of fabrication and integration with integrated circuits is an attractive candidate. However, microstrip antenna operating in the dominant mode has low gain usually 5-8 dBi [9]. Several single layer and multilayer techniques have been proposed over the years to overcome this issue. The gain of patch antenna can be improved using array, proximity coupling in horizontal (coplanar) or vertical (stacking) plane, and superstrate loading as shown in Fig. 2.1.

A microstrip patch array can be employed to increase the gain [1, 11]. However, feednetwork is required to excite the individual antennas which add complexity. Moreover, losses associated with feednetwork due to conductor, dielectric and radiation losses results in low antenna efficiency. Directivity can also be increased by utilizing parasitic patches either in the plane of antennas or vertically in a stacked configuration. In coplanar configuration, parasitic patches are coupled to a driven patch along the radiating and or non-radiating edges. However, this is primarily a bandwidth enhancement technique and directivity increases due to

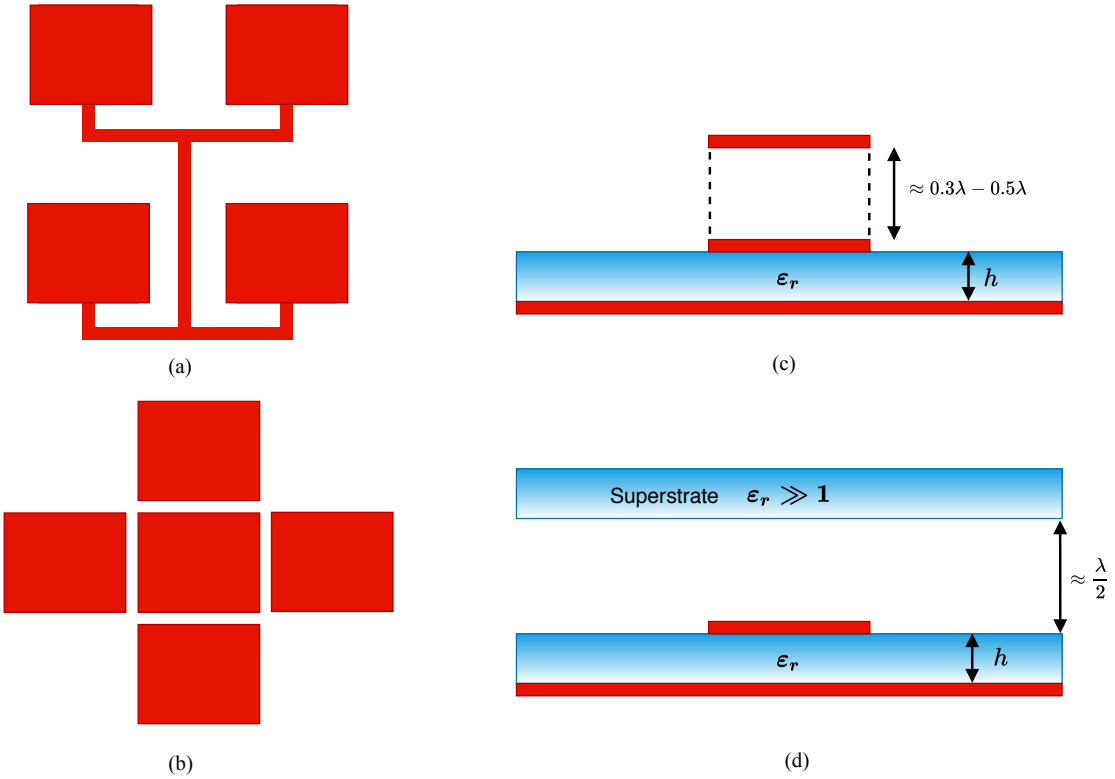

FIGURE 2.1: Gain enhancement techniques for patch antenna (a) Patch array (b) Proximity coupled patch (c) Stack patch configuration (d) Superstrate loading

increase in the surface area of the antenna. Moreover, radiation pattern is not stable and varies over the frequency band [10].

An electromagnetically coupled stacked patch configuration is proposed in [9, 21]. In this technique, a parasitic patch is placed vertically in a stacked configuration above a driven or fed patch. Bandwidth or directivity enhancement is possible depending on spacing between the driven patch and parasitic patch. For spacing less than 0.1λ, impedance bandwidth is increased due to close resonance frequencies of fed and parasitic patches, two-frequency resonance. When the spacing between the patches is on the order of half wavelength 0.3-0.5λ [9], gain is enhanced due to existence of standing wave in the cavity between patches. Both current and electric field of patches are 180^0 out of phase (resonance condition). The radiated field is in-phase in the broadside direction resulting in gain enhancement. Although, stacked patches can provide high directivity but distance between the patches needs to be order of half wave length thus occupying larger volume. Moreover,

antenna complexity increases due to multilayer structure.

Another technique for gain enhancement is to use high dielectric substrates known as superstrates above the patch antenna [22, 23]. The basic idea is to achieve resonance condition, substrate-superstrate resonance. In [24, 25] partially reflective surfaces (PRS) are used as superstrate for gain enhancement. However, in both dielectric and PRS superstrates half wavelength spacing is required (for forming Fabry-Perot type resonance) between the patch and the superstrate which increases the overall antenna profile. Another technique for directivity enhancement is to used metasurface lens [26] half wave distance above the patch antenna which reduce the half power beamwidth and thus enhances the overall antenna gain. Although, efforts have been made to reduce antenna profile using artificial magnetic conductor (AMC) and metamaterial supersubstrate [27, 28] but they increase the design complexity. Moreover, due to multilayer structure fabrication cost increases.

2.1.1 Use of Higher Order Modes for Gain Enhancement

Gain can be enhanced by using higher order localized modes known as fracton or fractino mode in boundary or mass fractal antennas respectively [29, 30]. Localized modes (fracton or fractino modes) are regions of high current densities. Gain increases because current density maxima are in phase and have large spacing between them in terms of wavelength, resulting in an antenna with larger electrical size and coherent radiation in broadside direction. It was shown by A.B.Younas and Z. Ahmed et al.[31] that directivity can be increased further by introducing another radiating surface in the form of a slot.

In case of Euclidean geometry, higher order mode patch antennas can provide high directivity due to increase in antenna size. For example, higher order TM_{m0} modes (with m odd) of rectangular patch have broadside pattern. The electric field distribution of TM_{m0} modes patch antenna are shown in Fig. 2.2. The theoretical E- and H-plane radiation patterns of TM_{m0} modes patch antenna are shown in

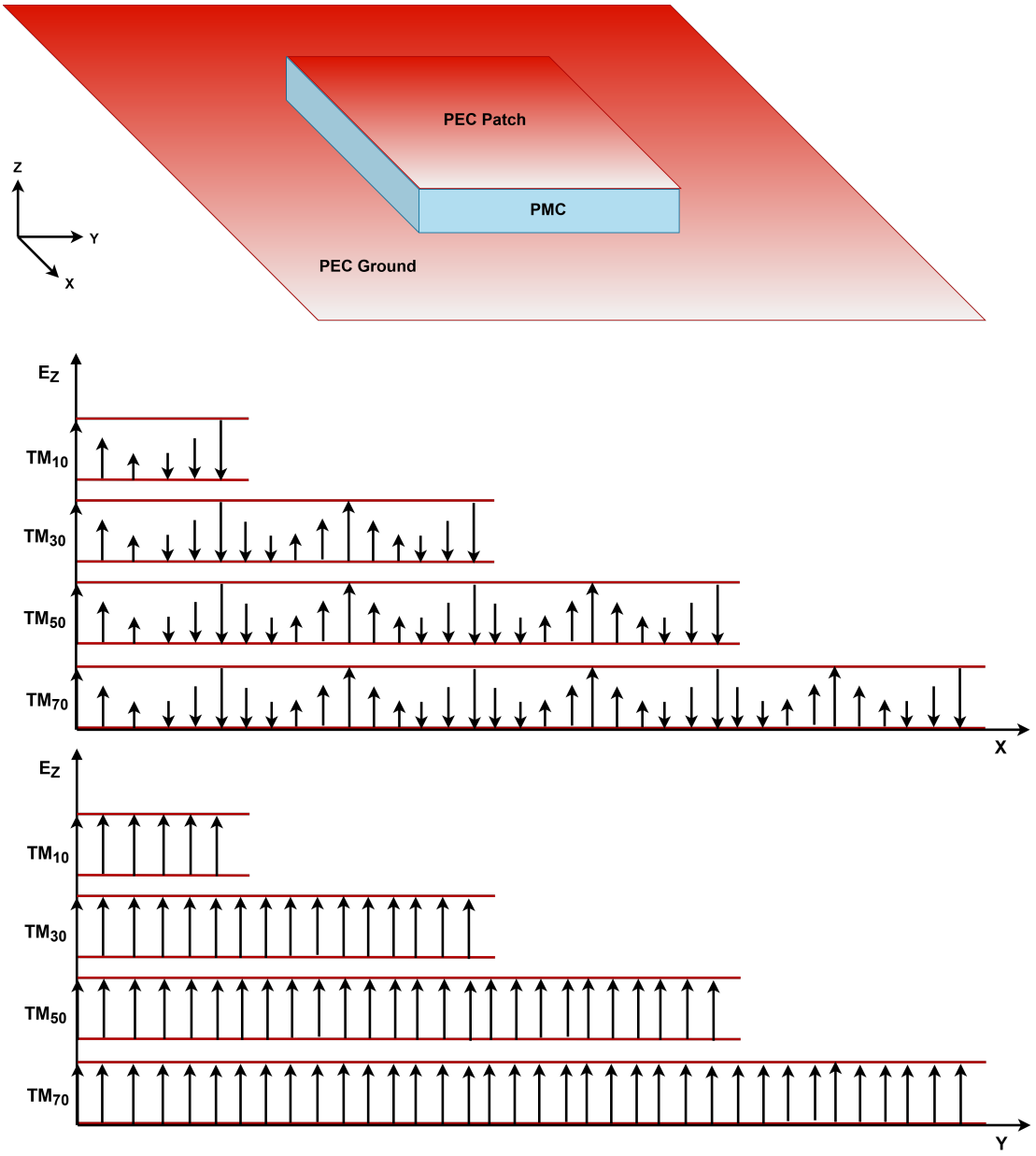

FIGURE 2.2: Electric field distribution in TM_{m0} mode patch cavity.

Fig. 2.3 (a) and 2.3 (b). It can be seen from Fig. 2.3 (a) that higher order TM_{m0} modes have high E-plane SLL, an issue which limits their use for practical applications. In addition, they have lower gain than their fractal counterpart e.g., a fractal antenna of size 1.38λ has a directivity of 12.7 dBi [29] while a TM_{30} mode patch antenna of size about 1.5λ has directivity of 9.09 dBi [13].

For TM_{m0} mode (with m odd) of rectangular patch several questions can be asked:

1. What are the possible causes of higher SLL in E-plane?

2. Why SLL are not high in H-plane?

3. What are the possible causes of lower directivity?

In order to answer these question let's take a closer look at the expression for radiation pattern of rectangular patch antenna. The radiation pattern of patch antenna can be calculated using transmission line model. This model assumes that radiated field is mainly due to two fringing fields located along the width of patch antenna (also called the radiating edges) which are separated by a half wave length distance L. The fringing fields from both ends add constructively in the broadside direction. The radiated field of patch antenna can be calculated by treating the fringing fields as two equivalent radiating slots separated by distance L. The radiated far field of patch antenna for TM_{m0} mode is given by [32]

$$E_\theta = E_0 \cos\phi \, f(\theta, \phi) \tag{2.1}$$

$$E_\phi = -E_0 \cos\theta \sin\phi \, f(\theta, \phi) \tag{2.2}$$

where

$$f(\theta, \phi) = \frac{\sin\left[\dfrac{\beta m W}{2} \sin\theta \sin\phi\right]}{\dfrac{\beta m W}{2} \sin\theta \sin\phi} \cos\left(\frac{\beta m L}{2} \sin\theta \cos\phi\right)$$

$E_0 =$ constant representing the maximum magnitude of field

$E_\theta =$ theta component of elctric field vector

$E_\phi =$ phi component of elctric field vector

$\beta = \dfrac{2\pi}{\lambda}$

Here, first factor of $f(\theta, \phi)$ is the element pattern (pattern factor) due to y-directed line source of width W and second factor is array factor due to two element array along x-axis. E- and H-plane patterns can be evaluated by putting $\phi = 0$ and $\phi = 90^0$ in above expressions.

For E-plane ($\phi = 0$)

$$E_\theta = E_0 \cos\left(\frac{\beta m L}{2}\sin\theta\right), E_\phi = 0 \tag{2.3}$$

For H-plane($\phi = 90$)

$$E_\phi = E_0 \cos\theta \frac{\sin\left[\frac{\beta m W}{2}\sin\theta\right]}{\frac{\beta m W}{2}\sin\theta}, E_\theta = 0 \tag{2.4}$$

In E-plane, pattern consists of only array factor (AF) term consisting of a cosine function while pattern factor (PF) is unity. The argument of cosine function is m times a constant. For higher order TM_{m0} modes (m=3,5,.....), multiple phase variation in aperture field which is also a cosine function (e.g., there are three half wave phase variation for TM_{30} mode) as well as large spacing between the radiating edges (not meeting Nyquist criteria) results in high E-plane SLL as shown in Fig. 2.3(a).

In H-plane, pattern consists of only PF term consisting of a sinc function whereas AF is 1. This makes sense because aperture field and far-field radiation patterns are Fourier transform pair and in present case both uniform aperture field and sinc function are transform pairs. The argument of sinc function is m times a constant term. H-plane pattern for TM_{m0} modes (m=1, 3, 5, $\cdots$) are shown in Fig.2.3(b). It can be seen that for m=1 and 3, there are no SLL in H-plane whereas for m=5 and 7, H-plane SLL corresponds to a sinc function and are less than -15 dB. The possible reason for lower directivity in TM_{m0} mode (for odd m) patch antenna can be associated to high SLL in E-plane. A second reason is out of phase surface current distributions regions of TM_{m0} mode patch.

Different methods are proposed in the past to overcome the drawbacks associated with the radiation properties of TM_{m0} mode (with odd m) of rectangular patch as well as other patch geometries. In [33, 34], a corporate feed network was used for excitation of an oversized higher mode patch in dominant mode. However, similar

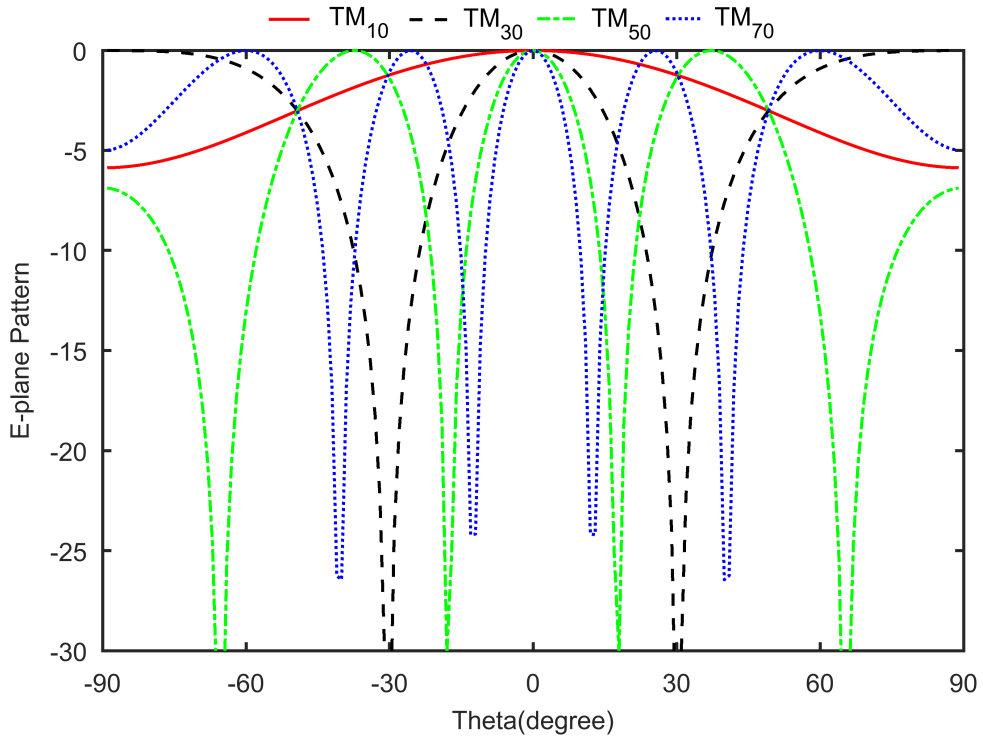

(a)

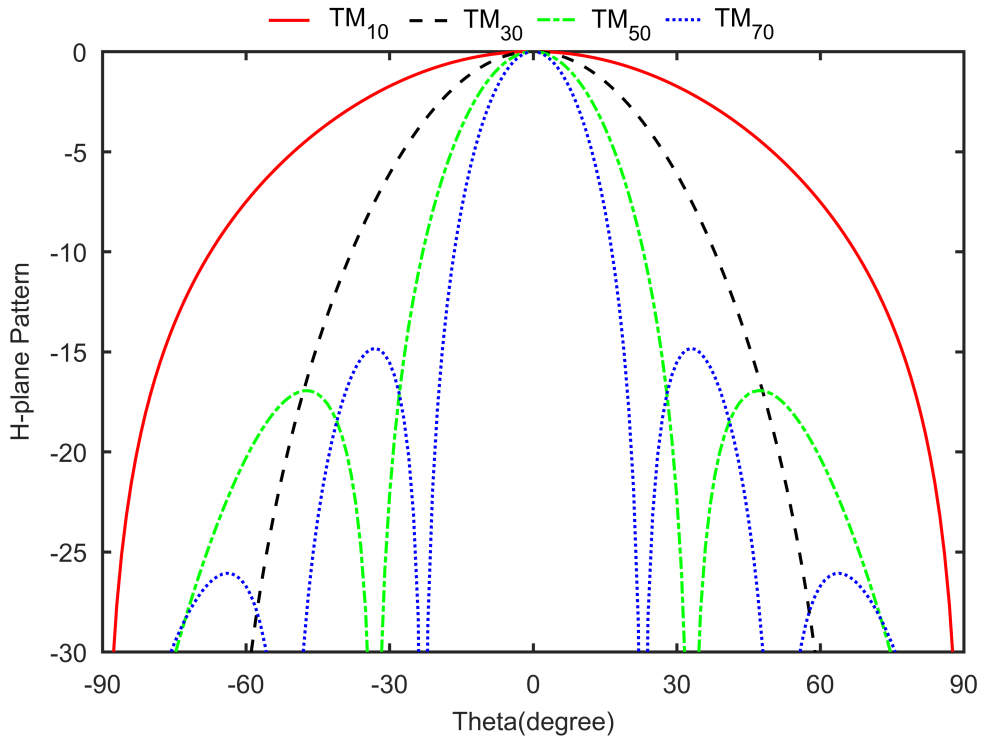

(b)

FIGURE 2.3: TM_{m0} mode (with odd m) patch antenna patterns (a) E-plane and, (b) H-plane.

to array antenna feed network is required which add complexity. In [35], genetic optimization was applied to a TM_{12} mode square patch having endfire radiation pattern to achieve a broadside radiation pattern.

Recently, there is a renewed interest to improve the radiation characteristics of higher order mode patch antennas [36–39]. A differential feeding was proposed in [36] to excite a shorted TM_{30} mode rectangular patch. Although, SLL are eliminated but resulting antenna gain is low and fabrication cost increases due to presence of via holes. In [37], E-plane SLL of TM_{12} mode circular patch antenna was reduced by employing a high dielectric constant substrate. However, surface wave losses in high dielectric substrates can cause ripple in main beam and reduction in antenna efficiency. A dual mode circular patch antenna was proposed in [38] wherein superposition of radiated field was used to achieve gain enhancement and SLL reduction by employing simultaneous excitation of TM_{11} and TM_{13} mode in a stacked configuration. However, due to multilayer nature antenna has complex geometry and is difficult to fabricate.

2.1.1.1 Slot Loading Technique

In the past, slot loading has been employed to improve the impedance bandwidth or SLL reduction of higher mode patch antenna. U, E and H slots [40–42] can be used to achieve wide impedance bandwidth in patch antennas by coupling the different resonance frequencies. Although, extensive literature can be found to improve impedance bandwidth using slot loading, but very few references are available for radiation pattern shaping using slot loading approach. Reactive slot loading can be employed to modify the higher mode current distribution and make it similar to dominant one. A dual band modified TM_{30} mode rectangular patch was proposed in [43] by placing two reactive slots along the radiating edges. As a result SLL are eliminated but at the expense of reduction in antenna directivity.

A modified TM_{12} mode patch with broadside pattern was presented in [44] by placing T-slots along the non-radiating edges. In [39], a non-resonant slot loading

TABLE 2.1: Comparison of single layer higher order mode patch antennas.

Ref.	Frequency (GHz)	Mode	Patch Shape	Height	Directivity (dB)	SLL (dB)
[29]	3.5	Fractino	Fractal	0.09λ	12.7	-4
[31]	3.3	Fractino	Fractal	0.093λ	14.15	-12.5
[36]	60	TM_{30}	RMPA	0.0254λ	10	-
[37]	10	TM_{12}	CMPA	0.042λ	10.55	-12.1
[39]	10	TM_{12}	CMPA	0.026λ	10.9	-20

is used to reduce the SLL of TM_{12} mode circular patch antenna. However, antenna has asymmetric radiation pattern and high cross polarization level.

A comparison of different single layer higher mode high gain patch antennas with broadside radiation pattern is shown in Table 2.1. Many observations can be made from Table 2.1 . First, both [29] and [31] use fractal gemetries operating in higher order mode. A fractal slot is used in [31] to increase the directivity and SLL suppression compared to orignal design presented in [29]. Second, patch antenna given in [36],[37] and [39] use Euclidian geometries. In [36], a differential-fed TM_{30} mode shorted patch with slot is used to achieve about 10 dBi gain. In [37], a stacked circular patch configuration operating in TM_{12} and TM_{11} modes is used to achieve high gain. As mentioned before, [39] use slot-loaded circular patch operating in TM_{12} for SLL reduction. It can be noted from Table 2.1 that higher mode patch antennas using Euclidean geometries have maximum directivity <11dBi. On the other hand, maximum directivity of patch antennas using fractal geometries is >14 dBi. Although, different techniques are available to reduce SLL in higher mode patch antenna with Euclidean geometries but no such technique is available for directivity enhancement and SLL reduction simultaneously.

2.1.1.2 Notch Loading Technique

One way to achieve patch antenna miniaturization is notching (cutting the slot or slit from) the patch radiator. Basic principle is to increase the path length of

surface current resulting in lowering of antenna resonant frequency. Different form of notch loading can be employed to achieve this goal. A C-shaped patch antenna with notch placed along one of non-radiating edge was proposed in [45, 46]. In [47–49] an H-shaped patch antennas were presented by cutting notches along both non-radiating edges. A variation of H-shaped patch antenna is a bowtie antenna in which triangular shaped notches are cut along the radiating edges [50]. Similarly, a rectangular ring microstrip antenna can be formed by cutting a notch in the center of patch antenna [47, 51]. In all these configurations, notch loading is used to reduce patch antenna size operating in fundamental TM_{10} mode. No significant work have been reported where notch loading is uses for gain enhancement and SLL reduction of higher order TM_{m0} modes.

2.2 Multiband Patch Antennas

Multiband planar antennas are essential for covering different wireless communication band using single antenna. In the past, different techniques have been used for achieving multiband planar antennas such as stacked patch configuration, using multiple broadside modes in patch, reactive loading in the form of slots, and metamaterial inspired antennas.

In stacked patch configuration, patches are placed vertically above each other. The top patch known as the driven patch is fed by a coaxial probe, whereas other patches beneath the driven patch are called the parasitic patches. The spacing between the patches and resonant length of each patch can be varied to control the frequency ratio. Dual band and multiband operation can be achieved using this arrangement depending on the number of patches. Dual band circular and annular ring patches are reported in [52, 53] using stack of two patches. Multiband patch antenna covering five bands using a stack of one driven and four parasitic rectangular patches is demonstrated in [54]. The drawbacks of stack patch configuration are fabrication difficulty and large volume. Another technique for achieving multiband operation is to use different patch modes having same polarization and

broadside radiation pattern. As an example, TM_{10} and TM_{30} mode of rectangular patch can be used to achieve dual band operation. However, frequency ratio is fixed in this case and is approximately equal to 3. Shorting pins can be placed on patch to lower the frequency ratio [55]. Alternately, reactive slots can be placed on the patch to decrease the frequency ratio [43]. Similarly, triband operation is possible using broadside TM_{10},TM_{20} and TM_{21} modes in triangular patch antenna [56]. However, frequency ratio is fixed in multi mode based multiband antennas which can cause difficulty for applications requiring exact frequency band.

Slot loading in the form of U slot can be used to achieve multiband behavior. A dual and triple band U slot patch antennas are presented in [57]. For dual band operation a single U slot is introduced whereas two U slots are required for tri band operation. A miniaturized multiband patch antenna using multiple inverted U slots and shorting pins is reported in [58]. Design of different multiband miniaturized patch antennas with dual band, triband and quadband operation are demonstrated.

2.2.1 Metamaterial Inspired Multiband Antennas

Left handed (LH) metamaterials exhibit both negative permittivity and permeability. One way to realize LH metamaterials is to use CRLH TL. CRLH TL based antenna can be designed to achieve miniaturization and multi band behavior. Zeroth order resonance (ZOR) mode which is independent of operating frequency is popular for antenna miniaturization application. Multifrequency operation is achieved by using negative order, zeroth order and positive order resonances. However, only fixed large frequency ratio is possible using this method [16]. In [59] single layer patch antenna partially filled with mushroom type CRLH structure was proposed to achieve non-integer frequency ratio. However, antenna has low efficiency at -1^{st} resonance. In [60] a patch antenna loaded with combination of mushroom type CRLH structure and reactive impedance surface was presented. It is shown that dual band dual linear polarization can be achieved by using two orthogonal -1^{st} modes. Moreover, single band circular polarization can be realized

TABLE 2.2: Comparison of different CRLH TL based dual band antennas.

Ref.	f_1/f_2 (GHz)	Gain (dBi)	Structure	Resonance Modes	Efficiency	Reconfig.
[59]	1.8/2.2	4.5/6.8	Single layer	$n = \mp 1$	60/83	No
[60]	2.4/2.9	2.25/3.11	Single layer	$n = -1$(x,y)	-	No
[61]	2.45/3.5	10.3/5.1	Multilayer	$n = \mp 1$	80/88	No

by exciting orthogonal -1^{st} modes with 90^0 phase shift. A multilayer CRLH TL based patch antenna is presented in [61] with improved efficiency but proposed structure is difficult to design and fabricate. It is worth mentioning that none of the aforementioned designs offers frequency reconfigurability. In this work single layer, dual band frequency reconfigurable CRLH TL based patch antennas with improved radiation efficiency will be explored.

2.3 Research Objectives

Recently, the need for low profile antennas with medium gain(about 10-16 dBi) is increasing. Higher order TM_{m0} (m = 3, 7,.....) mode rectangular patch antennas have broadside radiation patterns and higher gain than the fundamental TM_{10} mode. However, they suffer from high E-plane SLL and non-optimum gain. Very few work has been reported in this area and there is a need to develop new techniques for improving the radiation characteristics of TM_{m0} (m = 3, 7,.....) modes patch. In first part of research, main cause of high E-palne SLL and low directivity in rectangular patch antennas operating in higher order TM_{m0} mode will be explored. The objective is to design single layer higher order TM_{m0} mode rectangular patch antennas with improved gain and SLL performance. Two techniques namely slot loading and notch loading will be employed to achieve this objective. First, a slot loading approach will be used to improve the radiation characteristics of higher order mode rectangular patch antennas. Theoretical formulation of radiation characteristics of enhanced performance patch antennas will be explored.

In the past notch loading has been employed to reduce the size of patch antennas. No significant work have been reported to improve the gain enhancement and SLL reduction of higher mode patch antennas using notch loading. In this work, notch loading approach will be investigated to achieve gain enhancement and SLL reduction of higher order mode rectangular patch antennas.

Metamaterials, due to their unique properties enables new ways of antenna design. In particular, Composite Right Left Handed Transmission line (CRLH TL) based metamaterials are attractive due to their ease of fabrications. They can be used to achieve size reduction using zeroth order resonant (ZOR) mode. CRLH TL based antenna can also be used to achieve multiband operation but usually have fixed frequency ratio. Current techniques to address this issue using metamaterial loaded patches suffer from low efficiency or fabrication difficulty. Moreover, none of these technique offers frequency reconfigurability. In second part of research, different multiband patch antenna configurations consisting of patch and CRLH TL metamaterial will be investigated. The objective is to realize single layer multiband patch antennas having controllable frequency ratio and reconfigurability.

Chapter 3

Diffrential-Fed Slot-Loaded TM_{30} Mode Rectangular Patch Antenna

3.1 Introduction

High directivity planar antennas with low SLL are desired in various wireless communication applications. Although, higher order mode operation in patch antennas can be used to increase directivity due to increase in size but high E-plane SLL limits their use for most practical applications.

Recently, there is a renewed interest to improve the radiation characteristics of higher order mode patch antennas [36–39, 62]. A dual mode circular patch antenna was proposed in [38], wherein superposition of radiated field was used to achieve gain enhancement and SLL reduction by employing simultaneous excitation of TM_{11} and TM_{13} modes in a stacked configuration. However, due to multilayer nature, antenna has complex geometry which causes both design and fabrication difficulty. A differential fed shorted TM_{30} mode rectangular patch is presented in [36] which has no E-plane SLL but resulting antenna has low gain. Moreover, due to presence of via holes fabrication cost increases. In [37], E-plane SLL of TM_{12} mode circular patch antenna was reduced by employing a high dielectric constant

substrate. However, surface wave losses in high dielectric substrates can cause ripple in main beam and reduction in antenna efficiency.

As mentioned in Section 2.1.1, slot loading can also be used for SLL reducton in higher modes patch antennas. In this thesis, we propose a resonant slot loading technique and differential feeding to achieve high gain, low SLL single layer patch antenna with symmetric radiation pattern and low cross polarization. The method employs a linear 1×2 array of slots which perturbs the out of phase current distribution in TM_{30} mode patch to create additional in phase radiators. It is shown that by perturbing only out of phase higher mode current distribution while keeping in phase current distribution intact, both directivity enhancement and SLL reduction can be achieved simultaneously.

The slot loading technique presented here is different in the sense that it is used to improve the radiation characteristics of patch rather than impedance bandwidth enhancement. Moreover, in the proposed technique instead of removing the out of phase surface current distribution, it has been utilized to achieve performance enhancement of antenna. Different parameters that influence the performance of antenna are investigated. It is shown that by making the resonant frequency of patch and slots equal, good impedance matching and gain flatness can be achieved. It is worthwhile to mention that differential feeding is usually employed to suppress cross-polarization [63] or to achieve symmetric radiation pattern [36], whereas current work demonstrates that differential feeding can also be used to increase directivity. A peak directivity of 13.3 dB is achieved by means of proposed resonant slot loading and differential feeding technique with good SLL of -12.7 dB.

To the best of our knowledge, this is the highest reported peak directivity for TM_{30} mode patch antenna in single layer configuration using Teflon based substrate. In the past, fractal antennas operating in higher order fracton or fractino mode showed higher directivity [29] compared to their Euclidian counterpart. The proposed antenna demonstrates a practical realization of high directivity patch antenna employing simple Euclidian geometry and larger directivity compared to fractal antennas.

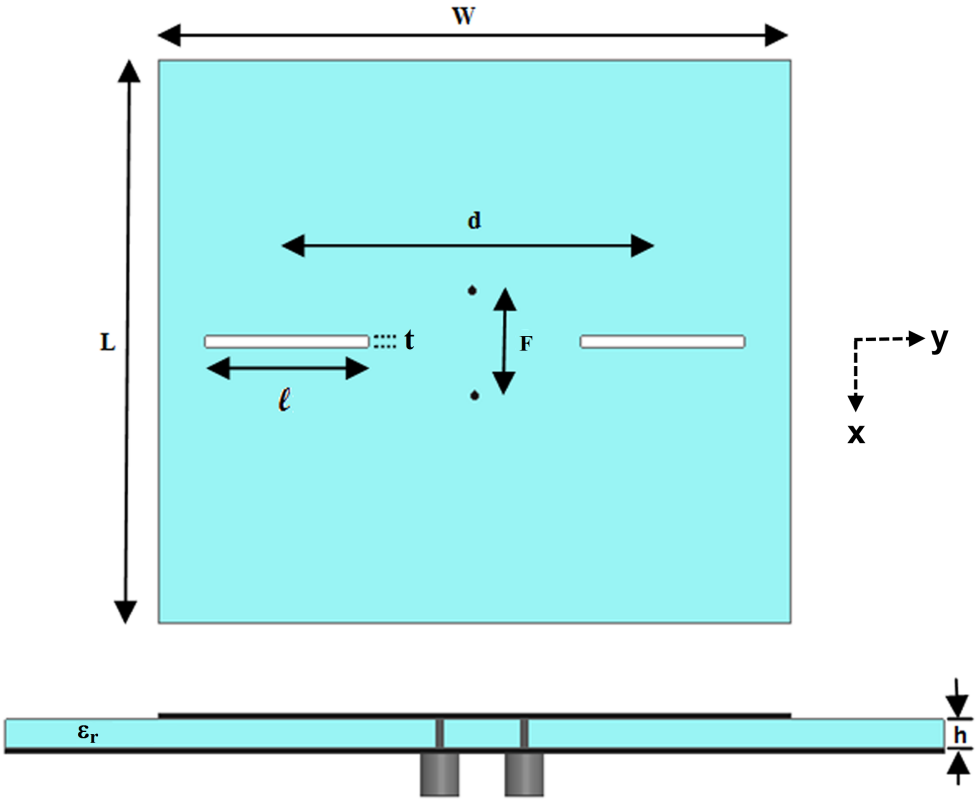

FIGURE 3.1: Geometry of the proposed antenna ($W = 10.1$, $L = 9$, $\ell = 2.6$, $d = 6$, $t = 0.18$, $F = 2$) all dimensions in cm.

3.2 Antenna Geometry and Radiation Mechanism

The proposed antenna geometry is shown in Fig. 3.2. The antenna is designed to operate at resonant frequency of 3 GHz. Arlon CuClad substrate having $\epsilon_r = 2.2$ and thickness $h = 1.524$ mm was used for antenna design. The rectangular patch has length L and width W. A pair of slots, each having length ℓ and width t is cut at the center of patch parallel to the radiating edges. The distance between the centers of slots is d. The antenna is fed using two differential probes symmetrically located around the center and a distance F apart.

The working of antenna can be explained by taking an analogy with slotted waveguide antenna. In a waveguide, radiating slot can be created by placing a resonant slot such that surface current lines are interrupted [64]. Simulated surface current distribution of conventional TM_{30} mode patch is shown in Fig. 3.1(a). It consists

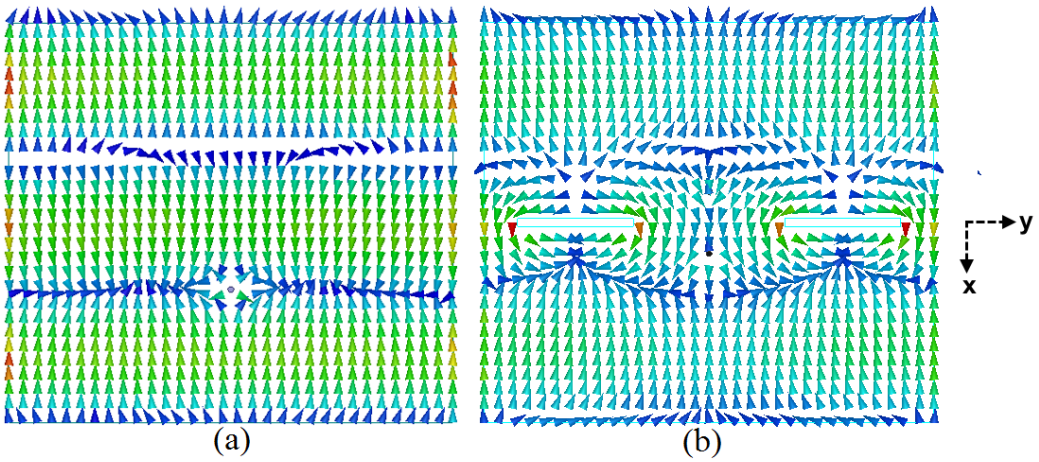

FIGURE 3.2: Simulated surface current distribution (a) Conventional TM_{30} mode patch, (b) Proposed antenna.

of two in phase regions located along the radiating edges and a center out of phase undesired region. By placing half wave length slots in the center region, slots can be excited in their fundamental mode as shown in Fig. 3.1(b). Use of differential feeding ensures the symmetric surface current distribution on the patch. The slots placed in the center portion of the patch interrupt the out of phase current distribution such that the induced slot field is in phase and polarization matched with the aperture field associated with the radiating edges of the TM_{30} mode patch. It is worthwhile to mention that a single higher order mode slot cannot be used in this case as in phase radiation condition would not be satisfied. An additional radiating edge is thus created in the form of two slots at the center of antenna. By combining the radiating field of higher order mode patch and fundamental mode of slots a simple single layer, low SLL and high directivity antenna is realized.

3.3 Theoretical E-plane Radiation Pattern

Theoretical radiation pattern of slot loaded patch antenna can be calculated by using superposition principle. The total far-field is given by the linear combination of patch and slot fields.

$$E_T = E_{\text{Patch}} + E_{\text{Slot}} \tag{3.1}$$

The equivalent aperture model of the antenna is shown in Fig. 3.3. Here slot 1 and 2 correspond to the effective radiating aperture of TM_{30} mode patch [65] with resonant length along x-axis and represent the patch field, while slot 3 and 4 are radiating aperture corresponding to the resonant slots of about half lambda located at the center of the patch and represent the slot field. The aperture E-field in center slots i.e., slots 3 and 4 is out of phase relative to radiating slots i.e., slot 1 and 2. Theoretical justification of why center slots aperture field distribution is out of phase with respect to radiating slots is given in [66]. It will be shown later that out of phase aperture field of center slots with respect to radiating slot field is necessary to make the radiated far-field in phase.

Assuming infinite ground plane, the E-plane (ϕ =0) radiated field of TM_{30} mode patch (slot 1 and slot 2) can be calculated [32] and is given as

$$E_{\theta}^{\text{Patch}} = C_1 \cos\left(\frac{3k_0 L}{2}\sin\theta\right) \tag{3.2}$$

where

$$C_1 = j\frac{k_0 E_a h W}{\pi}$$

$h =$ Substrate height

$E_a =$ Magnitude of slot aplerture elctric field

$$k_0 = \frac{2\pi}{\lambda}$$

The radiating field of slot (slot 3 and slot 4) due to two element y-directed slot array may be determined using pattern multiplication. For single resonant slot of about half lambda located at origin, electric field can be modeled as that of TE_{10} mode of rectangular waveguide [67] as shown in Fig. 3.3. The slot aperture field can be written as

$$E_x = E_a \cos\left(\frac{\pi y}{\ell}\right) \tag{3.3}$$

The radiated field of single slot can be calculated using equivalence principle and is given by

$$E_\theta = \frac{-jk_0E_a\ell t}{\pi^2}\frac{\cos\left(\frac{k_0\ell}{\pi}\sin\theta\sin\phi\right)}{1-\left(\frac{k_0\ell}{\pi}\sin\theta\sin\phi\right)^2}\frac{\sin\left(\frac{k_0t}{2}\sin\theta\cos\phi\right)}{\left(\frac{k_0t}{2}\sin\theta\cos\phi\right)}\cos\phi \tag{3.4}$$

Array factor due to two slots along y-axis a distance d apart is given by

$$\mathrm{AF}_{34} = 2\cos\left(\frac{k_0d}{2}\sin\theta\sin\phi\right) \tag{3.5}$$

Using pattern multiplication the radiated field of slot (slot 3 and slot 4) can be written as

$$E_\theta^{\mathrm{Slot}} = C_2\frac{\cos\left(\frac{k_0\ell}{\pi}\sin\theta\sin\phi\right)}{1-\left(\frac{k_0\ell}{\pi}\sin\theta\sin\phi\right)^2}\frac{\sin\left(\frac{k_0t}{2}\sin\theta\cos\phi\right)}{\left(\frac{k_0t}{2}\sin\theta\cos\phi\right)}\cos\phi\times\mathrm{AF}_{34} \tag{3.6}$$

where

$$C_2 = -j\frac{2k_0E_a\ell t}{\pi^2}$$

For t$\ll\lambda$ sinc function is approximately equal to 1 and we can write E-plane (ϕ=0) pattern as

$$E_\theta^{\mathrm{Slot}} = C_2 \tag{3.7}$$

Using Eq. (3.1) the radiated field of slot loaded patch becomes

$$E_\theta^T = C_1\cos\left(\frac{3k_0L}{2}\sin\theta\right) + C_2 \tag{3.8}$$

It is important to note that in (3.8) both terms are adding in phase because although slot far-field given by (3.7) has negative sign, recall that slot aperture field was also negative due to its out of phase nature with respect to radiating slot, making C_2 positive overall. In other words, by making the center slot field and radiating slot field of patch out of phase we make the radiated far-field in phase. Using the optimized slot-loaded patch antenna dimensions, given in Fig. 3.2, the far-field amplitude ratio was evaluated and is given by $\frac{C_2}{C_1} = 0.46$. Fig. 3.4 shows

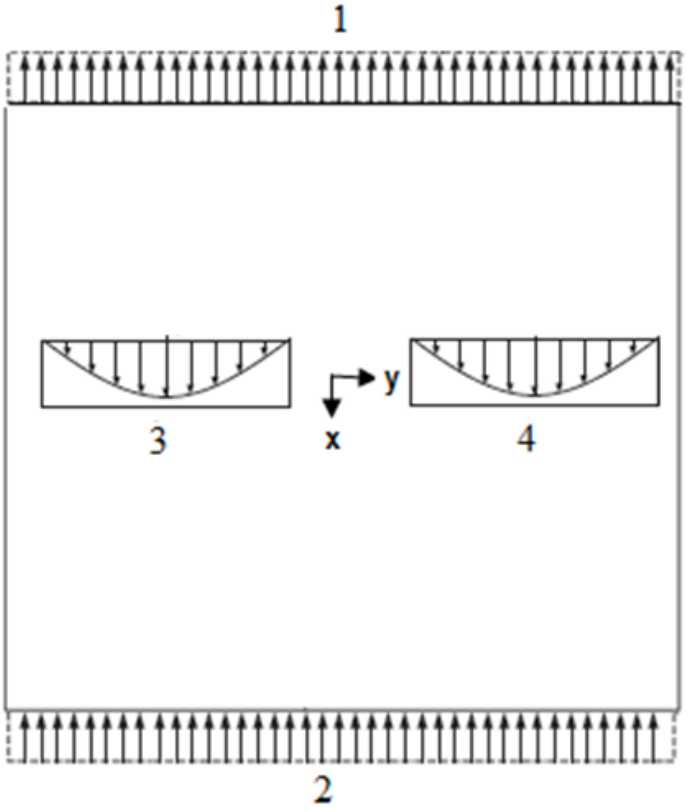

FIGURE 3.3: Equivalent aperture model of the proposed antenna.

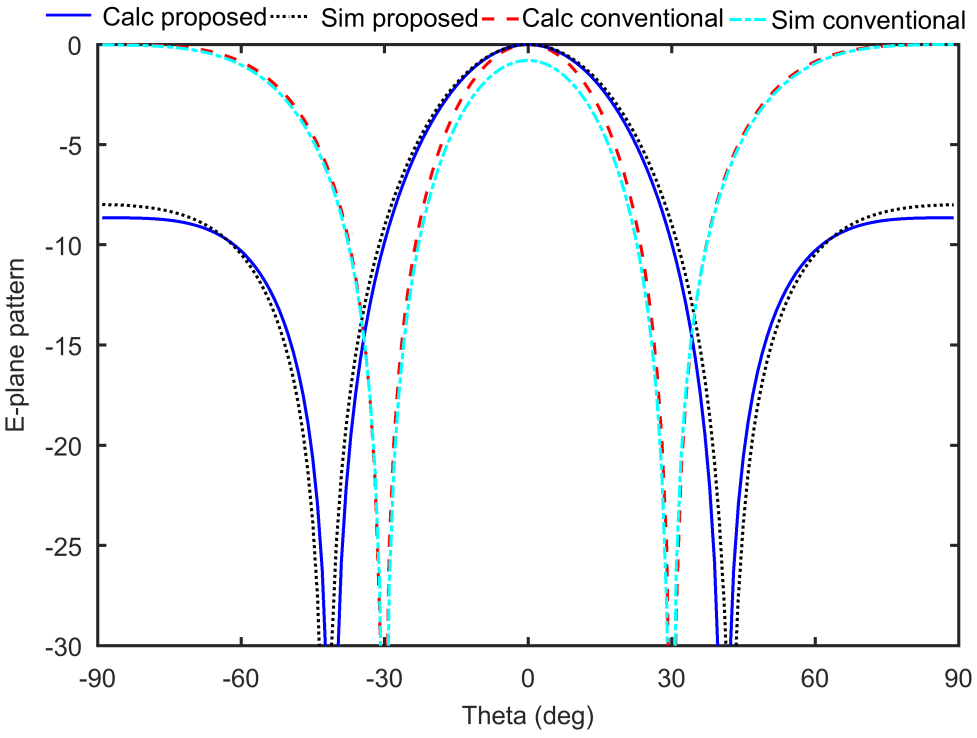

FIGURE 3.4: Simulated and calculated E-plane radiation patterns with infinite ground plane.

the theoretical and simulated E-plane radiation patterns of the proposed antenna. The simulation was performed in HFSS using infinite ground plane. Both simulated and calculated pattern are in good agreement thus validating the theoretical model. For reference theoretical E-plane radiation pattern of conventional (without slots) TM_{30} mode antenna is also shown in Fig. 3.4. The reduction in SLL compared to conventional TM_{30} mode patch antenna can be observed from the plot.

3.4 Parametric Study

The effect of various parameters on the performance of proposed slot loaded patch antenna has been investigated in this section. Commercial EM simulator Ansys HFSS was used for this parametric study. A finite ground plane 14cm x 15cm has been used, and all the simulations were performed in single fed configuration by changing only one parameter at a time while keeping all other parameters constant. The initial parameters of the antenna were $L = 9$ cm, $W = 10$ cm, $\ell = 2.9$ cm, $t = 0.21$ cm, $d = 6$ cm, and $F = 2$ cm (defined from patch center for single fed configuration). It is important to point that single-fed configuration suffers from pattern asymmetry due to asymmetric surface current distribution (see Fig. 5.7). A differential feeding can be used to circumvent this issue which will be discussed later on.

Simulated S_{11} and directivity plots of the proposed antenna are shown in Figs. 3.5(a, b). Two resonance peaks can be observed in the simulated S_{11} curve which correspond to resonance frequency of the patch and slot respectively (see Section 3.4.2). Moreover, it can be seen from the directivity plot that although antenna exhibit peak directivity of 12.97 dB at first resonance frequency of 2.915 GHz but directivity flatness is poor as directivity falls very sharply with frequency, reaching a value of -3 dB at 3 GHz. In addition, impedance matching is also poor at the first resonance peak where directivity is high. Impedance matching cannot be improved by just changing the feed point location. It is shown in Section 3.4.5

that by bringing these two resonance peaks together first and then changing the feed point location good impedance matching can be achieved.

3.4.1 Effect of Patch Width, W

It can be seen from Fig. 3.5(a) that with increase in W upper resonance peak moves downward while lower resonance peak moves upward. For $W = 10.5$ cm, both peaks merge together at $f = 2.935$ GHz with slightly better impedance matching. Moreover, Fig. 3.5(b) shows that with increase in W directivity flatness improves significantly. For $W = 10.5$ cm, good directivity flatness is achieved but at the expense of reduction in peak directivity.

3.4.2 Effect of Slot Length, ℓ

The slot length ℓ mainly influences the lower resonance peak of the S_{11} curve which corresponds to resonance frequency of slot. It is evident from Fig. 3.6(a) that lower resonance peak moves upward as ℓ decreases. The upper resonance frequency (patch resonance) is not influenced by changing slot length. For $\ell = 2.6$ cm, both peaks merge together at $f = 3$ GHz. By combining the two resonance peak together directivity flatness improves greatly as shown in Fig. 3.6(b). For $\ell = 2.6$ cm, good directivity flatnessis achieved but at the expense of reduction in peak directivity. Thus, resonant slot is more desired as it improves directivity flatness of antenna.

3.4.3 Effect of Patch Length, L

Effect of patch length L on S_{11} is shown in Fig. 3.7(a). By increasing length L both resonance peaks move downward. This makes sense as L corresponds to resonant length of the patch antenna and increase in resonant length should result in decrease in resonance frequency. A similar effect can be observed in directivity curve shown in Fig. 3.7(b) which also shifts downward with increase in L.

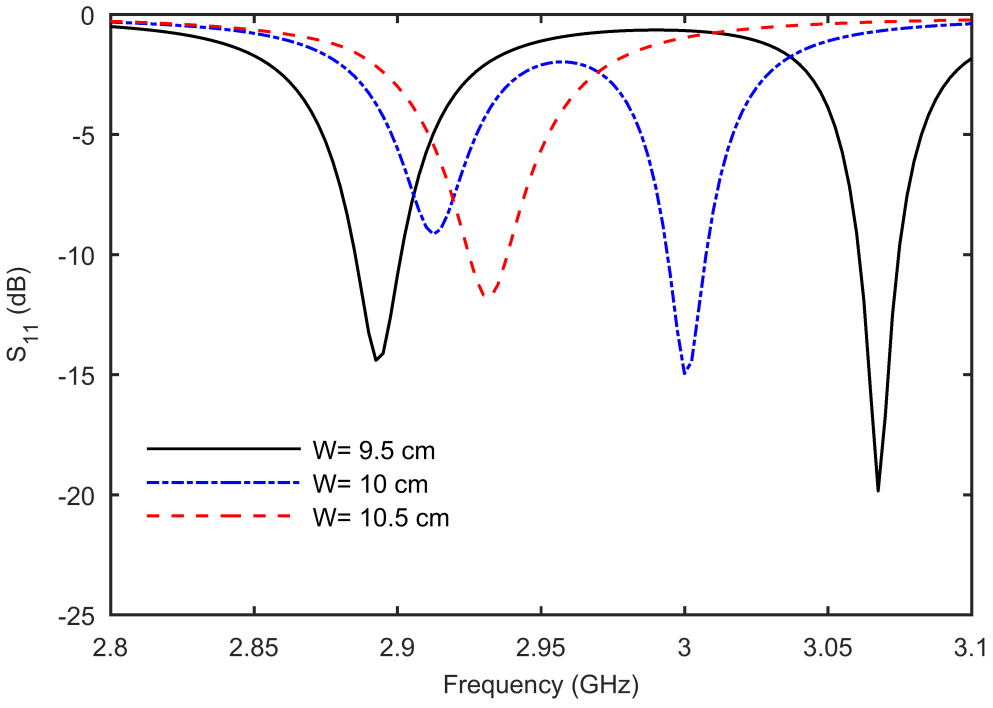

(a)

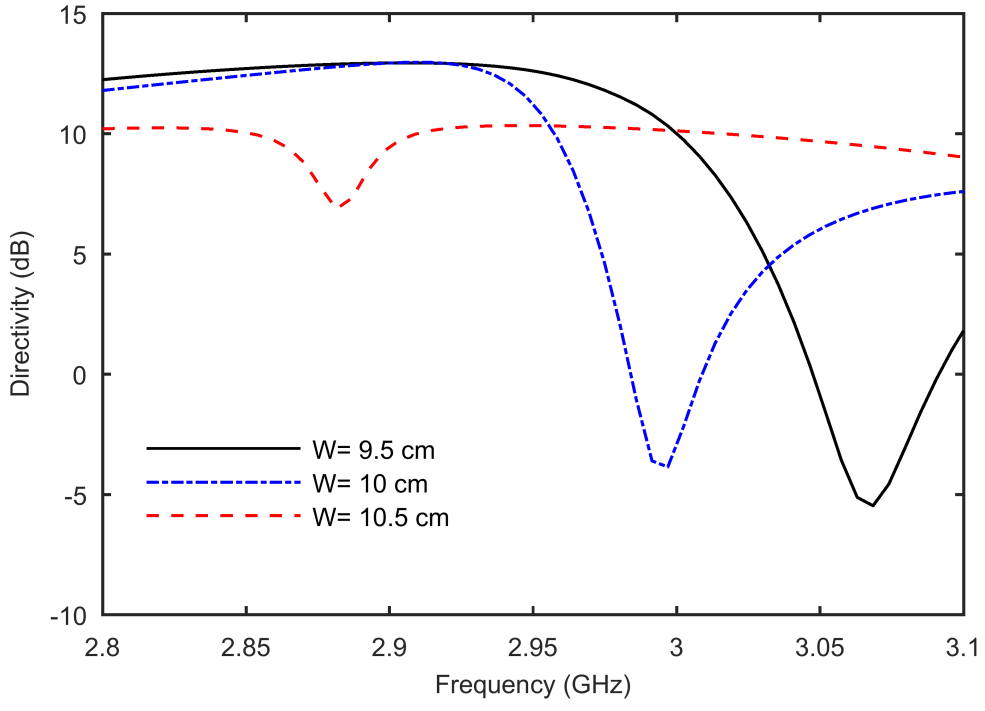

(b)

FIGURE 3.5: Effect of patch width W on the proposed slot loaded patch antenna (a) S_{11} and, (b) directivity.

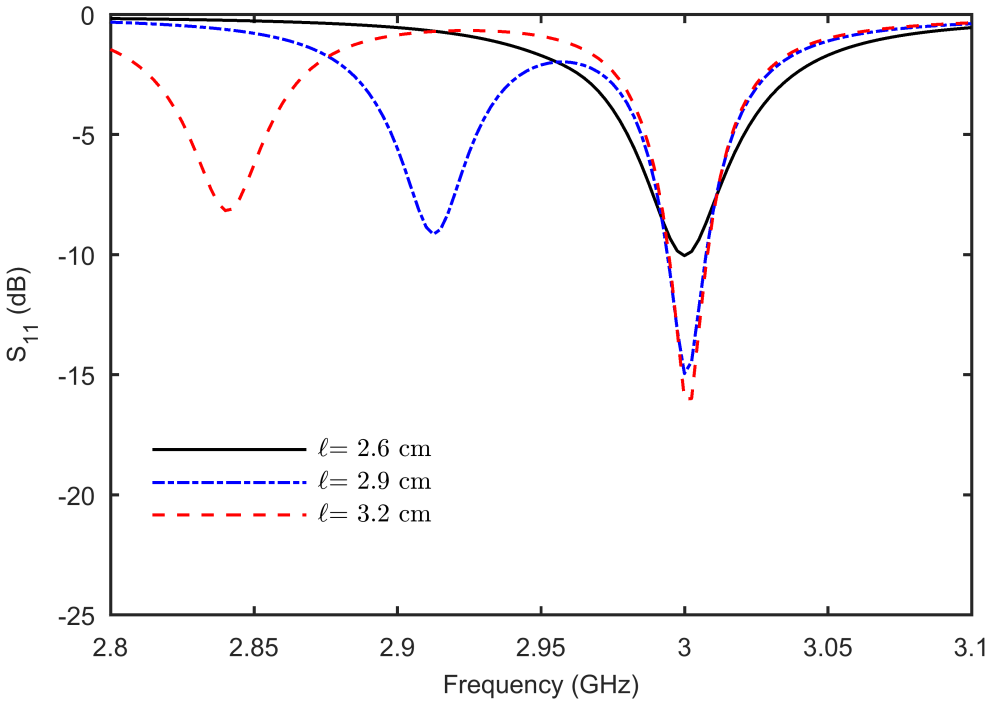

(a)

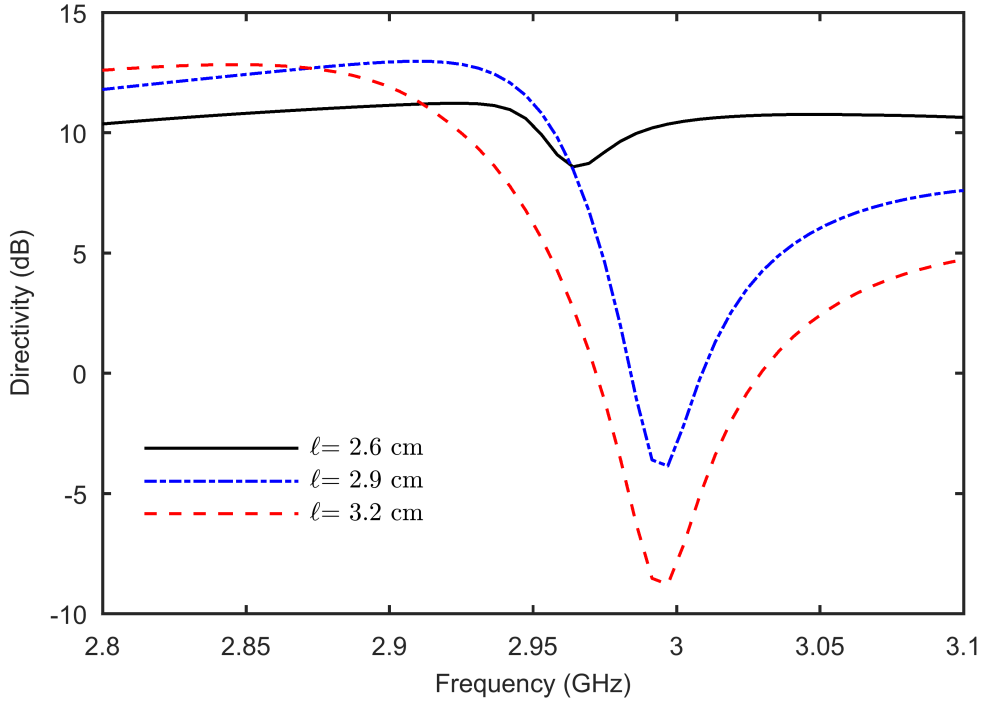

(b)

FIGURE 3.6: Effect of slot length ℓ on the proposed slot loaded patch antenna (a) S_{11} and, (b) directivity.

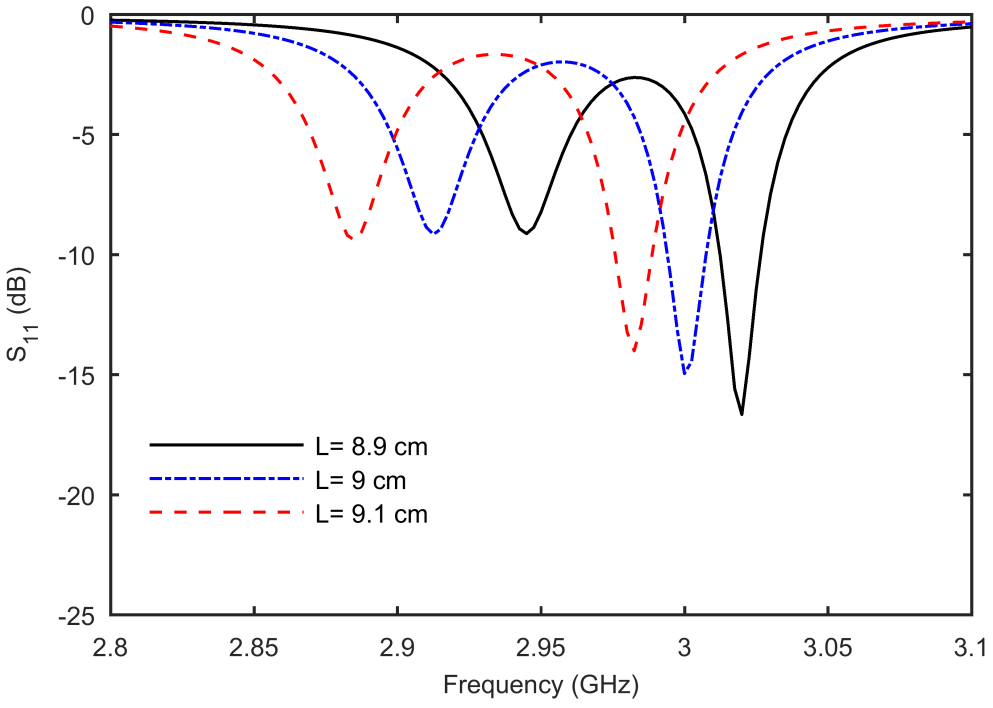

(a)

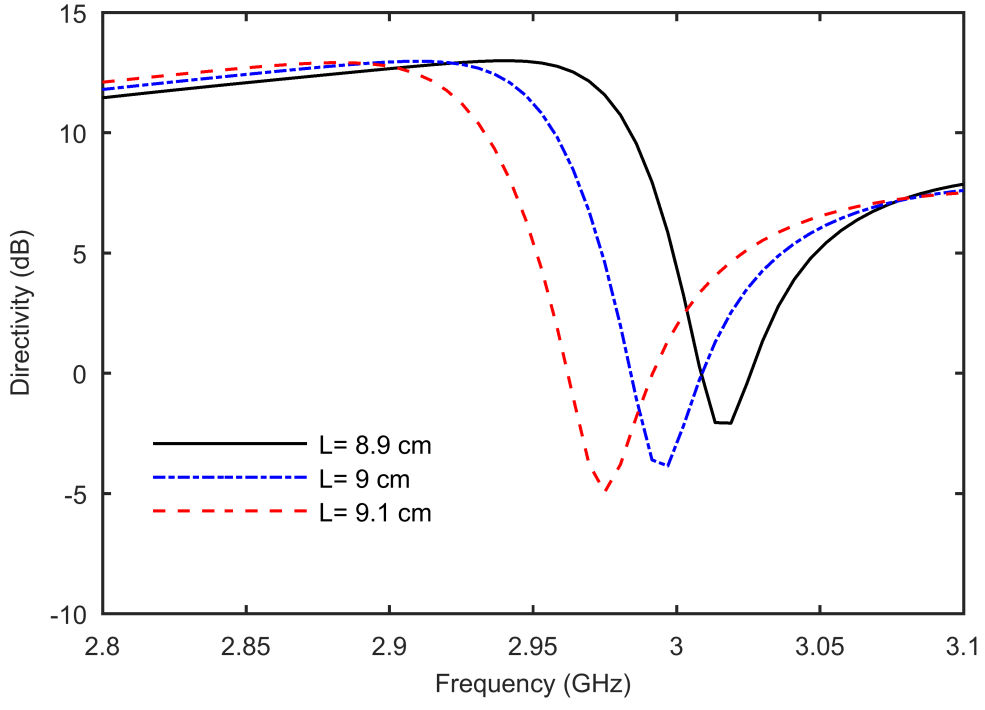

(b)

FIGURE 3.7: Effect of patch length L on the proposed slot loaded patch antenna (a) S_{11} and, (b) directivity.

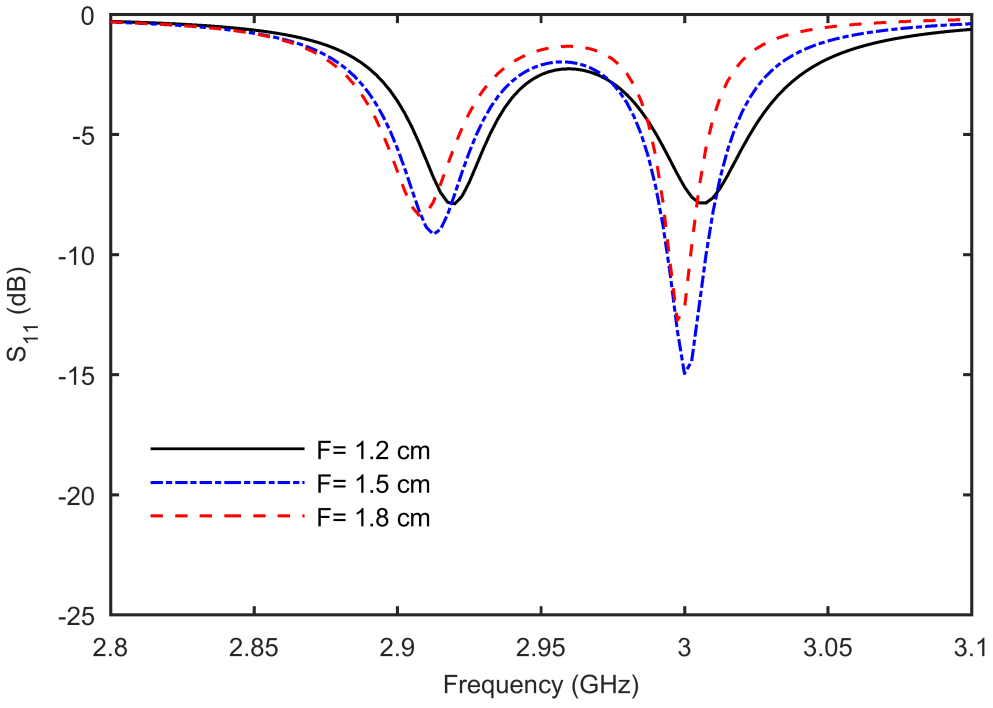

(a)

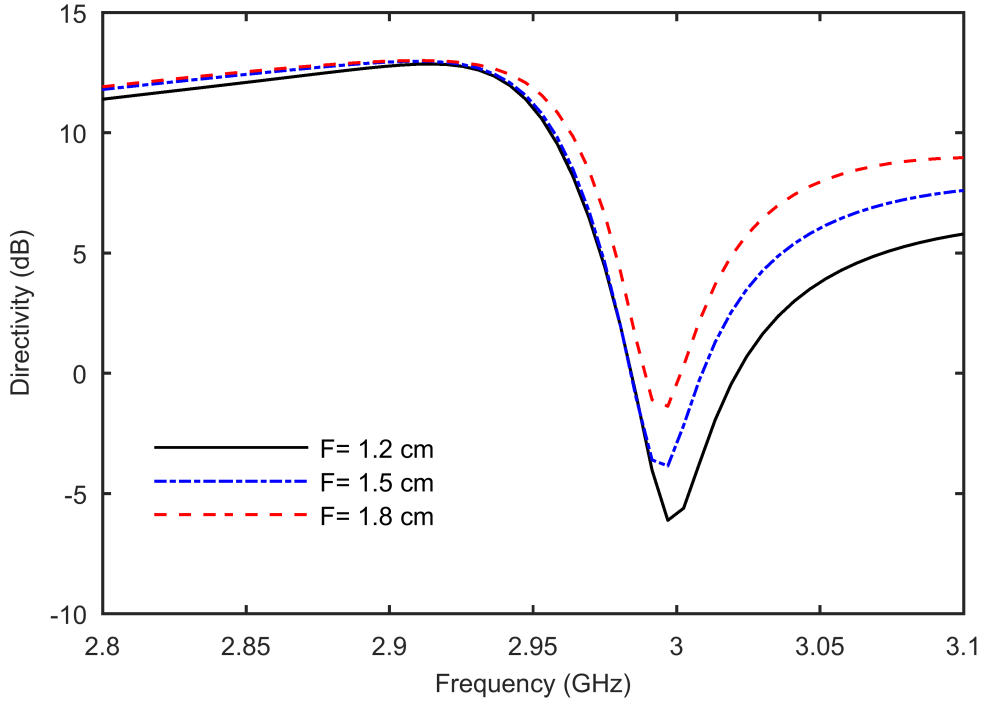

(b)

FIGURE 3.8: Effect of feed point position F (non-resonant slots, $\ell = 2.9$ cm) on the proposed slot loaded patch antenna (a) S_{11} and, (b) directivity.

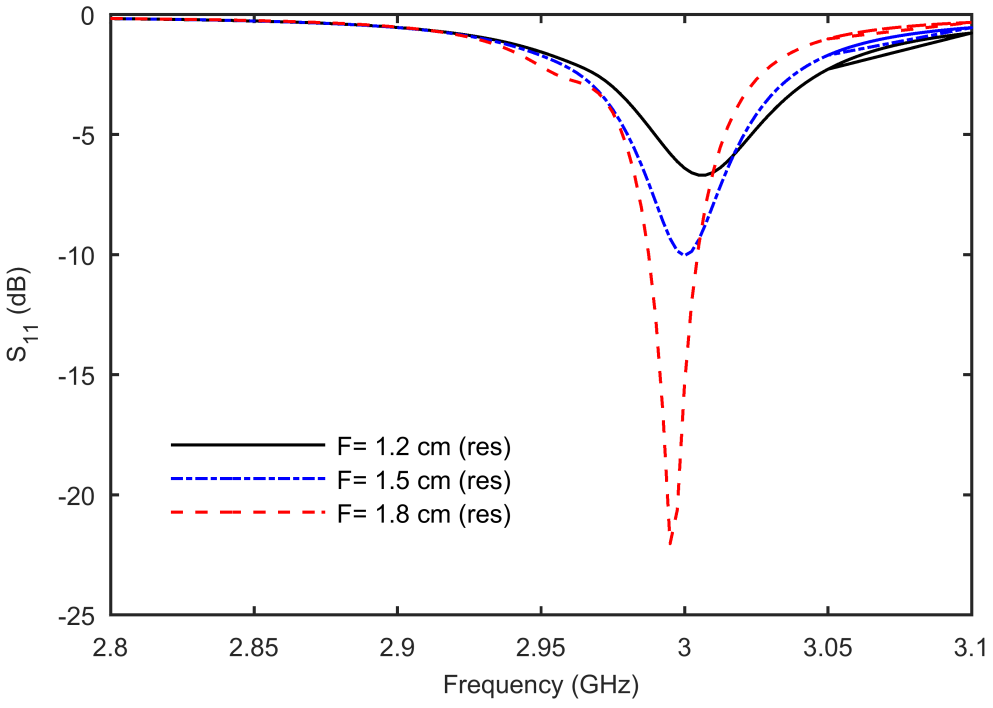

(a)

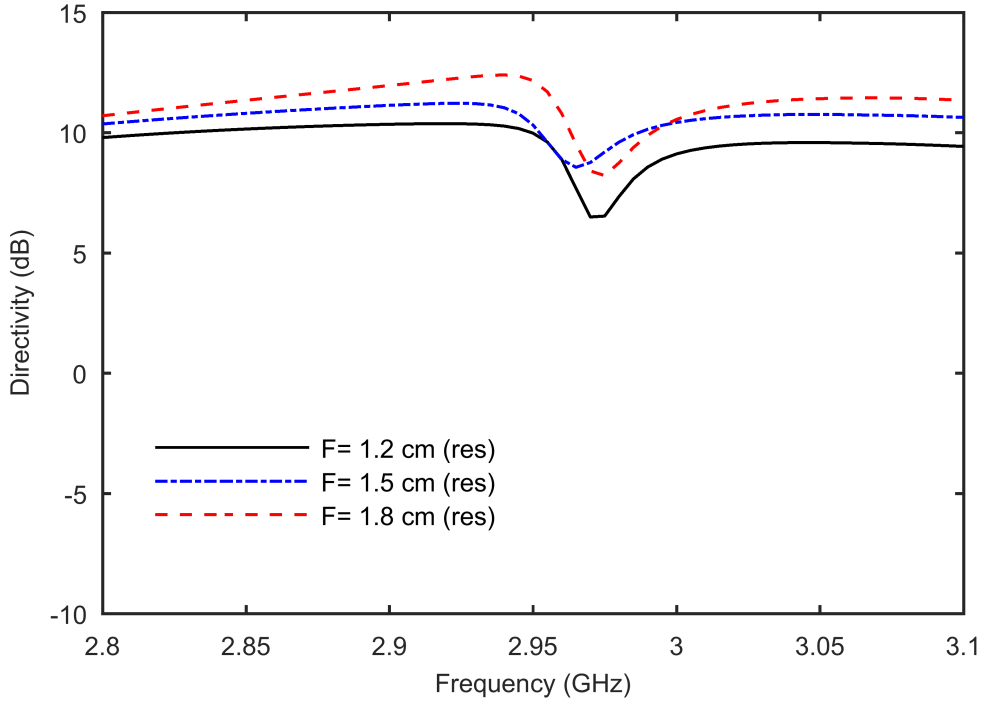

(b)

FIGURE 3.9: Effect of feed point position F (resonant slots, ℓ =2.6 cm) on the proposed slot loaded patch antenna (a) S_{11} and, (b) directivity.

3.4.4 Effect of Slot Width, t and Slot Spacing, d

No significant change in S_{11} and directivity was observed for small variation of slot width t and inter slot spacing d from the nominal values. However, their behavior is similar to that of slot length ℓ and lower resonance peak moves slightly upward as t or d decreases. Moreover, no significant change in directivity flatness was observed for both parameters due to slight change in resonance frequency. Nevertheless, directivity flatness improves slightly with decrease in either slot width t or inter slot spacing d.

3.4.5 Effect of Feed Point Location, F

The effect of feed point location$F$ on the S_{11} is shown in Fig. 3.8(a) and Fig. 3.9(a). As mentioned previously, the feed point location is defined from patch center for single fed configuration. Two cases are considered, namely resonant slot loading and non resonant slot loading. For resonant slots, slot length $\ell = 2.6$ cm whereas for non resonant slots, slot length $\ell = 2.9$ cm (same as the nominal value). It can be observed from Fig. 3.8(a) that S_{11} curve has two resonance peaks for non resonant slots. By varying the feed location F from the nominal value $F = 1.5$ cm, S_{11} at both peaks degrades. Thus no improvement in S_{11} can be achieved by changing the feed point location for non resonant slots. In contrary, for resonant slots varying the feed point location significantly improves the S_{11} and it can be observed from Fig. 3.9(a) that by changing the feed point F from 1.5 cm to 1.8 cm, the value of S_{11} decreases from –10 dB to –22 dB. Thus feed point location F improves the impedance matching only for resonant slots.

The effect of feed point location F on the directivity is shown in Fig. 3.8(b) and Fig. 3.9(b). In general, directivity flatness for resonant slots is much better compared to non resonant slots. Moreover, it can be observed that directivity flatness is also affected by change in feed location for both cases. This is due to modification of surface current distribution of patch with change in feed point location. The change in surface current also affects the pattern symmetry and

cross polarization levels. Thus if a single fed antenna is desired, feed position can be changed to achieve good matching but at the expense of asymmetric radiation pattern and directivity flatness. A differential feeding scheme can be employed to overcome these issues. It is shown in Section 3.5 that differential feeding scheme can be used to achieve symmetric radiation pattern, better directivity flatness and higher directivity compared to single fed design.

Based on the parametric study a slot loaded differential fed patch antenna was optimized. The optimized antenna dimensions are shown in Fig. 3.2.

3.5 Comparison of Conventional and Proposed Antenna

In this section, comparison of the proposed differential fed slot loaded patch antenna has been carried out with conventional (without slot) higher order TM_{30} mode patch antenna. Commercial EM simulator Ansys HFSS was used for all the simulations. Figure 3.10 shows the simulated E-plane radiation patterns for the proposed differential fed antenna along with single fed antenna and conventional TM_{30} mode patch antenna.

Significant reduction of SLL compared to conventional TM_{30} mode patch can be observed. The simulated E-plane SLL for TM_{30} mode patch antenna are –2.4 dB while the proposed differential fed slot loaded patch antenna shows SLL of –12.7 dB. Thus, the proposed slot loaded antenna can achieve SLL improvement of more than 10 dB compared to conventional antenna (TM_{30} mode patch without slot). Moreover, compared to single fed design, the differential fed antenna has symmetric radiation pattern. Moreover, the proposed antenna can be directly integrated with differential circuits.

As shown in Table 3.1, directivity of the proposed differential fed slot loaded patch antenna is 13.3 dB compared to 10.9 dB for conventional TM_{30} mode patch antenna. An improvement of 2.4 dB in directivity is thus achieved while the size

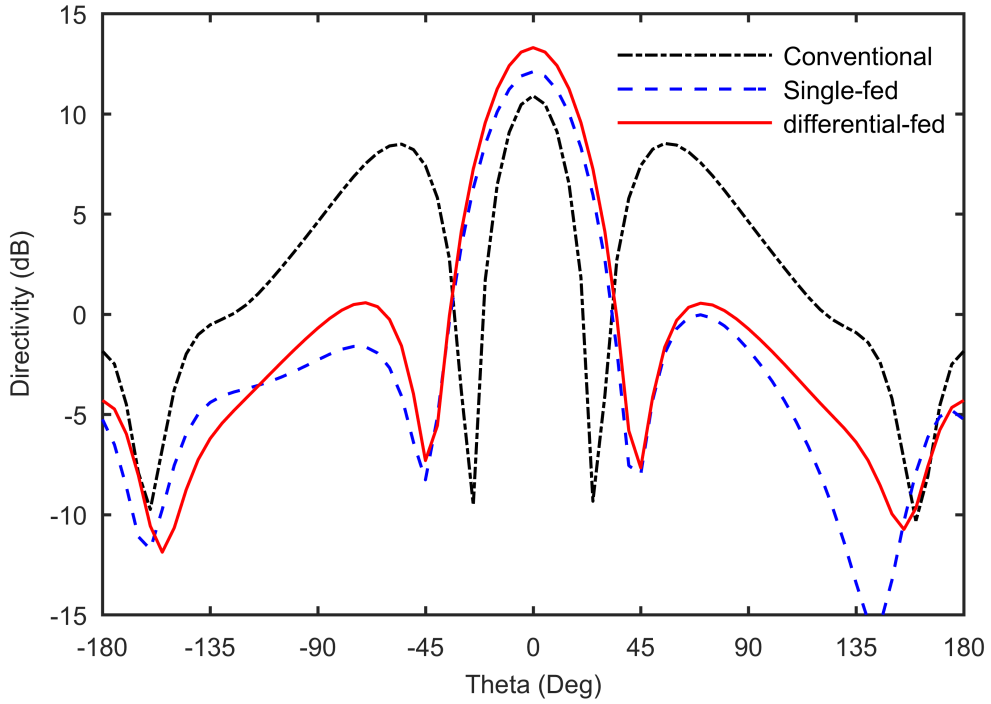

FIGURE 3.10: Comparison of simulated E-plane radiation patterns.

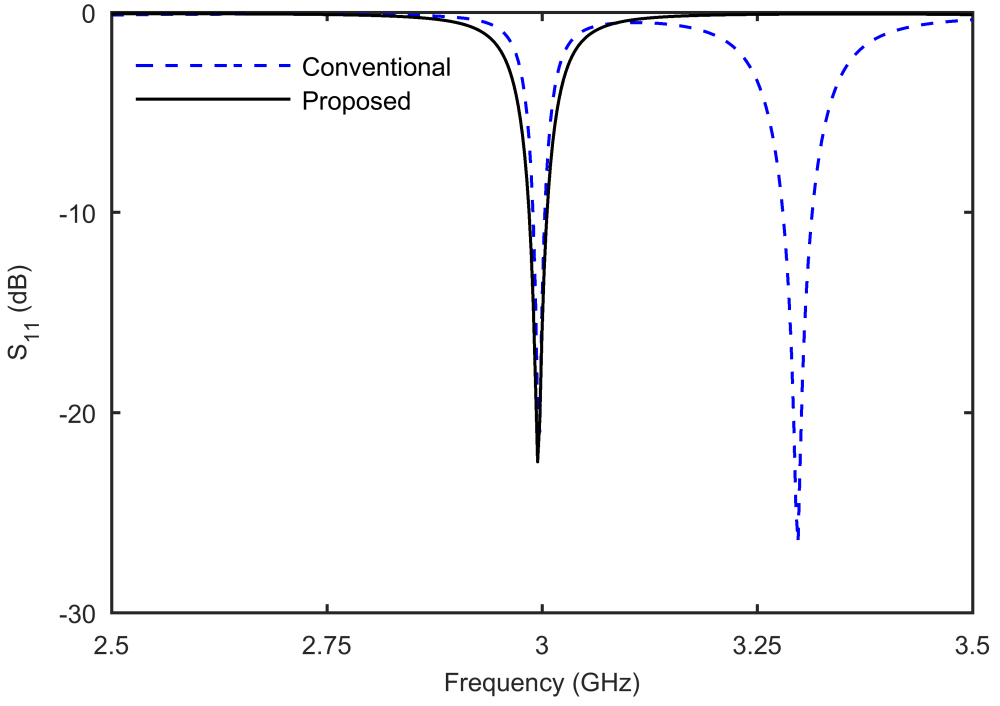

FIGURE 3.11: Simulated S_{11} of the proposed and conventional antenna.

TABLE 3.1: Comparision of the proposed, single fed and conventional patch antennas.

Antenna Type	SLL (E-plane)	3 dB Beamwidth	Directivity	Impedance Bandwidth
Conventional	-2.4 dB	25^0	10.9 dB	35 MHz
Single fed	-13.7 dB (L) -12.0 dB (R)	36^0	12.1 dB	20 MHz
Proposed	-12.7 dB	36^0	13.3 dB	21 MHz

remains the same. Moreover, compared to single fed scheme 1.2 dB enhancement of directivity is achieved using differential feeding because it ensures desired in-phase surface current distribution intact as shown in Fig. 3.1(b). It can be seen from Table 3.1 that the proposed antenna exhibits larger 3 dB beamwidth of 36^0 compared to conventional TM_{30} mode patch which has 3 dB beamwidth of 25^0. The beam broadening can be attributed to reduction in SLL.

The S_{11} plot of the proposed and conventional TM_{30} mode is shown in Fig. 3.11. Conventional TM_{30} mode patch antenna has a resonance frequency of 3.3 GHz as indicated by the dash line in Fig. 3.11. In addition, the second resonance frequency at 3 GHz can also be seen in the graph which corresponds to endfire TM_{22} mode. The resonance frequency of the proposed slot loaded patch antenna is at 3 GHz indicated by the solid line in Fig. 3.11. Thus, in comparison with TM_{30} mode patch having no slot loading, resonance frequency is shifted downward from 3.3 GHz to 3 GHz.

This can be attributed to the increase in current path length due to presence of slot. Moreover, as given in Table 3.1, slot loaded patch antenna shows reduction in impedance bandwidth compared to conventional antenna. The $S_{11} \leq -10$ dB impedance bandwidth of the proposed antenna is 21 MHz [2989.5 - 3010.5 MHz] compared to conventional TM_{30} mode patch which has an impedance bandwidth of 35 MHz [3282.5 - 3317.5 MHz]. The relative bandwidths of conventional (without slot) and proposed slot loaded patch are 1.06% and 0.7% respectively. Thus, the

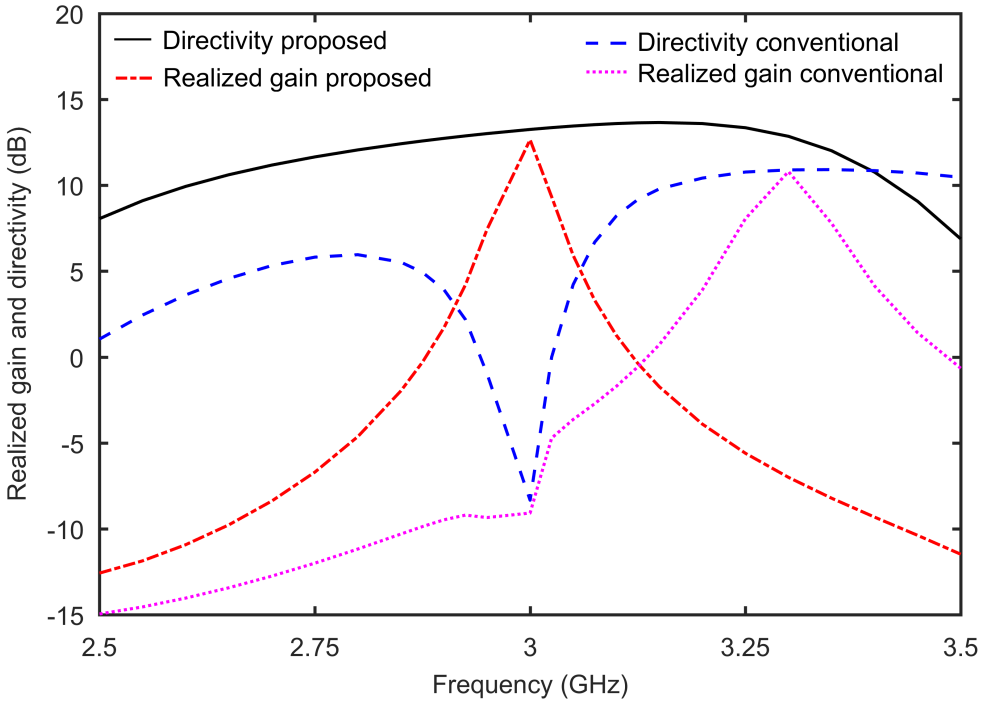

FIGURE 3.12: Simulated directivity and realized gain of the proposed and conventional antenna.

reduced impedance bandwidth is a drawback of the proposed solution. This reduction in impedance bandwidth can be attributed to increase in antenna directivity owing to fundamental gain bandwidth product.

The proposed antenna has narrow impedance bandwidth of 0.7% which might not be adequate for some parctical applications. However, the narrow impedance bandwidth of the proposed antenna can be increased by using different bandwidth enahancement techniques given in literature such as increase in substrate thickness, proximity coupling or stacked patch configuration. Thus narrow bandwidth of the proposed antenna is not a limitation and can be improved using the aforementioned techniques to meet the actual practical application requirement.

Figure 3.12 shows the directivity plot of the proposed and conventional antenna as a function of frequency. It is evident from Fig. 3.12 that the proposed slot loaded antenna has an improved directivity performance. Maximum directivity of the proposed slot loaded antenna is 13.6 dB at 3.15 GHz compared to conventional TM_{30} mode antenna which has maximum directivity of 10.9 dB. Moreover,

differential fed slot loaded antenna has better directivity flatness compared to conventional antenna. In fact, for conventional antenna, directivity decreases sharply and reaches a value of –8 dB at 3 GHz. This is due to presence of endfire TM_{22} mode at 3 GHz as shown in Fig. 3.11. TM_{22} mode is not supported in the proposed differential fed slot loaded antenna as a result it exhibits larger gain bandwidth than the conventional TM_{30} mode patch. Thus in contrary to conventional TM_{30} mode patch antenna, impedance bandwidth enhancement techniques can be utilized with only slight reduction in antenna directivity.

3.6 Simulated and Measured Results

In order to validate the performance of the proposed slot loaded patch antenna, a prototype was fabricated. Photograph of the fabricated antenna is shown in Fig. 3.13. The antenna was differentially fed by using 180^0 Wilkinson divider shown in Fig. 3.14. A meander line was utilized in one of the output ports to achieve the desired 180^0 phase shift. Agilent PNA Network Analyzer was used to measure the reflection coefficient. The simulated and measured S_{11} of the proposed antenna are shown in Fig. 3.15. The measured $S_{11} \leq$ –10 dB impedance bandwidth is 19 MHz compared to simulated S_{11} which was 21 MHz. The measured center frequency is 3.003 GHz whereas the simulated center frequency is 2.995 GHz. The slight shift in resonance frequency can be attributed to variation in substrate removal in the milling process used for fabricating the antenna. In addition, substrate parameters like permittivity and thickness can also vary from the nominal value due to fabrication tolerances. Figures 3.16 and 3.17 show the simulated and measured normalized co-polarization and cross-polarization E and H-planes radiation patterns of the proposed antenna. A compact antenna test range (CATR) was used to measure the far-field radiation patterns of the antenna. The measured antenna gain is 12.8 dBi at 3 GHz. The measured SLL of the antenna is –12 dB and –21.5 dB in E and H-planes, respectively. Moreover, the proposed antenna shows a measured cross-polarization level of less than 28.5 dB below co-polarization pattern in both E and H-planes.

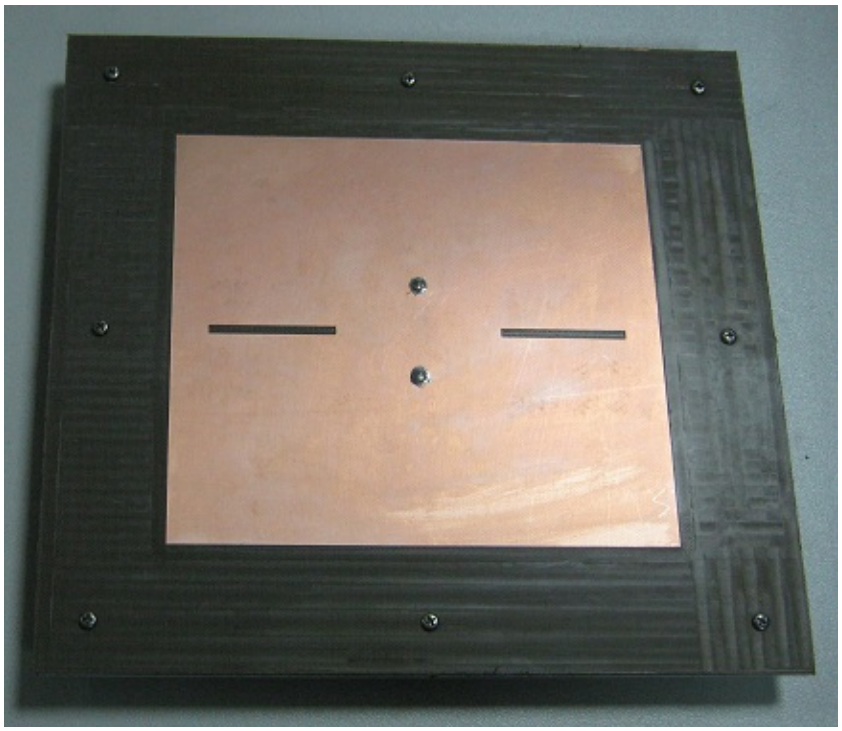

FIGURE 3.13: Prototype of the fabricated differential fed slot loaded TM_{30} mode patch antenna.

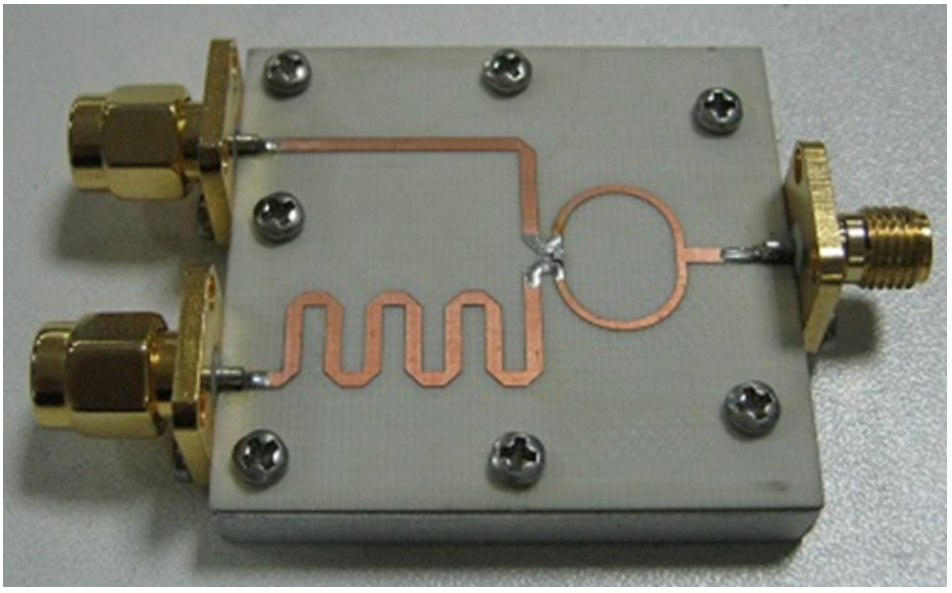

FIGURE 3.14: Fabricated 180^0 Wilkinson divider used for differential feeding.

Table 3.2 shows a comparison of different high gain single layer patch antennas found in literature. The proposed antenna demonstrates a high directivity of 13.3 dB using simple Euclidian geometry, previously achieved using Fractal geometries [29]. To the best of our knowledge this is the highest reported peak directivity for TM_{30} mode patch antenna in single layer configuration.

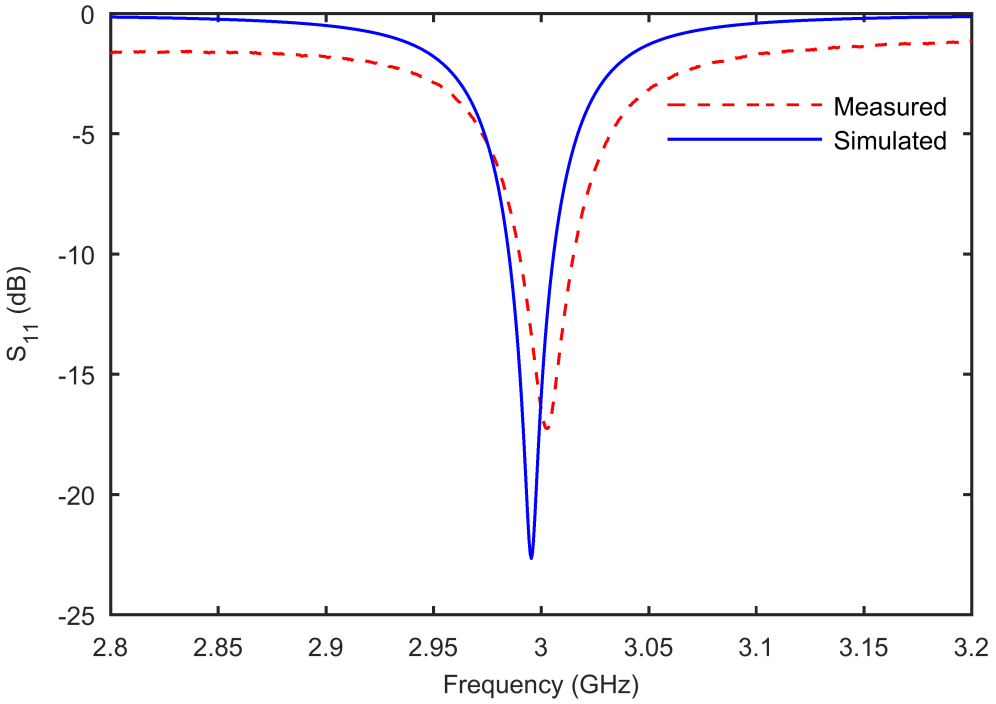

FIGURE 3.15: Simulated and measured S_{11} of the proposed differential fed slot loaded patch antenna.

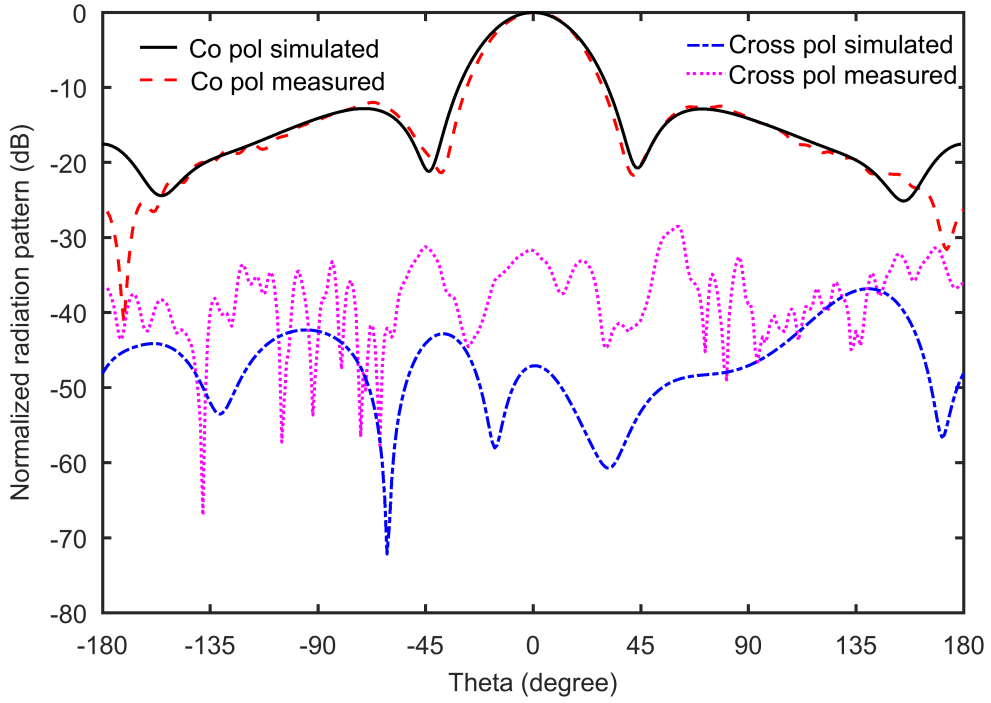

FIGURE 3.16: Simulated and measured E-plane radiation patterns of the proposed differential fed patch antenna.

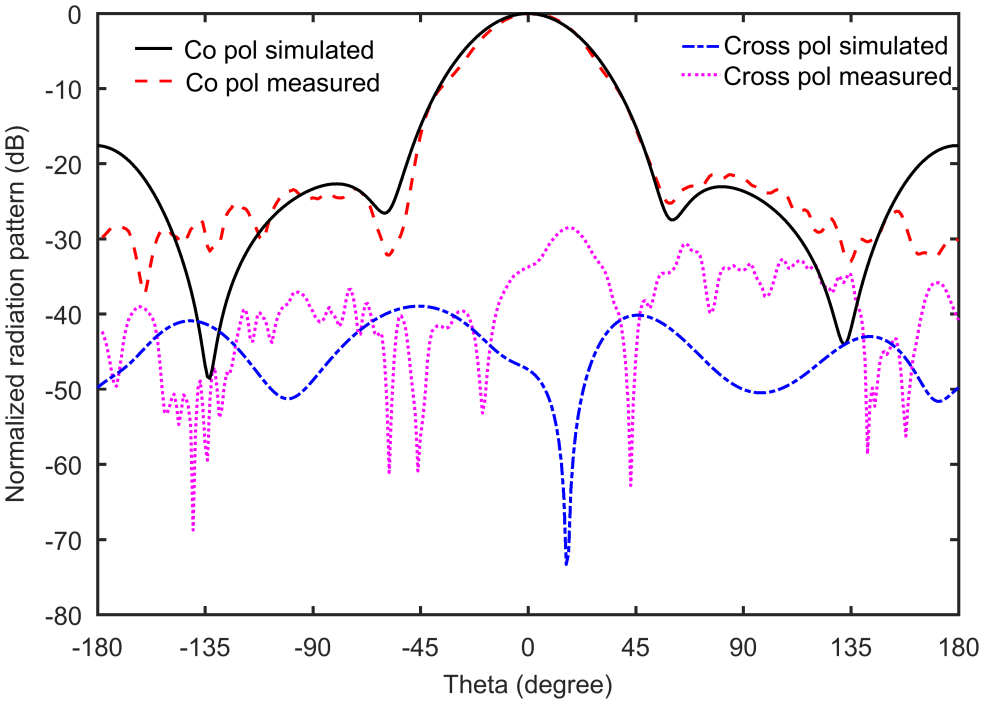

FIGURE 3.17: Simulated and measured H-plane radiation patterns of the proposed differential fed patch antenna.

TABLE 3.2: Comparison of single layer higher order mode patch antennas.

Ref.	Frequency (GHz)	Height	% BW	Directivity (dB)	SLL (dB)	Dimensions
[29]	3.5	$0.09\lambda_0$	12	12.7	-4	$1.38\lambda_0$
[36]	60	$0.025\lambda_0$	18	10	-	$2.26\lambda_0 \times 0.4\lambda_0$
[37]	10	$0.042\lambda_0$	0.7	10.55	-12.1	$0.34\lambda_0$
[39]	10	$0.026\lambda_0$	1.56	10.9	-20	$0.46\lambda_0$
Proposed	3	$0.015\lambda_0$	0.7	13.3	-12.7	$0.9\lambda_0 \times 1\lambda_0$

3.7 Summary

High E-plane SLL and low directivity problem of higher order TM_{30} mode patch antenna is resolved by employing resonant slot loading technique and differential feeding. Inspired by slotted waveguide antennas, a pair of resonant slots is placed in the center out of phase region of TM_{30} mode rectangular patch antenna which

acts as a new radiating edge. The basic idea of this scheme is to achieve superposition of radiated fields in single layer configuration. This is achieved practically by placing in phase slot radiators, operating in fundamental mode, in the out of phase current distribution region of TM_{30} mode patch antenna. Superposition of radiated fields of TM_{30} mode patch and fundamental mode of slots results in high directivity radiator with reduced SLL. It is shown that by making the resonant frequencies of patch and slots equal, good impedance matching and gain flatness can be achieved. The placement of resonant slots also has a slight adverse affect on the in phase current distribution resulting in asymmetric radiation pattern. It is demonstrated that a differential feeding scheme can be employed to achieve gain enhancement and symmetric radiation pattern by keeping the desired in phase current distribution intact. The proposed differential fed slot loaded patch antenna has symmetric radiation pattern with reduced cross polarization levels.

A novel low profile, single layer high gain patch antenna having dimensions of $0.9\lambda_0 \times 1\lambda_0 \times 0.015\lambda_0$ is demonstrated. It shows a measured gain of 12.8 dBi, SLL of –12 dB and $S_{11} \leq$ –10 dB impedance bandwidth of 21 MHz [2989.5 - 3010.5 MHz]. The proposed differential fed slot loaded higher order mode patch antenna exhibits a 2.4 dB increase in directivity and a reduction of about 10 dB in SLL compared to conventional TM_{30} mode patch antenna. The proposed antenna can be used as a substitute for 2×2 array of patch antennas (having outer dimensions 9 cm × 10.1 cm) operating in the fundamental mode and is suitable for integration with differential circuits. Moreover, the proposed technique can be utilized to improve the radiation characteristics of higher order mode rectangular patch antennas operating in TM_{m0} (m = 3,5,..) mode.

Chapter 4

Notch-Loaded TM_{30} and TM_{70} Modes Rectangular Patch

4.1 Introduction

In this chapter, a partial notch-loading technique for gain enhancement and SLL suppression of TM_{m0} mode (with odd m) rectangular patch antennas is presented. As mentioned previously, different methods can be used to overcome the low gain issue in patch antennas such as array design, stacked patch configuration, superstrate loading, shunt inductive loading and higher order mode operation.

Array design [8, 68] is the most common technique for gain enhancement in patch antenna operating in fundamental mode. However, it requires feed network which adds design complexity and reduces the radiation efficiency. In stacked patch configuration [9, 21], a parasitic patch is placed vertically above the driven patch, both operating in the dominant mode. The separation between the driven and parasitic patches can be chosen to enhance either the gain or the impedance bandwidth. For gain enhancement, separation between the patches need to be order of half wavelength which increases the antenna profile. Directivity can also be increased using superstrate loading. In this method, a high dielectric substrate [23, 69] or a partially reflective surface (PRS) [24, 70, 71] is placed about half wavelength

above the patch antenna. The main idea is to achieve cavity resonance condition which results in gain enhancement. However, this method increases the overall antenna profile. Another technique for gain enhancement is shunt inductive loading [72, 73]. In this technique, shorting pins are placed on the surface of patch antenna. The shunt inductive effect of these shorting pins increases the electrical size of patch at resonance. Gain enhancement is achieved due to enlarged radiating aperture of antenna.

Directivity of patch antenna can also be enhanced by using higher order mode operation. For example, rectangular patch antennas operating in higher order TM_{m0} ($m = 3, 5, 7, ..$) modes have broadside radiation pattern with higher directivity. The overall size of higher mode patch is larger than the dominant mode patch which results in increased directivity. However, higher order mode patch antennas suffer from high E-plane SLL and non-optimum gain. Over the years, different techniques have been proposed for SLL suppression and gain enhancement in higher order mode patch antennas. Radiation properties of higher order mode patch antennas can be improved using high dielectric substrate, superposition of broadside modes, and slot loading. In [37], a high permittivity substrate was used for E-plane SLL suppression of circular patch antenna operating in TM_{12} mode. The basic idea of this technique is to reduce the size of patch at resonance. However, due to surface wave losses radiation efficiency is also reduced. Another technique for SLL reduction of higher order mode patch antenna is to use linear superposition of different broadside modes. A dual mode circular patch antenna was proposed in [38] wherein a TM_{11} mode patch is placed above a higher order TM_{13} mode patch in a stacked configuration. SLL reduction and gain enhancement is achieved due to superposition of radiated fields of these two modes. The drawbacks of this technique are narrow impedance bandwidth and complex geometry. In [74], a single layer implementation of this technique was demonstrated using superposition of TM_{12} and TM_{14} modes. A wideband or dual band circular patch with high gain and low SLL was demonstrated in [75], which employed superposition of TM_{11} and TM_{13} modes at one frequency and superposition of TM_{12} and TM_{14} modes at another frequency.

Another way for improving the radiation properties of higher order mode patch antennas is to use slot loading technique [2, 39, 76–81]. In [2], SLL of a higher order TM_{30} mode patch antenna are eliminated by placing two reactive slots close to radiating edges. The main idea is to make the current distribution of higher order TM_{30} mode similar to fundamental TM_{10} mode, which eliminates the SLL but at the expense of antenna gain. A non-resonant slot loading technique was employed in [39] for E-plane SLL suppression of TM_{12} mode circular patch. However, antenna has high cross polarization and asymmetric radiation pattern. In [76], a low SLL differential fed TM_{30} mode slot loaded rectangular patch was demonstrated which can achieve low cross polarization and symmetric radiation pattern. A dual band differential fed high gain circular patch antenna operating in TM_{11} and TM_{12} modes was presented in [78] by using a combination of slot and shorting pins. In [79], a wideband low SLL differential fed rectangular patch antenna operating in TM_{10} and TM_{12} modes was realized by adding shorting pins and slots. A high gain slot loaded TM_{03} mode rectangular patch with reduced SLL and adjustable beamwidth was presented in [80]. Recently, a dual polarized slot loaded TM_{90} mode rectangular patch antenna with high gain and SLL suppression was demonstrated in [81].

In this chapter, a notch loading technique is proposed for gain enhancement and E-plane SLL reduction of higher order TM_{m0} ($m = 3, 7$) mode rectangular patch antennas. In this technique, out of phase surface current distribution regions of higher order mode patch antenna are partially removed. New in-phase radiating edges are created in this process. It is demonstrated that superposition of radiated field of these additional radiating edges and radiated field of unperturbed TM_{m0} ($m = 3, 7$) mode can be used to achieve both gain enhancement and SLL reduction. The proposed technique is different in the sense that it uses removal of out-of-phase surface current distribution regions to create new in phase radiators instead of reshaping it using slot [2, 39, 76–81]. A partial notch loaded TM_{70} mode patch is presented showing $>$ 16 dBi gain with good E-plane SLL of about -13 dB. As far as this author knows, this is the highest reported peak gain for single layer TM_{70} mode rectangular patch antenna. Previously, notch loading technique

has been used in the form of C and H slots [45, 82, 83] to achieve size reduction in patch antenna operating in fundamental mode; whereas, current work demonstrates use of notch loading for improving the radiation properties of higher order mode patch antennas.

4.2 Antenna Design and Modeling

In this section, working principle and theoretical analysis of two novel higher order TM_{m0} mode rectangular patch antennas namely notch loaded TM_{30} mode patch antenna (Antenna 1) and notch loaded TM_{70} mode patch antenna (Antenna 2) are described. Comparison of proposed notch loaded antennas with conventional (without notch) antennas is also presented.

4.2.1 Notch Loaded TM_{30} Mode Patch Antenna

4.2.1.1 Antenna Geometry and Working Principle

The proposed antenna geometry is shown in Fig. 4.1. It consists of rectangular patch of length L and width W fed by a coaxial probe at a distance F from the patch center. A partial notch loading of length ℓ and width w is applied at the center of both non-radiating edges. The ground plane size is given by $L_1 \times W_1$. Arlon CuCLad substrate having permittivity $\epsilon_r = 2.2$ and thickness $h = 0.15$ cm is used for antenna design. The operating frequency of notch-loaded TM_{30} mode patch is 3.23 GHz. The dimensions of proposed antenna are $L = 9$ cm, $W = 10.1$ cm, $\ell = 3$ cm, $w = 3$ cm, $L_1 = 14$ cm, $W_1 = 15$ cm and $F = 1.5$ cm.

The basic idea of proposed partial notch loading technique can be understood with the help of surface current distribution plot on higher order mode rectangular patch antenna. Figure 4.2(a) shows the surface current distribution plot of conventional TM_{30} mode patch antenna. Two in-phase and one out-of-phase regions can be identified between the two radiating edges. The out-of-phase current distribution

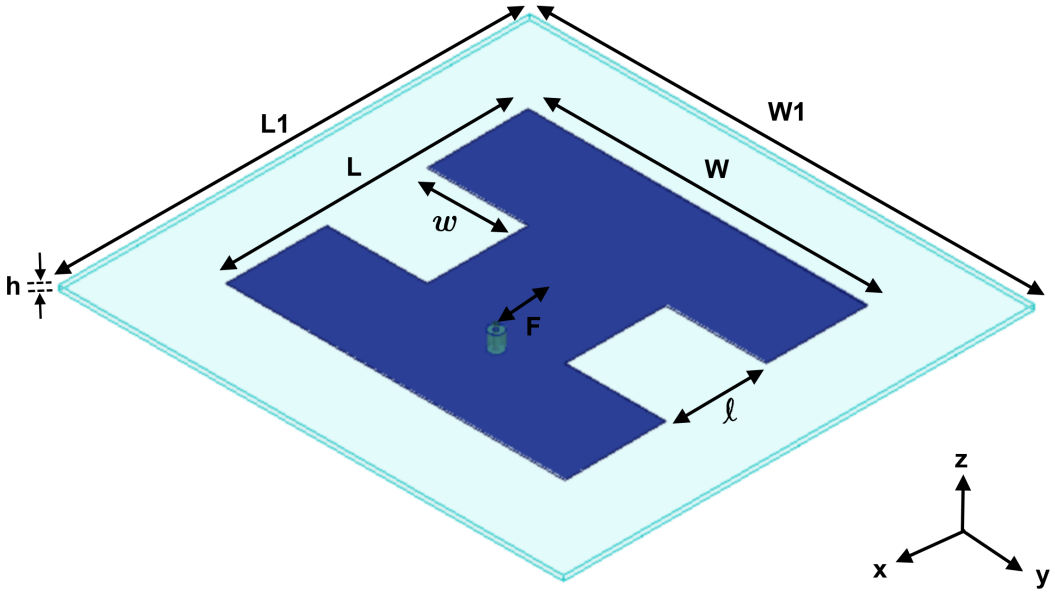

FIGURE 4.1: Geometry of the proposed notch loaded TM_{30} mode patch.

region is undesired as it causes reduction in directivity and raise in SLL [76]. Alternately, one can think that low directivity and high E-plane SLL is due to large inter element spacing between the two radiating edges of TM_{30} mode [80]. The main idea of proposed notch loading technique is to create new in-phase radiators between the two radiating edges by partially removing the undesired current distribution regions.

Figure 4.2(b) shows the surface current distribution plot of proposed notch loaded TM_{30} mode patch antenna. It can be seen that the surface current distribution of the desired in-phase regions is intact. In addition, new radiating edges are created in the process. This can be verified by looking at the electric field (E-field) plot of proposed antenna shown in Fig. 4.3(b).

The corresponding equivalent magnetic current lines of the proposed antenna are shown in Fig. 4.4. It can be observed that contrary to conventional TM_{30} mode patch four new in-phase radiating edges are created using proposed notch loading technique. It will be shown in Section 4.2.1.2 that superposition of radiated field of these new radiating edges and radiated field of unperturbed (without notch) TM_{30} mode results in SLL reduction and gain enhancement.

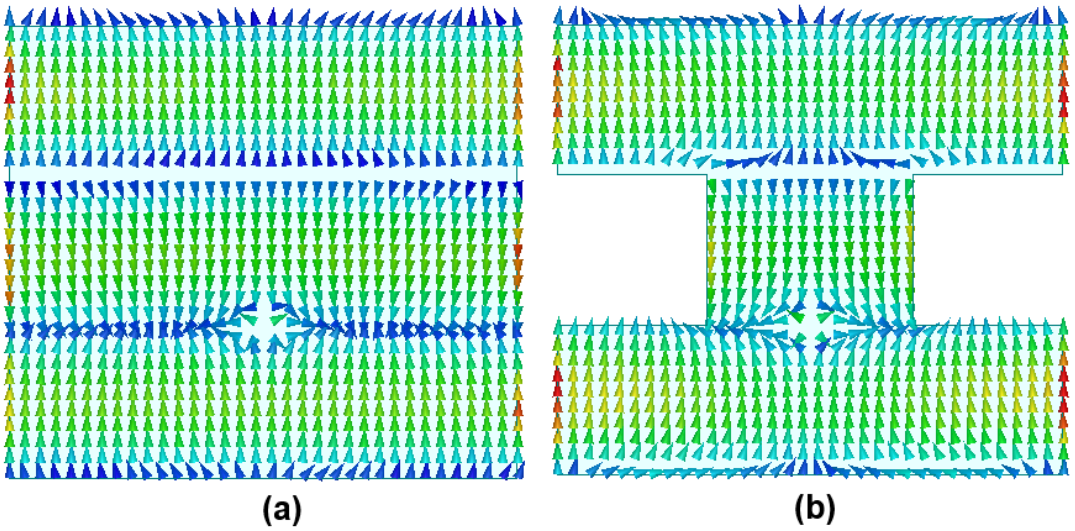

FIGURE 4.2: Surface current distribution plots (a) TM_{30} mode, (b) Notch loaded TM_{30} mode.

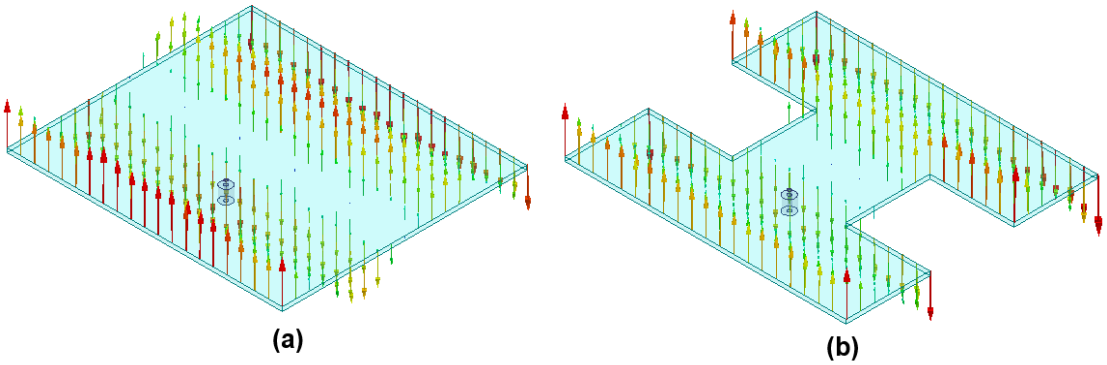

FIGURE 4.3: Electric field plots (a) TM_{30} mode, (b) Notch loaded TM_{30} mode.

4.2.1.2 Theoretical Analysis

Theoretical radiation characteristics of the proposed notch loaded TM_{30} mode patch antenna are presented in this section. An infinite ground plane is assumed for all the calculations. Figure 4.4 shows the equivalent aperture model for proposed antenna. It consists of y-directed magnetic line sources which can be found using equivalence principle and small substrate height assumption [67]. Here, two magnetic line sources of width W represent aperture field of conventional (without notch) TM_{30} mode, whereas four magnetic line sources of width w represent the aperture field created due to notch loading. Theoretical radiation pattern of notch

loaded TM_{30} mode patch antenna can be found using superposition principle and can be written as the linear combination of unperturbed TM_{30} mode patch far field E_1 and far field due to notch loading E_2

$$E = C_1 E_1 + C_2 E_2 \tag{4.1}$$

The radiated far field components of E_1 and E_2 can be calculated using the cavity model [32] and are given by

$$E_\theta = \cos\phi \left[C_1 f_1(\theta, \phi) + C_2 f_2(\theta, \phi)\right] \tag{4.2}$$

$$E_\phi = -\cos\theta \sin\phi \left[C_1 f_1(\theta, \phi) + C_2 f_2(\theta, \phi)\right] \tag{4.3}$$

where

$$f_1(\theta, \phi) = \frac{\sin(WY)}{WY} \cos(LX) \tag{4.4}$$

$$f_2(\theta, \phi) = \frac{\sin(wY)}{wY} [\cos(\ell X) \cos((W - w)Y)] \tag{4.5}$$

$$X = \frac{k_0}{2} \sin\theta \cos\phi \tag{4.6}$$

$$Y = \frac{k_0}{2} \sin\theta \sin\phi \tag{4.7}$$

Here k_0 is free space phase constant. The first factor, i.e. sine terms in Eqs. (4.4) and (4.5) are the pattern factors for y-directed magnetic line sources of widths W and w, respectively. Second term in Eq. (4.4) is the array factor due to two element array of distance L along x-axis. Whereas second term in Eq. (4.5) is the array factor due to 2×2 array of distance ℓ along x-axis and $W - w$ along y-axis.

The E-plane ($\phi = 0$) radiation pattern is given by

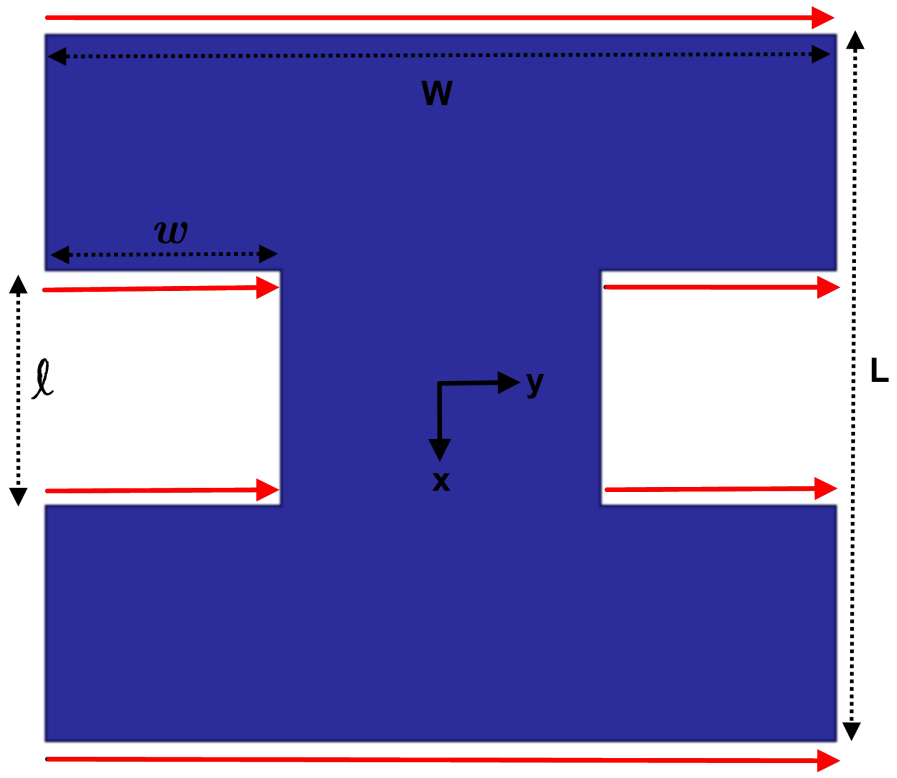

FIGURE 4.4: Equivalent magnetic current lines for the proposed notch loaded TM_{30} mode patch.

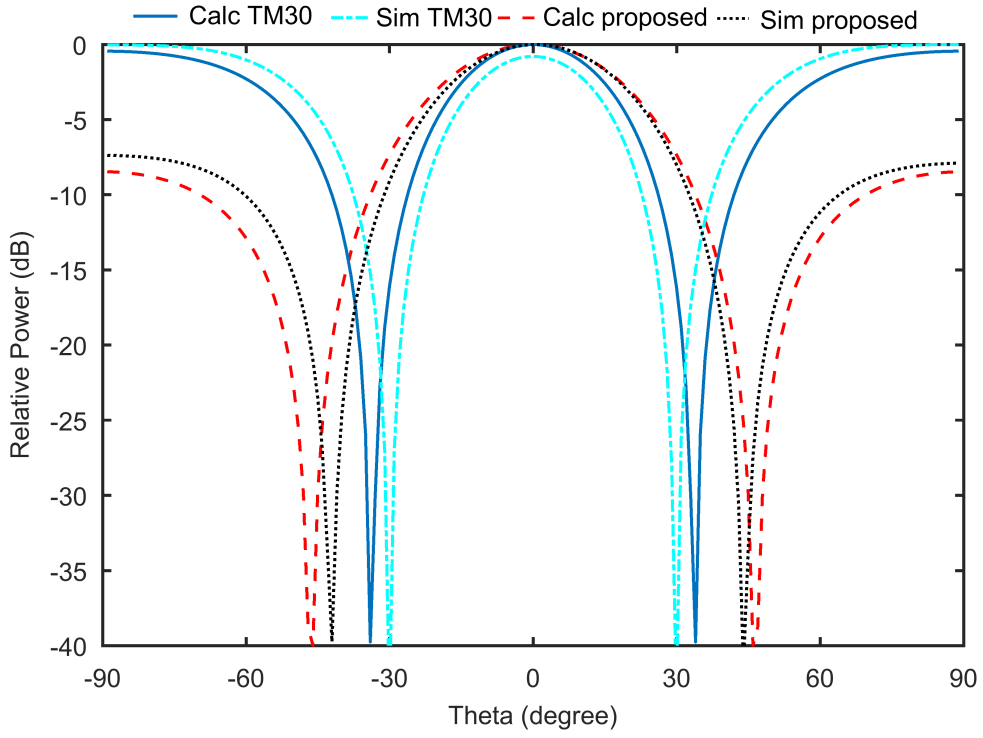

FIGURE 4.5: Simulated and theoretical normalized E-plane radiation patterns of Antenna 1.

$$E_\theta = C_1 \cos\left(\frac{k_0 L}{2}\sin\theta\right) + C_2 \cos\left(\frac{k_0 \ell}{2}\sin\theta\right) \tag{4.8}$$

Here amplitude ratio $\left|\frac{C_2}{C_1}\right| = \frac{2w}{W}$. Theoretical normalized E-plane radiation pattern of notch loaded TM_{30} mode patch antenna, for the dimension given in Sec. 4.2.1.1, is shown in Fig. 4.5. For comparison, simulated radiation pattern of antenna is also plotted. Simulation were performed using commercial EM simulator HFSS with infinite ground plane. Theoretical and simulated results are in reasonable agreement thus, validating the theoretical formulation. Theoretical and simulated radiation patterns of conventional TM_{30} mode patch are also plotted in Fig. 4.5. It can be seen that compared to conventional TM_{30} mode patch antenna, proposed notch loaded TM_{30} mode patch has reduced E-plane SLL. Theoretical directivity of the proposed notch loaded patch antenna can be evaluated using

$$D = \frac{4\pi U_{max}}{P_{rad}} \tag{4.9}$$

where $U = \frac{1}{2\eta}|E|^2$ and $P_{rad} = \int\int U sin\theta d\theta d\phi$. Using E-field expressions given by Eqs. (4.2) and (4.3), the directivity of the proposed notch loaded TM_{30} mode patch is evaluated numerically and is found to be equal to 13.11 dB. For comparison, the directivity of conventional patch antenna is also evaluated by setting $C_2 = 0$ in Eqs. (4.2) and (4.3). The directivity of conventional TM_{30} mode patch is found to be equal to 10.04 dB. Thus compared to its conventional counterpart about 3 dB improvement in directivity is achieved in the proposed notch load TM_{30} mode patch antenna.

4.2.1.3 Parametric Study

In this section, effect of notch dimensions on the E-plane SLL and return loss of proposed antenna is studied. As mentioned before, one objective of notch loading is to remove the undesired out of phase surface current distribution region of higher mode patch antenna.

For TM_{30} mode patch we have one center out-of-phase region as shown in Fig. 4.2(a). For patch of length L, length of undesired region is about $L/3$, whereas its width is equal to W. However, complete removal of undesired region is not possible as it results in two separate antennas. One solution is to apply partial notch loading and use two notches at the center of both non-radiating edges as shown in Fig. 4.1. Here, lengths of both notches is fixed and equal to $L/3$, wheres width w is varied to achieve the optimum results. It is worthwhile to mention that a rectangular notch offer two advantages compared to other geometries such as circular notch. First, it ensures complete removal of undesired reigion in the x-direction. Second, it simplfies the theoretical modeling of the proposed antenna.

Figure 4.6 shows the effect of notch width w on E-plane SLL and S_{11} of the proposed antenna. It can be seen from Fig. 4.6(a) that by changing the notch width w from 2 to 4 cm, SLL are decreased from -7.7 dB to -12.5 dB, showing an improvement of about 4.8 dB. An asymmetry in radiation pattern can also be observed for $w = 4$ cm. Figure 4.6(b) shows the effect of notch width w on the S_{11} of antenna. It can be seen that by increasing the notch width w from 2 to 4 cm, S_{11} is degraded from -20.6 dB to -11.8 dB. A downward shift in resonant frequency can also be observed. Thus, decrease in SLL is possible by increase in notch width w but at the cost of degradation in S_{11} and asymmetric radiation pattern. For this particular case, a square notch loading of $w = \ell$ is selected which gives a symmetric pattern with SLL of -10.8 dB and S_{11}= -16.1 dB.

It is worthwhile to point out that coaxial probe position in notch loaded TM_{30} mode patch is fixed, located at $L/3$ from edge or $\ell/2$ from center of patch, see Fig. 4.1. We can not change the location of probe because it will in turn change the surface current distribution of TM_{30} mode patch. As a result for a given notch width w, return loss of notch loaded TM_{30} mode patch is also fixed. A technique for improvement in return loss of notch loaded TM_{30} mode patch will be presented in Chapter 5. It will be shown that improvement in SLL and S_{11} of Antenna1 can be achieved by introducing a slot at the center of notch loaded patch antenna. The slot can be cut in different shapes such as circular, or a fractal slot.

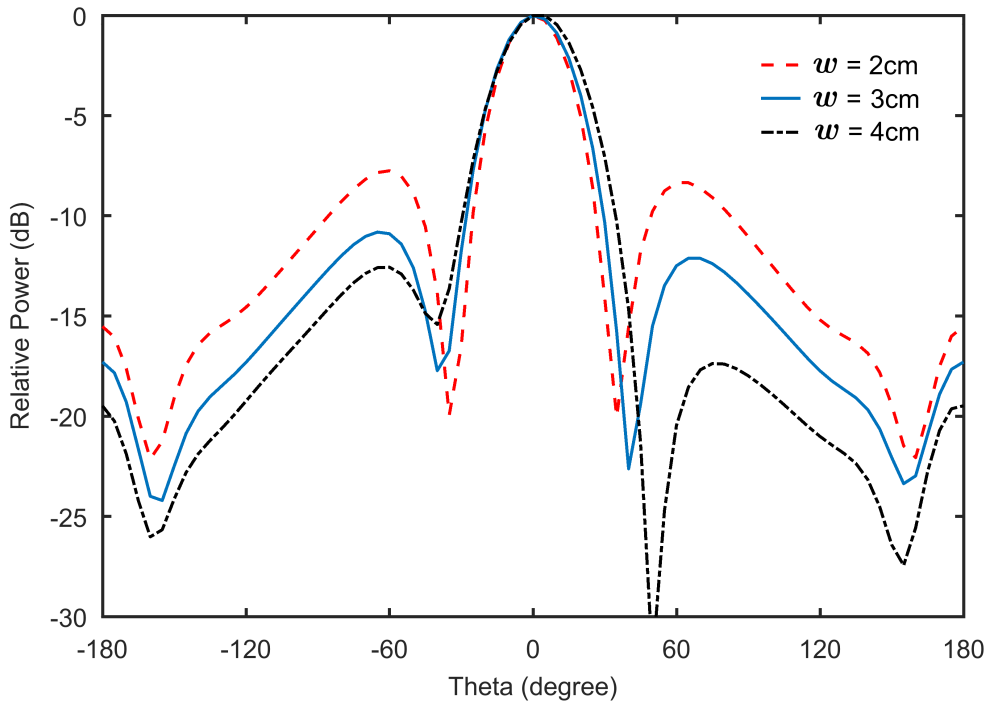

(a)

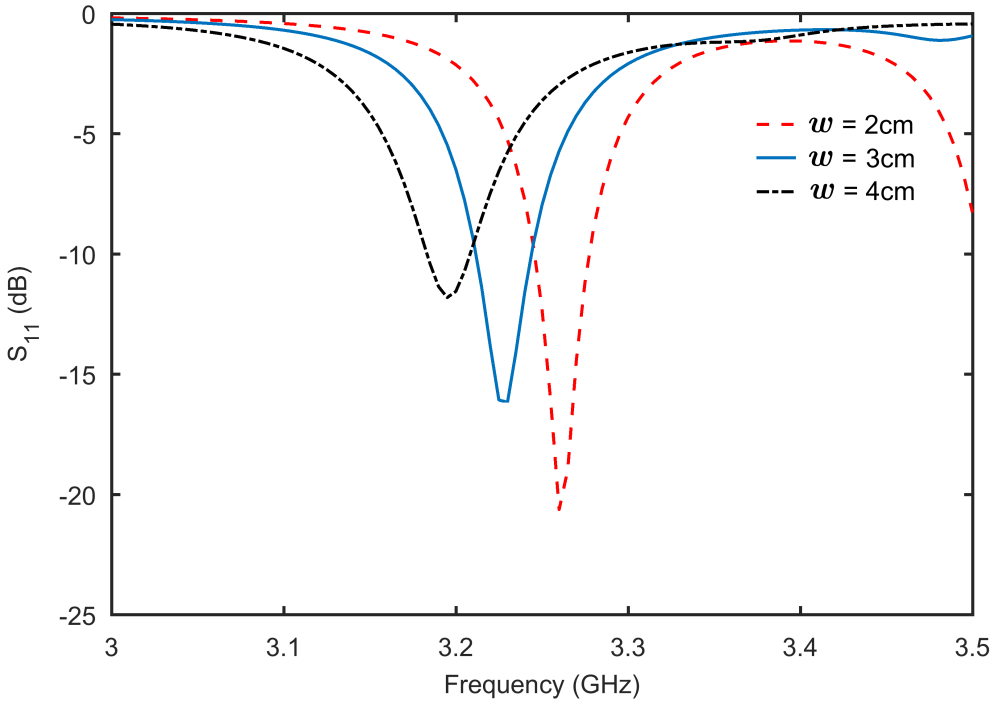

(b)

FIGURE 4.6: Effect of notch width w on (a) E-plane SLL, (b) S_{11}.

4.2.1.4 Comparison of Conventional and Notch Loaded TM_{30} Mode Antenna

As mentioned before, notch loading was applied to remove the undesired surface current distribution regions of TM_{30} mode which results in SLL reduction and gain enhancement. However, the effect of notch loading on surface current distribution of other TM modes will be quite different. So it is worthwhile to investigate the effect of notch loading on other higher order modes. In this section, the effect of notch loading on the resonance frequencies of different TM modes, gain, SLL, and cross-polarization of Antenna1 is investigated. Figure 4.7(a) shows the input resistance of Antenna1 as a function of frequency before and after the notch loading. Four resonance peaks can be observed for conventional antenna which corresponds to TM_{30} ,TM_{22},TM_{12} and TM_{20} modes. The resonance frequency of desired TM_{30} mode is 3.3 GHz which has broadside pattern. All other higher order modes are undesired as they have end fire pattern. For notch loaded antenna, a downward shift in the resonance frequencies of all TM modes can be observed. The resonance frequency of desired TM_{30} mode is 3.23 GHz.

The effect of notch loading on the gain of TM_{30} mode patch is shown in Fig. 4.7(b). For conventional antenna, gain at TM_{30} mode is 10.9 dBi, whereas notch loaded antenna has gain of 13.9 dBi. A 3 dB improvement in gain is thus achieved for notch loaded antenna compared to conventional antenna. The effect of notch loading on E-plane SLL of Antenna 1 is shown in Fig. 4.7(c). The SLL of conventional antenna for TM_{30} mode is -2.4 dB compared to notch loaded antenna, which has a SLL of -10.8 dB. An improvement of about 8 dB in SLL is achieved for notch loaded TM_{30} antenna compared to its conventional counterpart. The H-plane cross polarization of conventional and notch loaded antenna are shown in Fig. 4.7(d). For conventional antenna, maximum cross-polarization level below main lobe is 27.6 dB, whereas notch loaded antenna has cross polarization level of 35 dB below main lobe. Notch loaded antenna shows about 7 dB improvement in cross-polarization level compared to conventional antenna. The effect of notch loading on E-plane cross- polarization is negligible and not shown here.

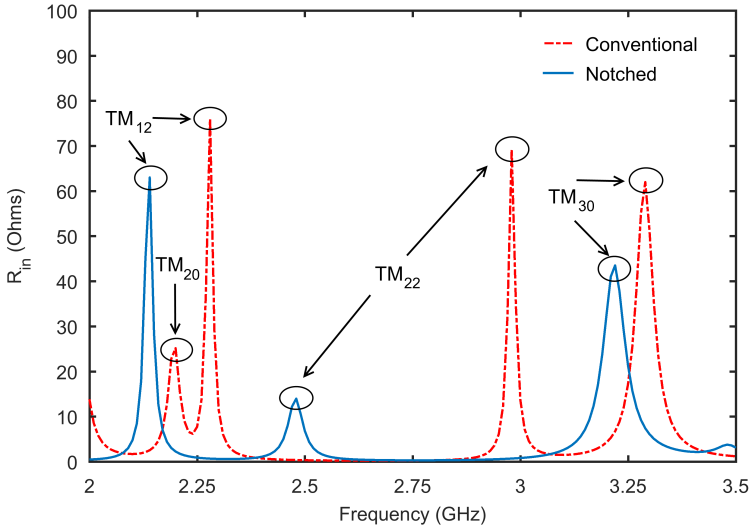
Conventional
Notched
TM12
TM20
TM22
TM30
Rin (Ohms)
Frequency (GHz)

(a)

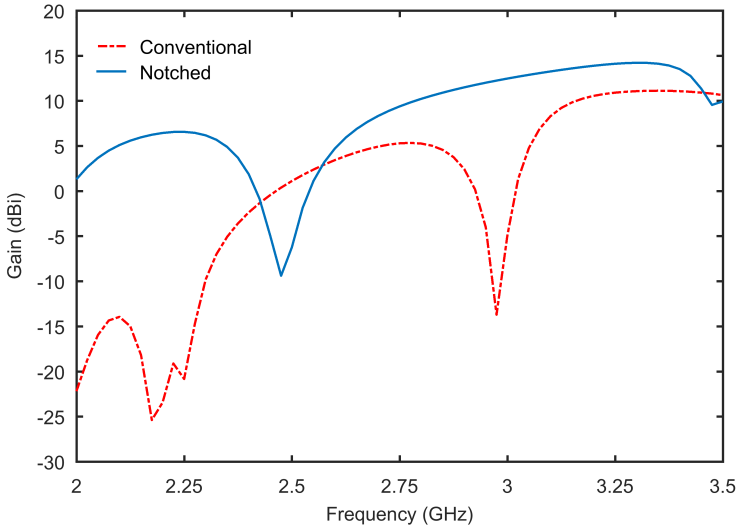
Conventional
Notched
Gain (dBi)
Frequency (GHz)

(b)

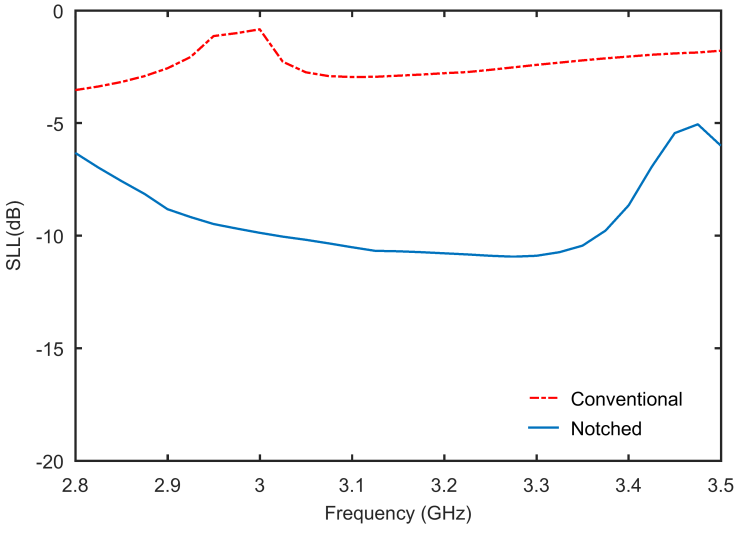
Conventional
Notched
SLL(dB)
Frequency (GHz)

(c)

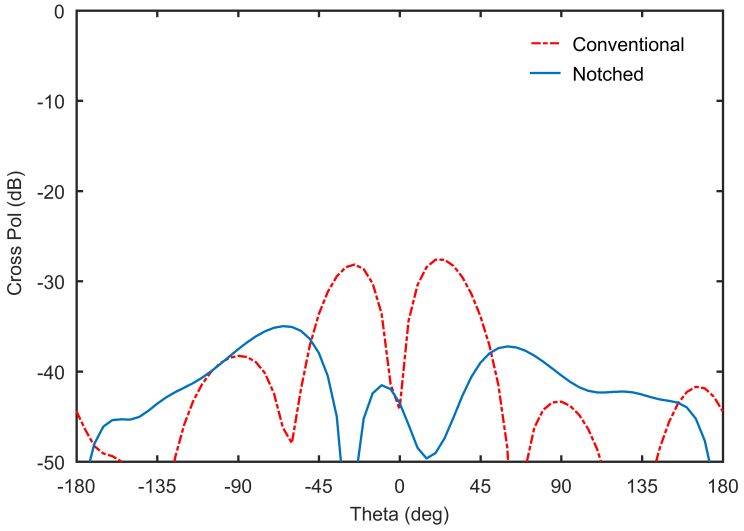

(d)

FIGURE 4.7: Comparison of conventional and notch loaded Antenna 1 (a) Input resistance, (b) Gain, (c) SLL and, (d) Cross polarization

4.2.2 Notch Loaded TM_{70} Mode Patch Antenna

4.2.2.1 Antenna Configuration and Working Principle

Figure 4.8 shows the geometry of proposed notch loaded TM_{70} mode patch antenna. The antenna is designed to operate in TM_{70} mode at 7.7 GHz. Arlon CuCLad substrate having permittivity $\epsilon_r = 2.2$ and thickness $h = 0.15$ cm is used for antenna design. The dimensions of the antenna are $L = 9$ cm, $W = 9$ cm, $\ell = 1.28$ cm, $w_1 = 0.64$ cm, $w_2 = 1.92$ cm, $w_3 = 1.28$ cm, $L_1 = 14$ cm, $W_1 = 14$ cm and $F = 0.64$ cm.

The working principle of the proposed antenna can be understood using the surface current distribution plot of the conventional TM_{70} mode patch antenna shown in Fig. 4.9(a). It consists of alternate in-phase and out-of-phase current distribution regions. Four in-phase and three out-of-phase current distribution regions can be identified. The fundamental idea of proposed notch loading technique is the partial removal of undesired current distribution regions. It is worthwhile to mention that full removal of these undesired regions is not possible as it will result in four separate antennas. The proposed partial notch loading scheme is shown in

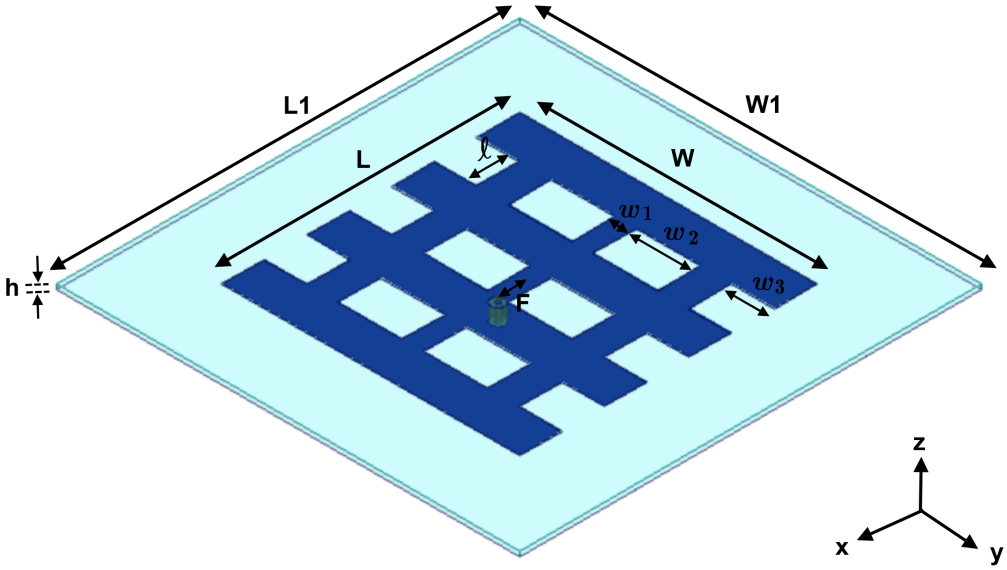

FIGURE 4.8: Geometry of the proposed notch loaded TM_{70} mode patch

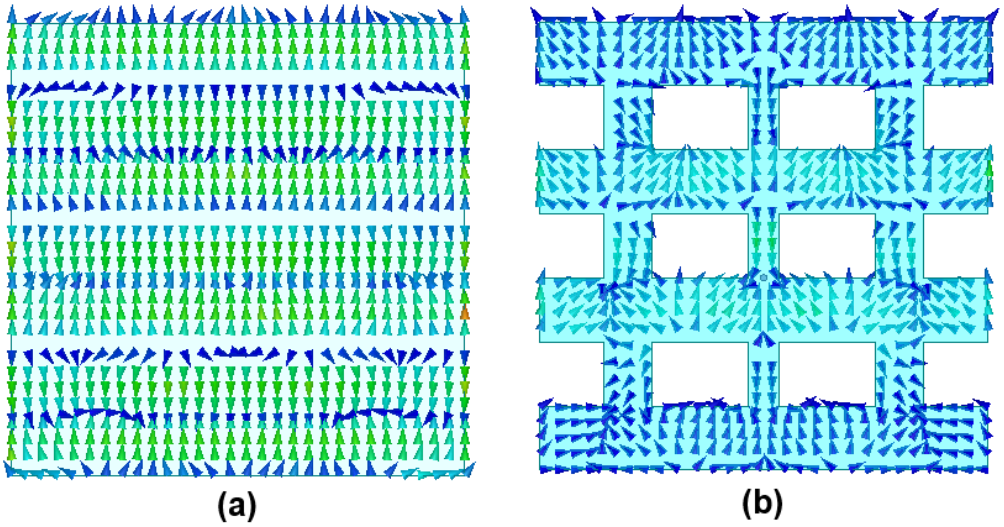

FIGURE 4.9: Surface current distribution of patch (a) Conventional TM_{70} mode, (b) Proposed notch loaded TM_{70} mode

Fig. 4.8. Each undesired region is notch loaded with four slots. The notches are symmetric with respect to y-axis. The widths of notches are w_2 and w_3, whereas length of each notch is fixed and is equal to $L/7$. The partial notch loading creates 24 new in-phase radiating edges between the two radiating edges of unperturbed TM_{70} mode patch as shown in Fig. 4.10. It will be shown in the next section that superposition of radiated field of these additional radiating edges and that of unperturbed TM_{70} mode results in SLL reduction and gain enhancement.

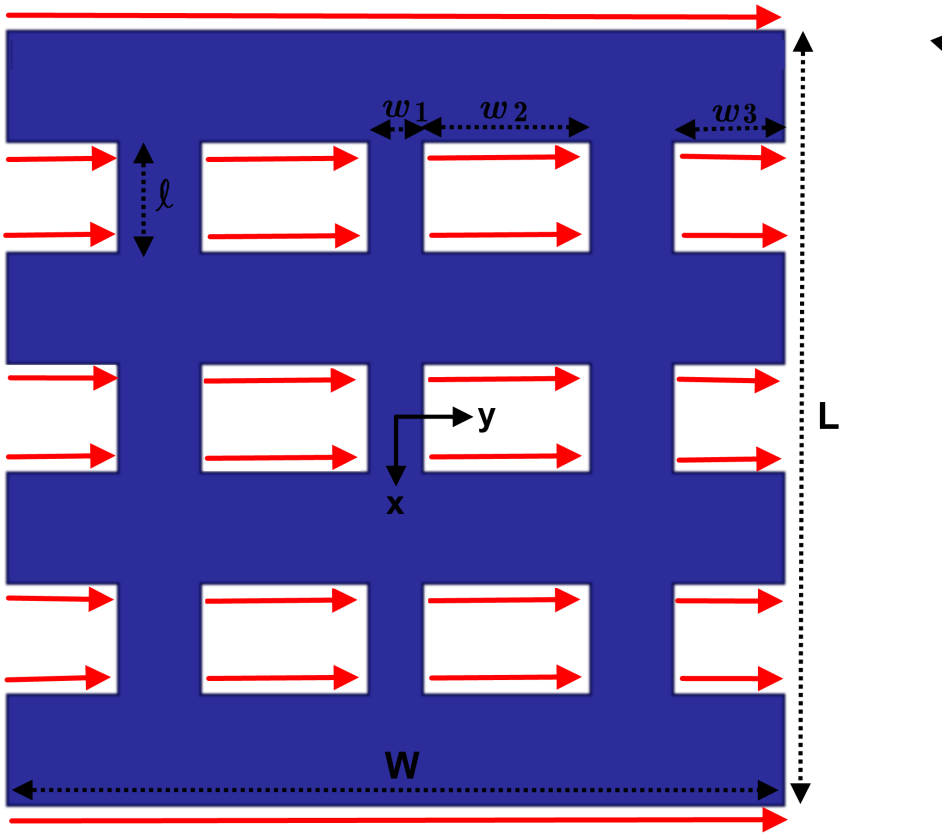

FIGURE 4.10: Equivalent magnetic current lines of the proposed notch loaded TM_{70} mode patch

4.2.2.2 Theoretical Radiation Characteristics

The equivalent aperture model of the proposed notch loaded TM_{70} mode patch antenna is shown in Fig. 4.10. Using the equivalent principle and small substrate height assumption, the aperture field of the radiating edges can be represented by y-directed magnetic line currents. Here, two magnetic line sources of width W represents the radiating edges of unperturbed TM_{70} mode, whereas 24 new radiating edges created due to partial notch loading are represented by magnetic line sources of width w_2 and w_3.

Theoretical radiation patterns of notch loaded TM_{70} mode patch can be found using the superposition principle. The total far field can be written as the linear combination of field due to unperturbed TM_{70} mode and field due to notch loading.

$$E = C_1E_1 + C_2E_2 + C_3E_3 \tag{4.10}$$

Here, E_1 represents the field of unperturbed TM_{70} mode due to 2 magnetic line currents of width W, E_2 represents the field due to 12 magnetic line currents of width w_2 and E_3 represents the field due to 12 magnetic line currents of width w_3. The radiated far field components of E_1, E_2 and E_3 can be calculated using the cavity model [32] and are given by

$$E_\theta = \cos\phi\,[C_1f_1(\theta,\phi) + C_2f_2(\theta,\phi) + C_3f_3(\theta,\phi)] \tag{4.11}$$

$$E_\phi = -\cos\theta\sin\phi\,[C_1f_1(\theta,\phi) + C_2f_2(\theta,\phi) + C_3f_3(\theta,\phi)] \tag{4.12}$$

where

$$f_1(\theta,\phi) = \frac{\sin(WY)}{WY}\cos(LX) \tag{4.13}$$

$$f_2(\theta,\phi) = \frac{\sin(w_2Y)}{w_2Y}[\cos((w_1+w_2)Y)\sum_n \cos(\ell X)] \tag{4.14}$$

$$f_3(\theta,\phi) = \frac{\sin(w_3Y)}{w_3Y}[\cos((W_1-w_3)Y)\sum_n \cos(\ell X)] \tag{4.15}$$

where

$n = 1, 3, 5;\ X = \frac{k_0}{2}\sin\theta\cos\phi;\ Y = \frac{k_0}{2}\sin\theta\sin\phi$

The E-plane ($\phi = 0$) radiation pattern is given by

$$E_\theta = C_1\cos\left(\frac{k_0L}{2}\sin\theta\right) + (C_2+C_3)\sum_n \cos\left(\frac{k_0\ell}{2}\sin\theta\right) \tag{4.16}$$

Figure 4.11 shows the theoretical normalized E-plane radiation pattern of the proposed notch loaded TM_{70} mode antenna. Simulated radiation pattern of antenna

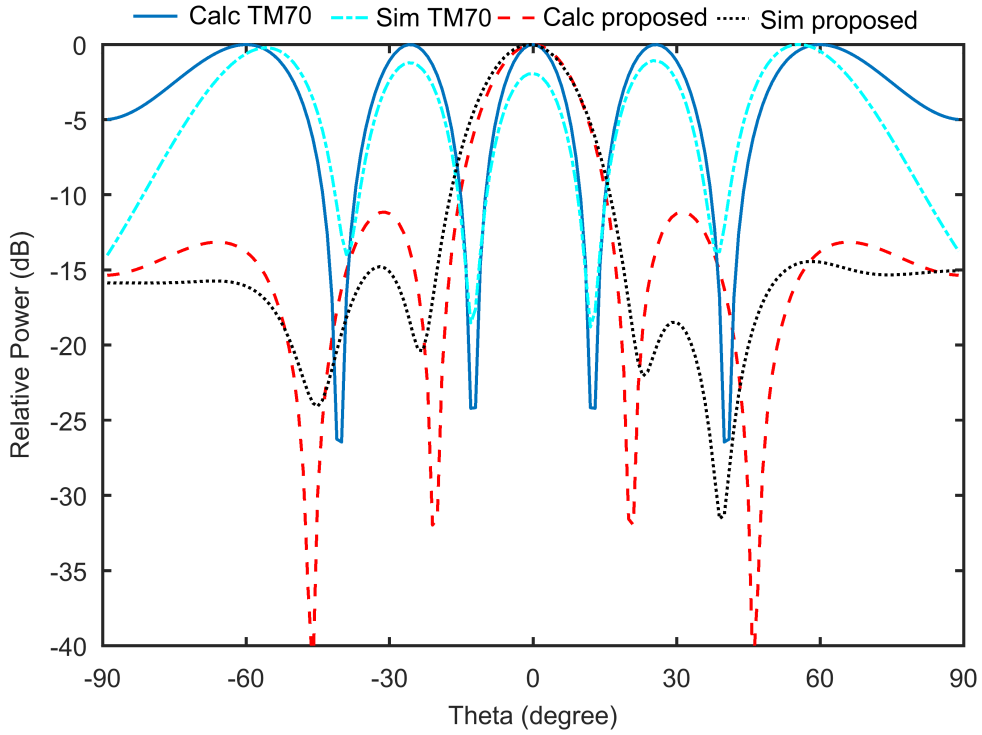

FIGURE 4.11: Simulated and theoretical normalized E-plane radiation patterns of Antenna 2

is also shown for comparison. Theoretical and simulated radiation patterns are in reasonable agreement. Small discrepancy in the result can be attributed to excitation of undesired higher order modes present in the EM simulation. Contribution of these modes are not taken into account in the theoretical analysis. It can be seen from Fig. 4.11 that proposed antenna has reduced SLL compared to its conventional counterpart. Directivity of the proposed antenna is calculated using Eq. (4.9) and is equal to 17.3 dB. In comparison, directivity of conventional TM_{70} mode patch antenna is equal to 12 dB. An improvement of > 5 dB in directivity is thus achieved using the proposed notch loading scheme.

4.2.2.3 Effect of Notch Loading on Performance of Antenna 2

In this section, effect of notch loading on resonance frequencies of different TM modes, gain, E-plane SLL, and cross-polarization of Antenna 2 is investigated. Figure 4.12(a) shows the input resistance of Antenna 2 as a function of frequency, before and after the notch loading. For conventional antenna (without

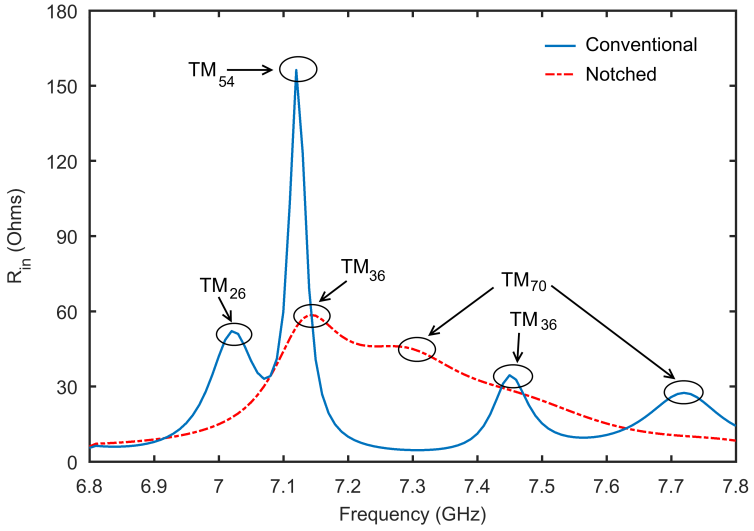
Conventional
Notched
TM54
TM26
TM36
TM70
TM36
Rin (Ohms)
Frequency (GHz)

(a)

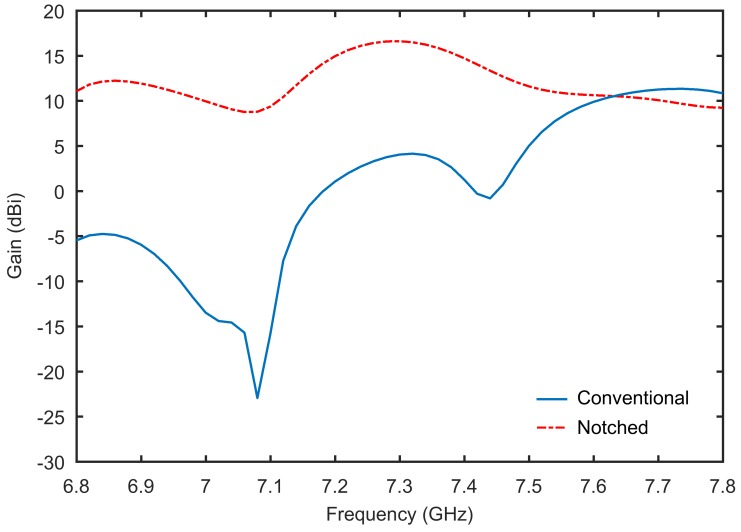
Gain (dBi)
Conventional
Notched
Frequency (GHz)

(b)

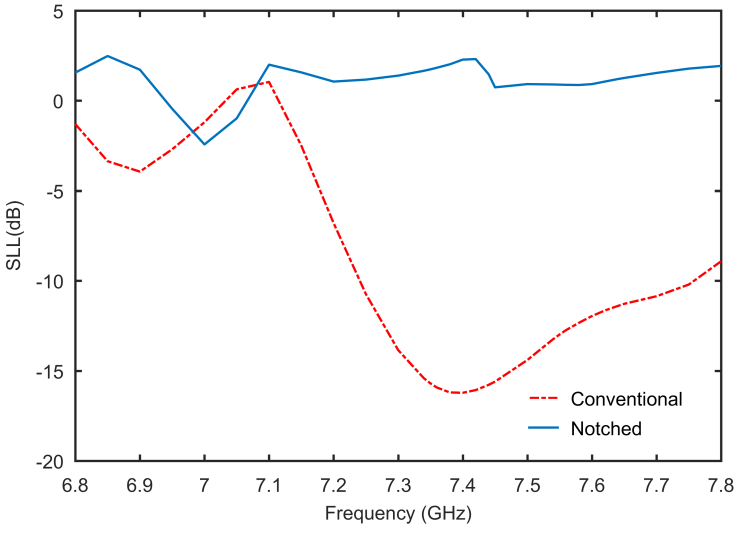
SLL(dB)
Conventional
Notched
Frequency (GHz)

(c)

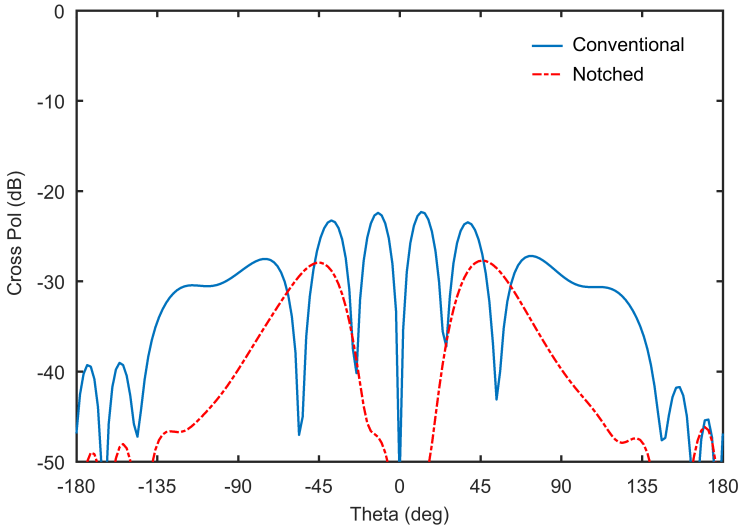

(d)

FIGURE 4.12: Comparison of conventional and notch loaded Antenna 2 (a) Input resistance, (b) Gain, (c) SLL and, (d) Cross polarization.

notch loading), four resonance peaks can be observed which corresponds to TM_{26}, TM_{54},TM_{36}, and TM_{70} modes. The desired TM_{70} mode has resonance frequency of 7.72 GHz. The TM_{36} mode is the closest higher order mode having a resonant frequency of 7.45 GHz. However, there is significant difference in antenna gain at both frequencies. The antenna gain for TM_{70} mode is 11.3 dBi and it drops to 0 dBi for TM_{36} mode as shown in Fig. 4.12(b). In addition, SLL of conventional antenna at TM_{36} and TM_{70} mode are 0.7 and 1.5 dB, which are undesirable for many practical applications.

The effect of notch loading on the resonance frequencies of antenna after the notch loading is shown in Fig. 4.12(a). Two resonance peaks can be observed for notch loaded antenna. The upper peak having resonance frequency of 7.28 GHz corresponds to TM_{70} mode, whereas lower peak having resonance frequency of 7.14 GHz corresponds to TM_{36} mode. The resonance frequencies of both modes are close to each other, resulting in wide impedance bandwidth. The antenna gain at TM_{70} and TM_{36} modes is 16.6 and 11.7 dBi as shown in Fig. 4.12(b). Significant improvement in antenna gain is achieved for notch loaded antenna compared to conventional antenna. An enhancement in antenna gain of about 5dB at TM_{70} mode and more than 11 dB at TM_{36} mode is achieved. Figure 4.12(c) shows the

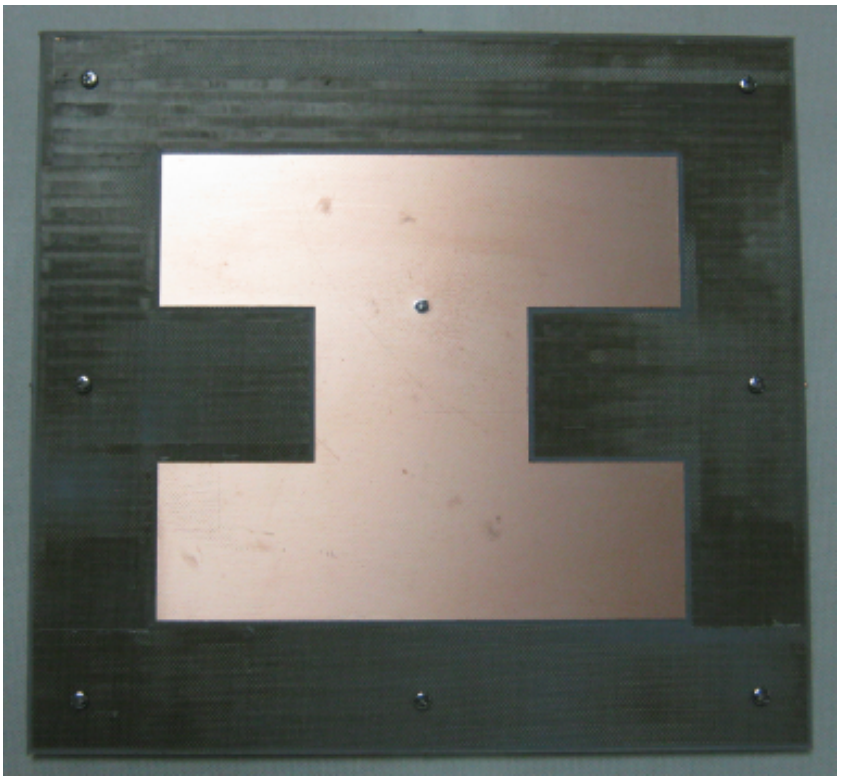

(a)

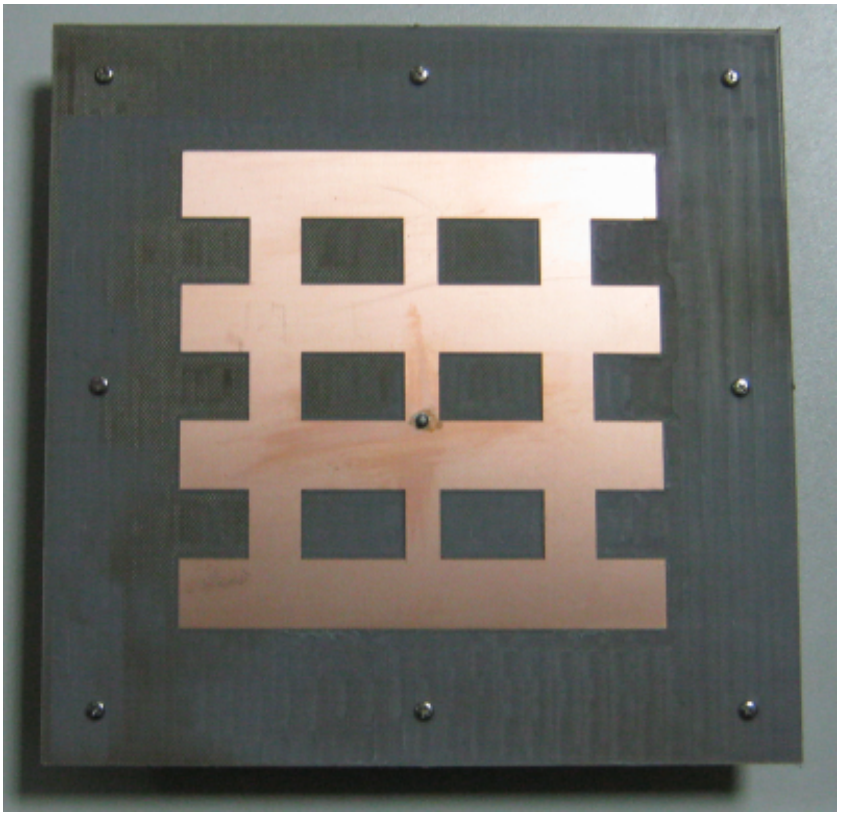

(b)

FIGURE 4.13: Fabricated notch loaded patch antennas (a) Antenna 1, (b) Antenna 2

E-plane SLL of notch loaded antenna as a function of frequency. The SLL of notch loaded antenna at TM_{36} and TM_{70} mode are -2.5 dB and -13.8 dB, respectively. The notch loaded antenna has lowest SLL of -16 dB at 7.4 GHz. Moreover, SLL of notch loaded antenna remains < -10 dB in frequency range of 7.25-7.75 GHz.

The H-plane cross-polarization of TM_{70} mode patch before and after the notch loading is shown in Fig. 4.12(d). The cross-polarization level of conventional antenna is 22.3 dB below main lobe, whereas notch loaded antenna has cross-polarization level of 27.7 dB. An improvement of about 5 dB in cross-polarization is thus achieved for notch loaded antenna compared to conventional antenna.

4.3 Results and Discussions

Prototypes of the proposed notch loaded higher mode patch antennas are fabricated and measured. The snapshots of fabricated antennas are shown in Fig. 4.13. Antennas were fabricated with CNC milling process using LPKF protomat H60. Agilent PNA network analyzer E220 was used for S-parameter measurements. Aluminum plates were used at the back of both antennas for mechanical support and SMA connector assembly.

4.3.1 Simulated and Measured Results of Antenna 1

Simulated and measured E- and H-planes radiation patterns of the proposed notch loaded TM_{30} mode patch antenna are shown in Fig. 4.14. Reasonable agreement between simulated and measured results is achieved. It can be observed from Fig. 4.14(a) that measured E-plane SLL are -10.5 dB compared to simulated value of -10.8 dB. Simulated and measured H-plane SLL of the antenna are -17.6 dB as shown in Fig. 4.14(b). The measured realized gain of the antenna is equal to 12.9 dBi. The measured efficiency of proposed Antenna 1 is about 79%. Simulated and measured S_{11} of the antenna are shown in Fig. 4.15. It can be seen that measured resonance frequency is shifted slightly upward compared to simulated

one, which may be attributed to fabrication tolerances. The measured $S_{11} \leq$ -10 dB impedance bandwidth of the antenna is 33 MHz around a center frequency of 3.25 GHz. Table 4.1 shows a summary of simulated and measured results of Antenna 1. Simulated results of conventional TM_{30} mode patch antenna are also shown for comparison. It can be observed that proposed antenna shows an improvement of 8 dB in E-plane SLL compared to conventional TM_{30} mode patch. In addition, 3 dB improvement in gain is also achieved, while size remains same.

4.3.2 Simulated and Measured Results of Antenna 2

Figure 4.16 shows the simulated and measured E- and H-planes radiation patterns of Antenna 2. The measured E-plane SLL of the antenna are -12.8 dB compared to simulated value of -14.4 dB. The measured and simulated H-plane SLL of the antenna are -24.9 dB and -21 dB, respectively. The measured realized gain of the antenna is 16 dBi. The measured efficiency of proposed Antenna 2 is about 87%. The simulated and measured return loss of Antenna 2 are shown in Fig. 4.17. The measured $S_{11} \leq$ -10 dB impedance bandwidth of the antenna is 280 MHz from 7.21 GHz to 7.49 GHz. The measured bandwidth of Antenna 2 is almost 4% which is about 4 times greater than Antenna 1 having bandwidth of 1%. The reason for wider bandwidth of Antenna 2 is existance of closein TM_{36} mode as shown in Fig. 4.12(a).

Table 4.1 shows a summary of simulated and measured results of Antenna 2. Simulated results of conventional TM_{70} mode patch antenna are also shown for comparison. It can be observed that proposed antenna shows an improvement of about 15 dB in E-plane SLL compared to conventional TM_{70} mode patch. Moreover, $>$ 5 dB improvement in gain is also achieved. The proposed antenna shows measured gain of 16 dBi. As far as this author knows, this is the highest reported gain for higher order TM_{70} mode rectangular patch antenna in single layer configuration.

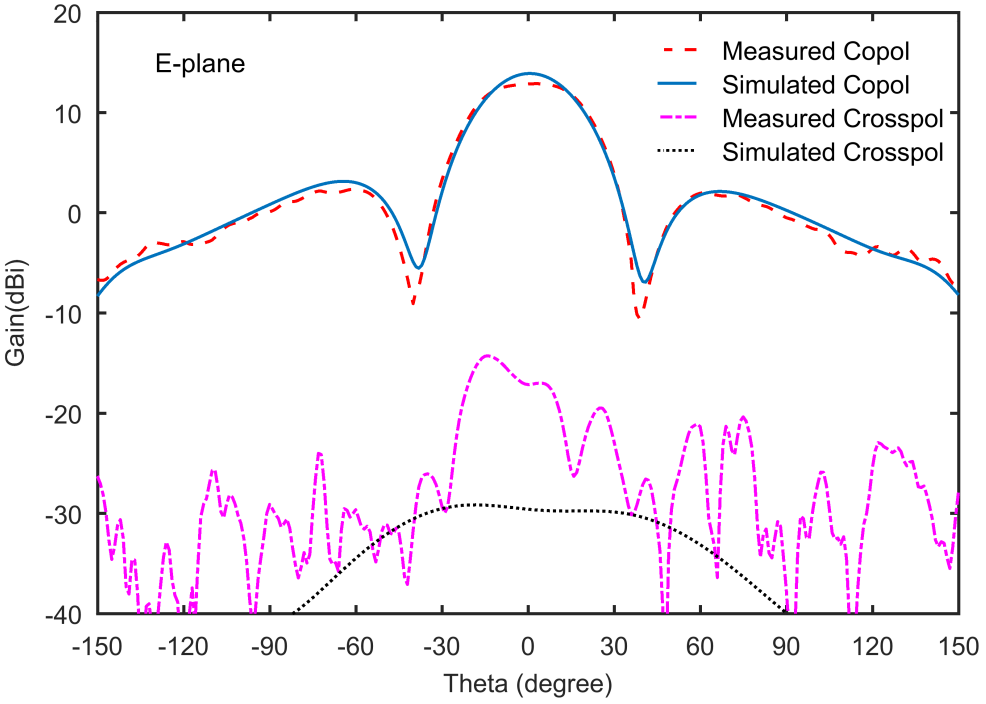

(a)

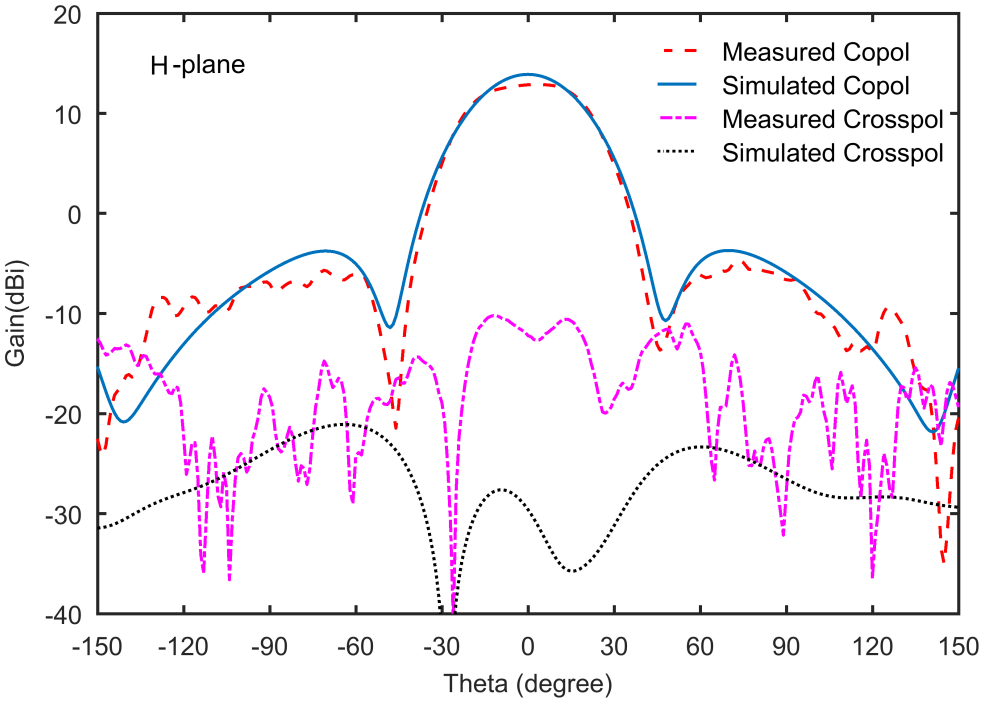

(b)

FIGURE 4.14: Simulated and measured radiation patterns of Antenna 1 (a) E-plane, (b) H-plane

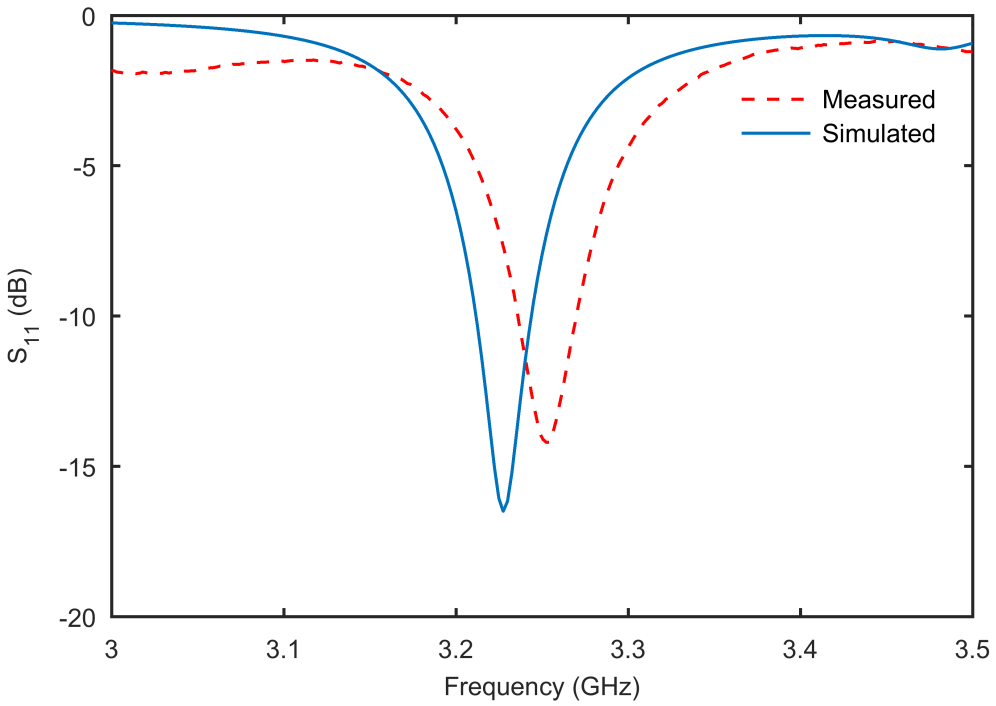

FIGURE 4.15: Simulated and measured S_{11} of Antenna 1

TABLE 4.1: Simulated and measured radiation characteristics.

Antenna	Gain (dBi)		E-plane SLL (dB)	
	Sim	Meas	Sim	Meas
Proposed TM_{30}	13.9	12.9	-10.8	-10.5
Conventional TM_{30}	10.9	-	-2.4	-
Proposed TM_{70}	16.6	16	-14.4	-12.8
Conventional TM_{70}	11.1	-	0.9	-

4.3.3 Comparison With Other Related Works

Over the years, different techniques have been employed to improve the radiation characteristics of higher order mode patch antennas. Table 4.2 shows a comparison of proposed antenna with the previous reported single-layer higher order mode patch antennas operating in a single band. It can be seen that the proposed antenna gives a reasonable compromise in terms of gain, SLL, and impedance bandwidth. The antenna reported in [81] shows the a high measured gain of 15.5 dBi. However, due to TM_{90} mode operation it has large aperture size of 2.92 λ_0 $\times$

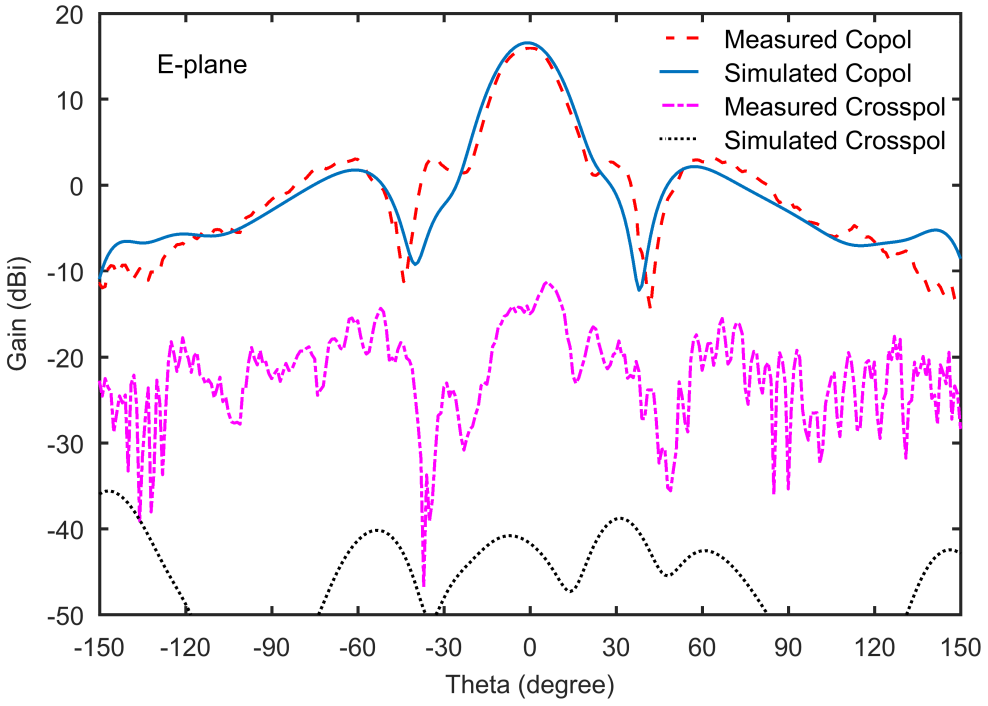

(a)

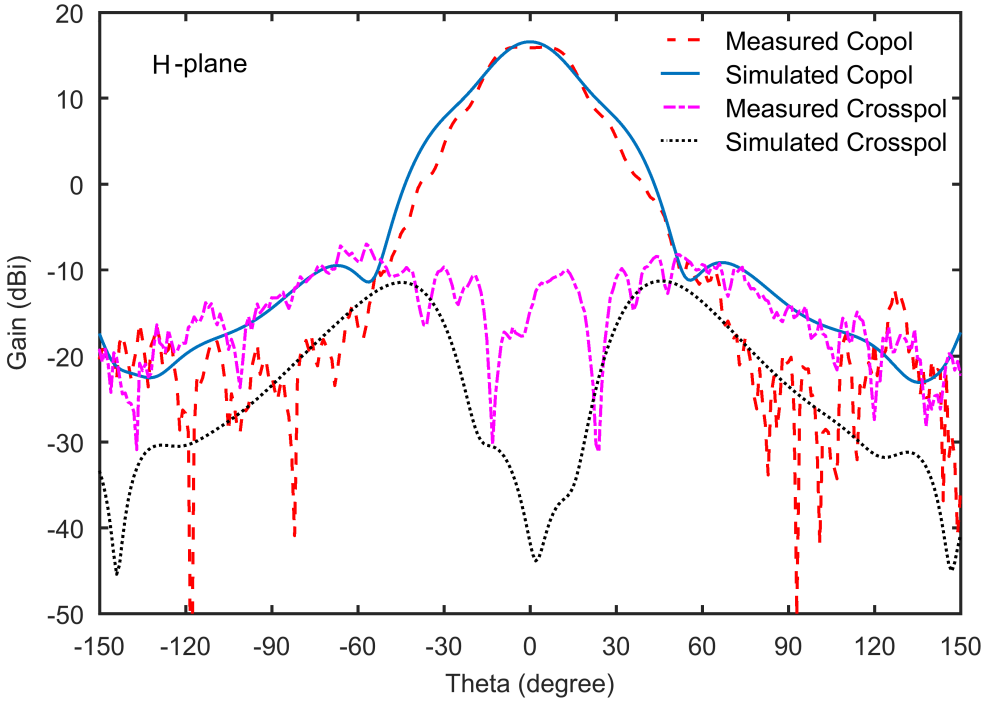

(b)

FIGURE 4.16: Simulated and measured radiation patterns of Antenna 2 (a) E-plane, (b) H-plane

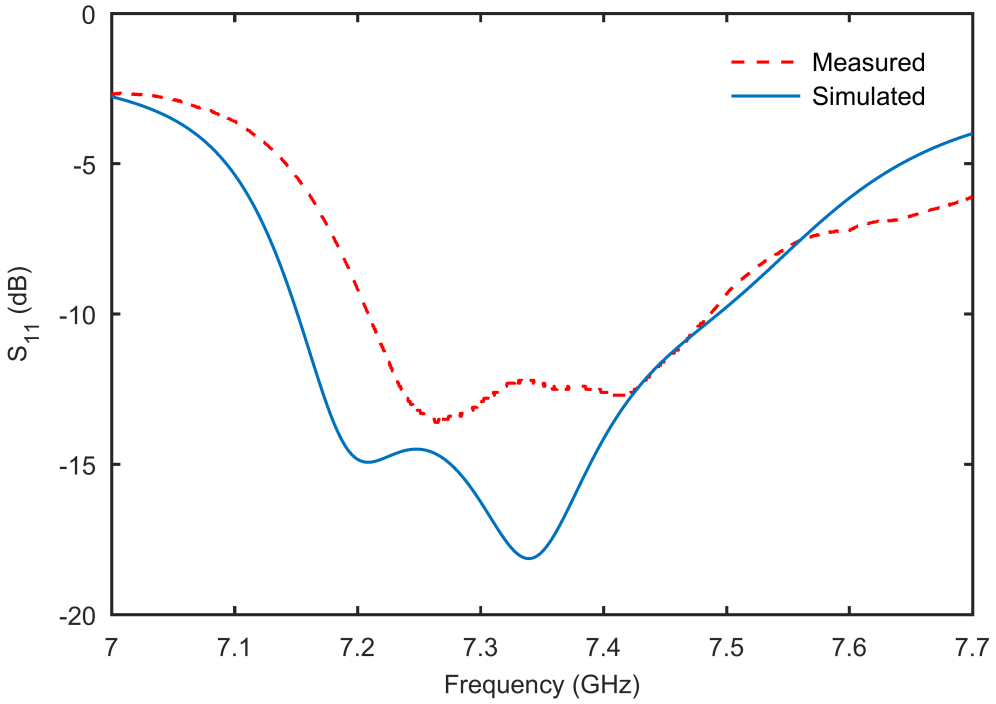

FIGURE 4.17: Simulated and measured S_{11} of the Antenna 2

TABLE 4.2: Comparison of single layer higher order mode patch antennas.

Ref.	Frequency (GHz)	Mode	Measured Gain (dBi)	E-plane SLL (dB)	Bandwidth (%)
[74]	11	TM_{12}	14.8	-11	1
[39]	10	TM_{12},TM_{14}	9.9	-20	1.56
[76]	3	TM_{30}	12.8	-12	0.7
[79]	1.9	TM_{12}	10	-12	10
[80]	4.2	TM_{03}	12.7	-18.6	0.4
[81]	12.5	TM_{70}	15.5	-11	2.3
This work	7.3	TM_{70}	16	-12.8	3.8

2.92 λ_0 × 0.06 λ_0. The measured gain of antenna presented in [74] is 14.8 dBi but it has narrow impedance bandwidth 1%. The technique presented in [39] achieves the lowest SLL of -20 dB but it has low gain and narrow impedance bandwidth. The antenna reported in [79] has largest impedance bandwidth of 10% but it has low gain of about 10 dBi. The proposed antenna has the highest reported measured gain in single-layer higher order mode patch antennas. It shows a measured gain

of 16 dBi along with good SLL of about -13 dB. In addition, it has reasonable impedance bandwidth of 3.8%. The aperture size of antenna is 2.2 λ_0 × 2.2 λ_0 × 0.04 λ_0. Due to its high gain, large bandwidth and good SLL proposed antenna is attractive for medium range wireless communication applications such as Wi-Fi directional antennas working in 900 MHz (902- 928 MHz), 2.4 GHz (2.4-2.4835 GHz), 3.6 GHz (3.655–3.695 GHz), 4.9 GHz (4.94-4.99 GHz) or 5 GHz (5.15-5.25 GHz, 5.25-5.35 GHz, 5.725-5.825 GHz) bands.

4.4 Summary

A new notch loading technique for gain enhancement and E-plane SLL suppression in higher order TM_{30} and TM_{70} mode rectangular patch antennas is presented. In this technique, out of phase surface current distribution regions of TM_{m0} ($m = 3, 7$) mode patch antennas are partially removed to create new in-phase radiators between the two radiating edges of conventional higher mode patch antennas. In this way, problem of large inter element spacing between the radiating edges of higher order mode patch is resolved. Due to superposition of radiated far fields, a high directivity patch antenna with reduced SLL is realized. Notch loading technique, which has been used previously for size reduction in patch antenna operating in fundamental mode, is used here to achieve E-plane SLL reduction and gain enhancement in higher order mode patch antennas.

Two novel single layer, easy to fabricate higher order mode patch antennas, namely, notch loaded TM_{30} mode patch antenna (Antenna 1) and notch loaded TM_{70} mode patch antenna (Antenna 2) are presented. Antenna 1 shows a measured gain of 12.9 dBi and E-plane SLL of -10.5 dB, whereas Antenna 2 shows a measured gain of 16 dBi and SLL of -12.8 dB. To the best of our knowledge, this is the highest reported antenna gain for single layer TM_{70} mode rectangular patch antenna. It is demonstrated that the proposed notch loaded TM_{30} mode patch can achieve about 8 dB reduction in SLL and 3 dB improvement in gain compared to conventional TM_{30} mode patch, whereas the proposed notch loaded TM_{70} mode patch antenna

shows about 15 dB reduction in SLL and > 5 dB improvement in gain compared to its conventional counterpart. Due to their high gain proposed antennas are suitable for short range point to point communication applications. The proposed notch loading scheme can also be used to improve the radiation properties of higher order mode patch antennas with circular and triangular geometries.

Chapter 5

Some Methods for Improving the Performance of TM_{30} Mode Patch

5.1 Introduction

In this chapter, two methods for improving the performance of slot and notch loaded TM_{30} mode patch antennas are presented. First, it is demonstrated that SLL and return loss performance of notch loaded TM_{30} mode patch described in Chapter 4 can be improved by etching a fractal slot at the center of patch. Second method is applicable to slot loaded TM_{30} mode patch antenna presented in Chapter 3 wherein symmetric radiation pattern and gain enhancement was realized using differential feeding. However, in some applications single coaxial feed is more preferred. It is demonstrated that by using a two dimensional 2×2 slot array, single-fed TM_{30} mode patch antennas can be realized.

5.2 Notch and Slot Loaded TM_{30} Mode Patch

It is demonstrated in Section 4.2.1 that notch loading technique can be applied for gain enhancement and SLL reduction in conventional TM_{30} mode patch antenna. It is shown that notch loaded TM_{30} mode patch has reduced SLL of about -11 dB,

an improvement of 8 dB compared to its conventional counter part. However, in many applications low SLL are desired. Thus, it is useful to look for techniques resulting in further reduction in SLL. Moreover, coaxial probe position in notch loaded TM_{30} mode patch is fixed, located at $L/3$ from edge or $\ell/2$ from center of patch, see Fig. 4.1. As a result return loss of notch loaded TM_{30} mode patch is also fixed. Since we can not change the location of probe because it will in turn change the surface current distribution of patch, we need to explore other mechanism for improvement in return loss. In this section, it will be demonstrated that by using a fractal slot loading at center of TM_{30} mode patch both SLL reduction and return loss improvement in TM_{30} mode patch can be realized.

5.2.1 Antenna Geometry

The proposed notch loaded TM_{30} mode patch with fractal slot loading is shown in Fig. 5.1. Please note that all the antenna dimensions as well as the substrate parameters are same as that of notch loaded TM_{30} mode patch given in Chapter 4. An additional fractal slot is embedded in the center of patch. In order to understand the working principle it is useful to look at the surface current distribution of the fractal loaded patch as shown in Fig. 5.2. It can be seen that fractal slot mainly affects center undesired current distribution whereas its effect on outer desired surface current distribution regions is negligible. By introducing a fractal slot undesired surface current distribution is reduced.

A question can be asked how this will effect the radiation characteristics such as gain, SLL and cross polarization of antenna? A related question is that how will it influence the impedance matching of patch? In the next section, answers of these questions will be explored. It will be demonstrated that improvement in SLL of notch loaded TM_{30} mode patch antenna can be achieved by introducing a fractal slot at the center of notch loaded patch. Moreover, it will be shown that introduction of additional slot adds a new degree of freedom for S_{11} improvement, rather than to move the feed.

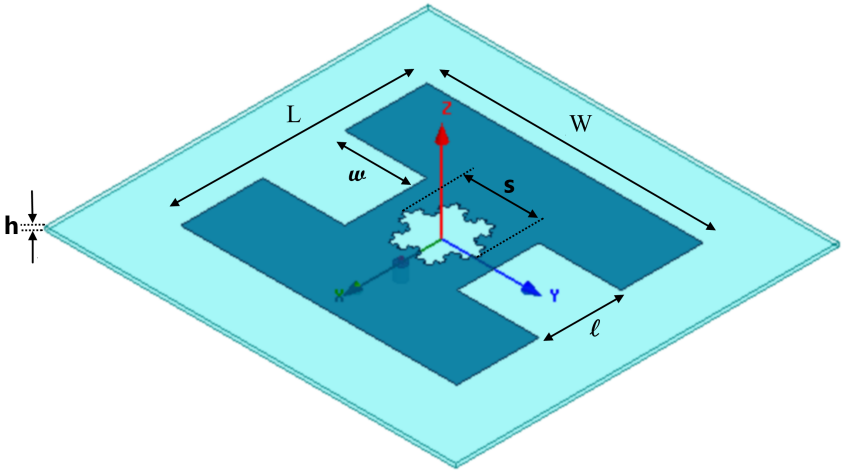

FIGURE 5.1: Geometry of notch and fractal slot loaded TM_{30} mode patch.

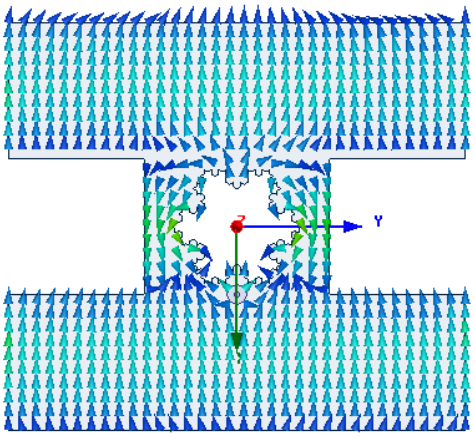

FIGURE 5.2: Surface current distribution of notch and fractal slot loaded TM_{30} mode patch.

5.2.2 Fractal Slot Loading for Improvement in SLL and Return Loss

A 3^{rd} iteration koch fractal slot is created at the center of notch loaded TM_{30} mode patch antenna as shown in Fig. 5.1. The fractal slot is obtained by applying three fractal iterations to an equilateral triangle (also known as initiator) with side length of 2.51 cm. The effect of fractal slot size on the SLL and S_{11} of proposed antenna is shown in Fig. 5.3. Three normalized slot sizes namely: $s = 0$, $s = 0.5$ and $s = 1$ are investigated. Here, zero slot size represent no fractal slot loading i.e., notch loaded patch without fractal loading, whereas slot size equal to 1 represents the full slot loading with initiator edge length of 2.51 cm (Fig. 5.1). It is shown

in Fig. 5.3(a) that by changing the slot size s from 0 to 1, E-plane SLL are reduced from -10.8 dB to -16.1 dB. An improvement of about 5.3 dB in SLL is thus achieved by using fractal slot loading. Figure 5.3(b) shows the effect of slot size on S_{11} of the proposed antenna. It can be observed that by increasing the slot size, resonant frequency is shifted downward. More importantly impedance matching is also improved with the introduction of slot. The value of S_{11} changes from -16 dB to -23 dB by increasing the slot size s from 0 to 1. An improvement of around 7 dB in S_{11} is thus achieved by using a fractal slot loading. Thus, introduction of frcatal slot adds a new degree of freedom for S_{11} improvement, rather than to move the feed.

5.2.3 Simulated Radiation Characteristics

Simulated radiation characteristics namely E and H-plane radiation patterns, gain, SLL , and cross polarization of notch and fractal slot loaded TM_{30} mode patch are investigated in this section. Fractal slot size $s = 1$ is used in all the cases.

Simulated E- and H-plane co-polarization radiation patterns are shown in Fig. 5.4(a). The simulated gain of fractal and notch loaded TM_{30} patch is 13.4 dBi. E-plane SLL of the antenna is -16.1 dB whereas simulated H-plane SLL are less than -26 dB. However, it is important to note that in H-plane back lobes levels are higher than the SLL. Infact, if we consider the backlobe levels as SLL then simulated H-plane SLL are -19.3 dB. The simulated E- and H-plane cross polarization radiation patterns are shown in Fig. 5.4(b). It can be seen that H-plane cross polarization are more dominant compared to E-plane. The peak value of cross pol in H-plane is -22 dB which is about 35 dB below main lobe.

5.2.4 Simulated S_{11} and Impedance Bandwidth

Simulated S_{11} of fractal loaded antenna is shown in Fig. 5.3(b), ($s = 1$). The resonant frequency of the antenna is 3.09 GHz. The value of S_{11} at the resonant frequency is -23 dB. The impedance bandwidth of the antenna, $S_{11} \leq -10$dB, is

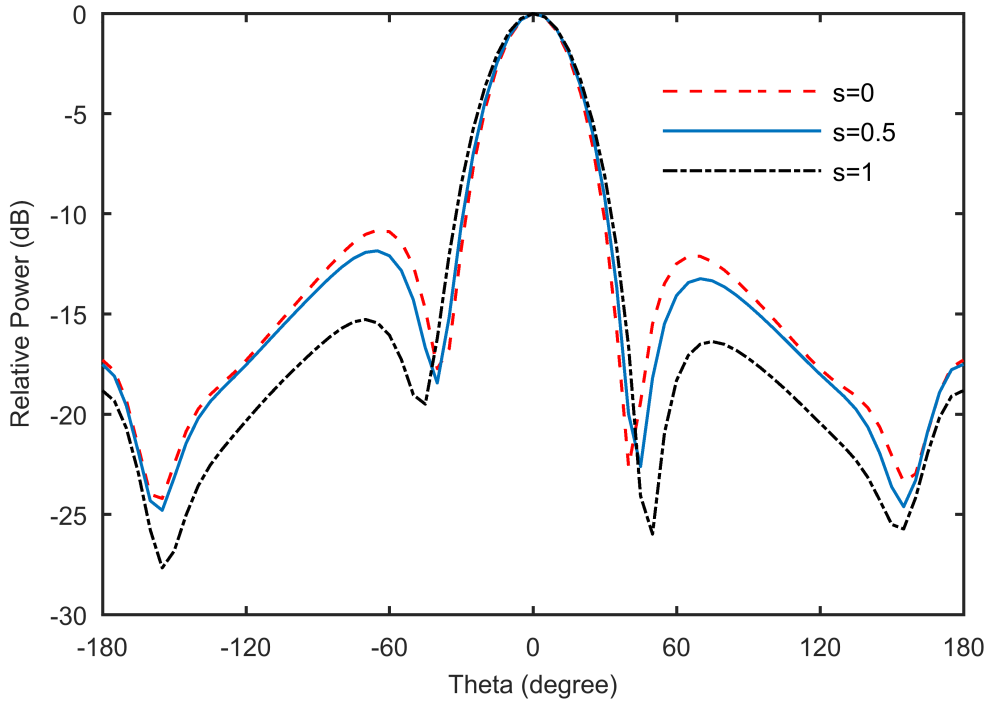

(a)

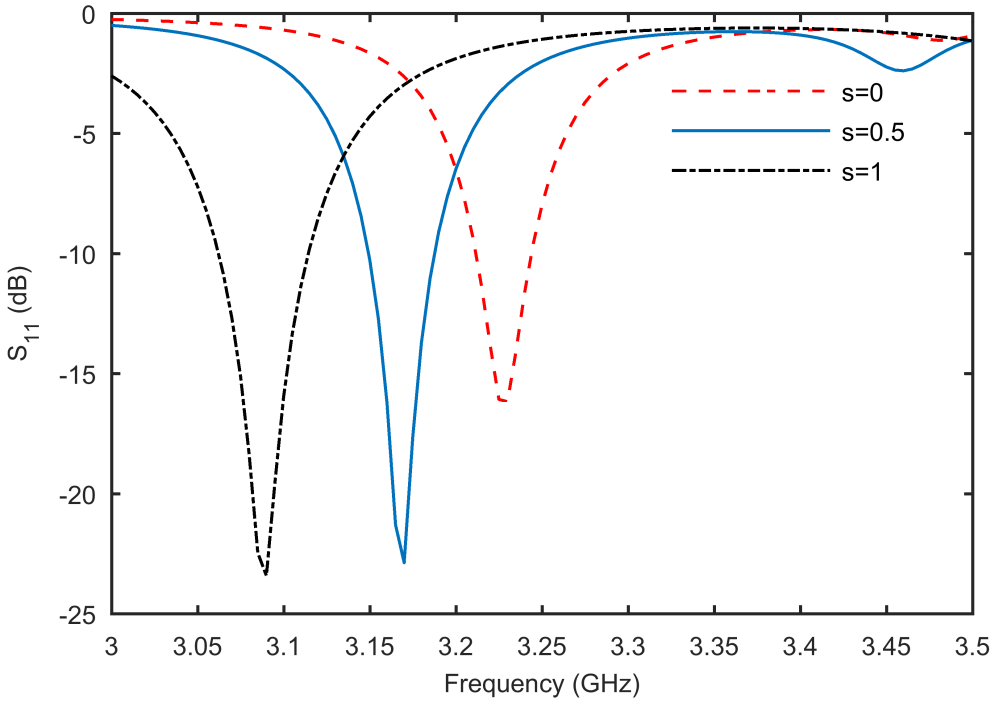

(b)

FIGURE 5.3: Effect of fractal slot size s on (a) E-plane SLL, (b) S_{11}.

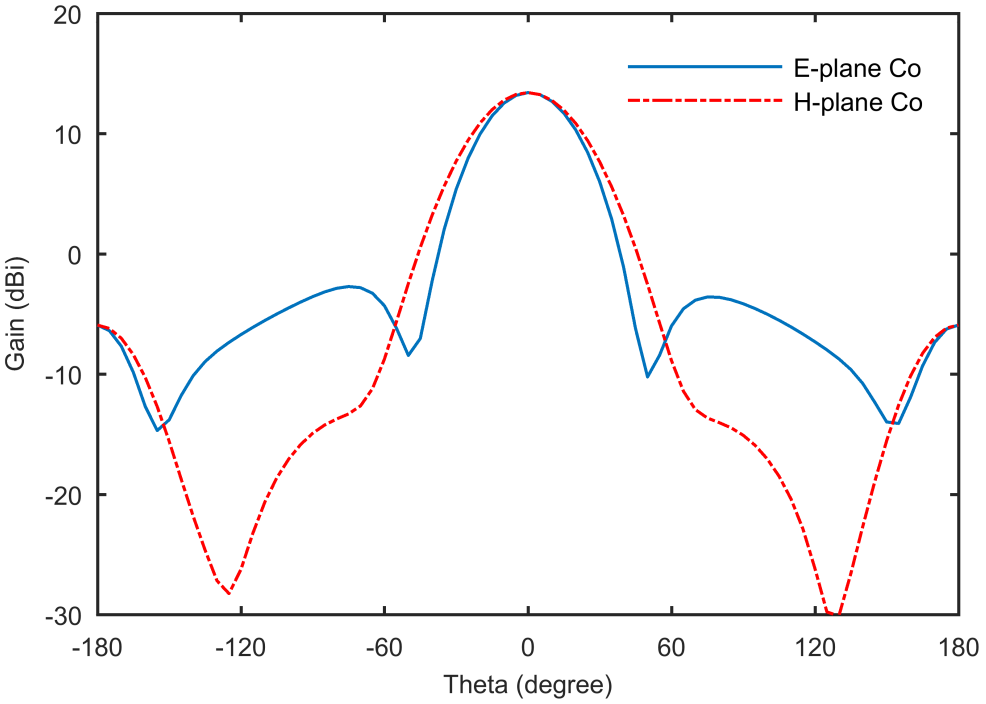

(a)

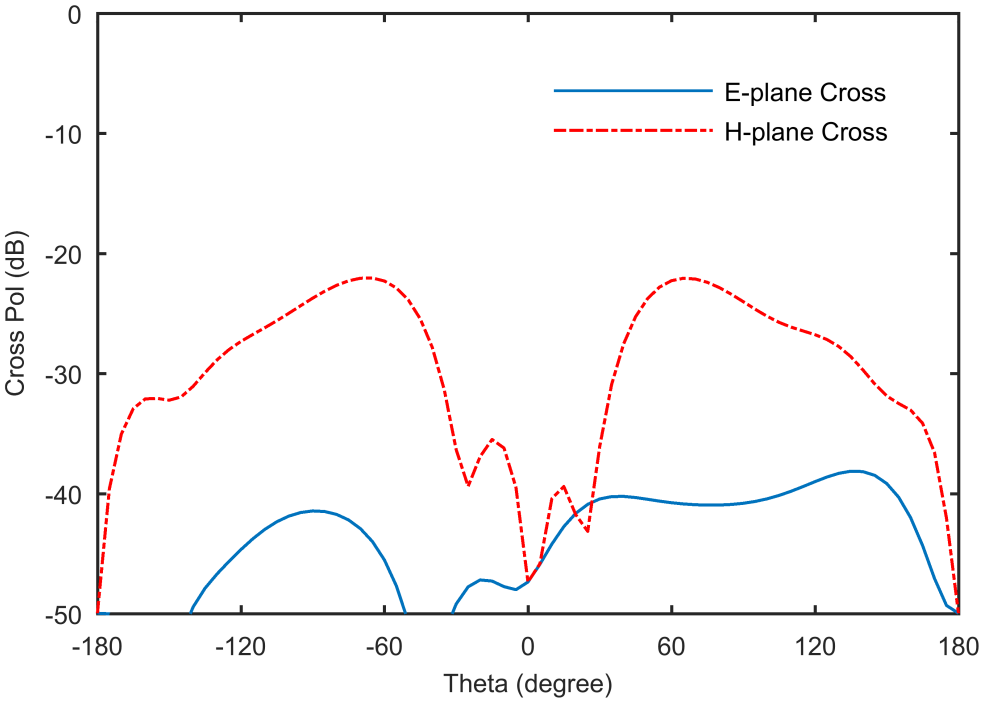

(b)

FIGURE 5.4: Simulated E and H-plane radiation patterns for fractal and notch loaded TM_{30} mode patch (a) Co, (b) Cross.

TABLE 5.1: Notch loaded TM_{30} mode patch with and without slot loading.

Antenna	Frequency (GHz)	Gain (dBi)	SLL (dB)	Return Loss (dB)	Bandwidth (MHz)
Notch loaded	3.23	13.9	-10.8	16	32
Notch and fractal slot loading	3.09	13.4	-16.1	23	52
Notch and circular slot loading	3.14	13.6	-14.5	38	51

52 MHz (1.68%). The relative bandwidth of TM_{30} mode patch with and without fractal slot loading is about 1% and 1.68%, respectively. Thus, fractal slot loading also improves the impedance bandwidth of the antenna by a factor of 1.68.

Table 5.1 shows a comparison of notch loaded TM_{30} mode patch with and without fractal slot loading. Introduction of fractal slot results in about 5 dB reduction in E-plane SLL and 7 dB improvement in return loss. Slight reduction of 0.5 dB in fractal slot loaded patch antenna gain can also be observed which can be attributed to reduction in resonance frequency resulting in decrease in the effective area of antenna.

5.2.5 Possiblities of Using Non-Fractal Slot Loading

It is shown that a fractal slot loading in notch loaded TM_{30} mode patch can be used for improvement in E-plane SLL and return loss. A question can be asked that why is fractal slot needed? Is it possible to use simpler slot geometry for instance a circular slot? To answer this question a circular shape slot of varying radius was investigated. It was found that for a circular slot radius of r= 1.3 cm gives better return loss compared to fractal slot. However, SLL and bandwidth are slightly degraded compared to fractal slot as shown in Table 5.1. Thus, a simple circular slot gives almost similar performance as that of fractal slot and can also be used to improve the notch loaded TM_{30} mode patch performance.

5.3 Single Fed Slot Loaded TM_{30} Mode Patch

It is demonstrated in Chapter 3 that slot loading technique, in the form of a 1×2 slot array located at the center of patch, can be used for gain enhancement and SLL reduction in conventional TM_{30} mode patch antenna. However, slot loading results in asymmetric radiation pattern and reduction in gain which can be circumvented by using differential feeding. In some applications single fed antennas are more desired. Thus, it is useful to look for techniques which can be used to realize single-fed slot loaded TM_{30} mode patch. Since the main cause of asymmetric radiation pattern in slot loaded TM_{30} mode patch proposed in Chapter 3 was asymmetric surface current distribution. If somehow symmetric surface current distribution can be realized then it is possible to achieve single-fed slot loaded TM_{30} mode patch antenna. How can we realize symmetric current distribution without differential feeding? In this section, it will be demonstrated that by using a 2×2 slot array at the center of patch single fed high gain TM_{30} mode antenna with symmetric radiation pattern can be realized.

5.3.1 Antenna Design

The proposed slot loaded TM_{30} mode patch with a planar 2×2 slot array etched at the center is shown in Fig. 5.5. Please note that all the antenna dimensions as well as the substrate parameters are same as that of slot loaded TM_{30} mode patch given in Chapter 3. The only difference is that now we are employing a planar 2×2 slot array instead of a linear 1×2 slot array used previously.

The design of antenna was carried out based on the maximum directivity criterion. First, a single slot was introduced at the center region of the patch and its length and width were optimized to achieve the maximum directivity at the center frequency. Next a linear 1×2 array of optimized slot was created on one side of the patch center. The slots dimensions and inter slot spacing were optimized again with the goal of achieving maximum directivity. The optimized 1×2 linear slot array dimensions were then used as a starting point for creating planar 2×2 slot

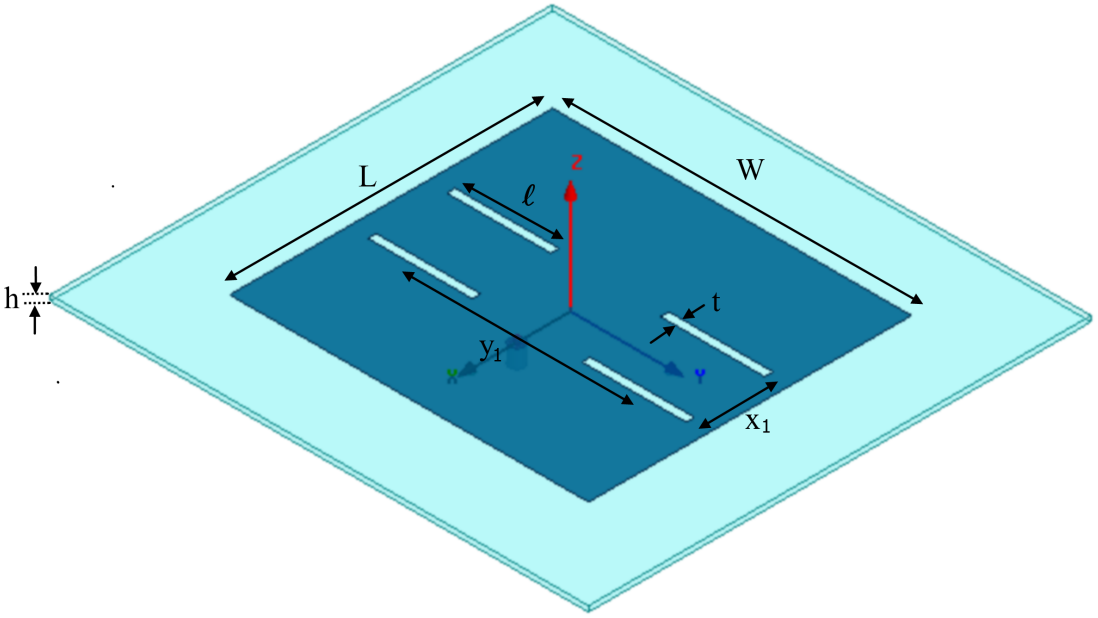

FIGURE 5.5: Geometry of single-fed slot loaded TM_{30} mode patch.

array. The slots dimensions and inter slot spacing in x and y directions were optimized again to achieve the maximum directivity. Final 2×2 slot array dimensions are $\ell = 2.9$ cm, $t = 0.23$ cm, $x_1 = 2.19$ cm,and $y_1 = 5.98$ cm.

It is worthwhile to look at the surface current distribution of the single-fed 2×2 slot loaded TM_{30} mode patch antenna and compare it with single-fed 1×2 slot loaded patch. Fig. 5.6 shows the surface current distribution of 2×2 slot loaded TM_{30} mode patch antenna. It can be seen that contrary to surface current distribution of single-fed 1×2 slot loaded antenna shown in Fig. 5.7, the proposed single-fed 2×2 slot loaded antenna has symmetric current distribution. This is very important as surface current distribution and far-field radiation pattern are related to each other. As we will see in the next section, 2×2 slot loaded antenna yields a symmetric pattern. This is not surprising because if cause (surface current distribution) is symmetric effect(radiation pattern) will also be symmetric.

5.3.2 Simulated Radiation Characteristics

Simulated radiation characteristics namely E and H-plane radiation patterns, gain, SLL , and cross polarization of single-fed 2×2 slot loaded TM_{30} mode patch are

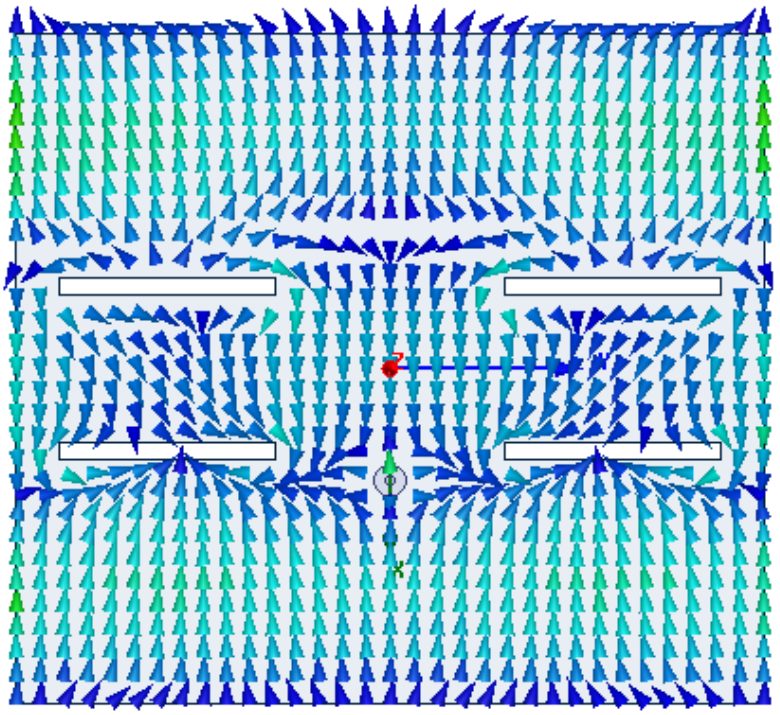

FIGURE 5.6: Surface current distribution of single-fed 2×2 slot loaded TM_{30} mode patch.

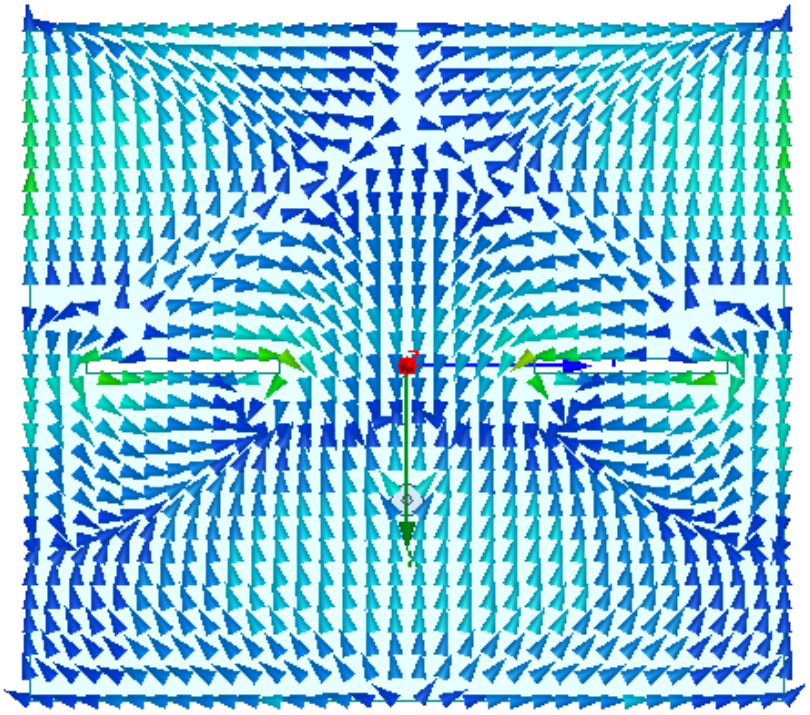

FIGURE 5.7: Surface current distribution of single-fed 1×2 slot loaded TM_{30} mode patch.

investigated in this section. All the simulations were performed in full-wave EM simulator HFSS.

Simulated E- and H-plane co-polarization radiation patterns are shown in Fig. 5.8(a). The simulated gain of 2×2 slot loaded TM_{30} patch is 13.3 dBi. E-plane SLL of the antenna is -9.2 dB whereas simulated H-plane SLL are -23 dB. However, it is important to note that in H-plane back lobes levels are considerably higher than the SLL. Infact, if we consider the backlobe levels as SLL then simulated H-plane SLL are -16 dB. The simulated E and H-plane cross polarization radiation patterns are shown in Fig. 5.8(b). It can be seen that H-plane cross polarization are more dominant compared to E-plane. The peak value of cross polarization in H-plane is -17 dB which is about 30 dB below main lobe.

5.3.3 Simulated S_{11} and Impedance Bandwidth

Simulated S_{11} of 2×2 slot loaded TM_{30} mode patch is shown in Fig. 5.9. The resonant frequency of the antenna is 3.18 GHz. The value of S_{11} at the resonant frequency is -18 dB. The impedance bandwidth of the proposed antenna, $S_{11} \leq -10$dB, is about 30 MHz (relative bandwidth of 0.94 %).

Table 5.2 shows a comparison of slot loaded TM_{30} mode patch with 1×2 (differential fed) and 2×2 (single-fed) slot loading. Both antennas have similar gain performance. E-plane SLL of 2×2 slot loaded TM_{30} mode patch is -9.2 dB whereas 2×2 slot loaded patch has SLL equal to -12.7 dB. Therefore 1×2 slot loaded patch shows about 3 dB reduction in E-plane SLL compared to 2×2 slot loaded patch. The possible reason for degraded SLL in 2×2 slot loaded patch can be attributed to the maximum directivity design criteria used for antenna optimization which ignores the SLL performance. The impedance bandwidth of 2×2 and 1×2 slot loaded TM_{30} mode patch antennas are 30 MHz (relative bandwidth of 0.94%) and 21 MHz (relative bandwidth of 0.7%), respectively. Therefore, single fed 2×2 slot loaded TM_{30} mode patch has better bandwidth performance.

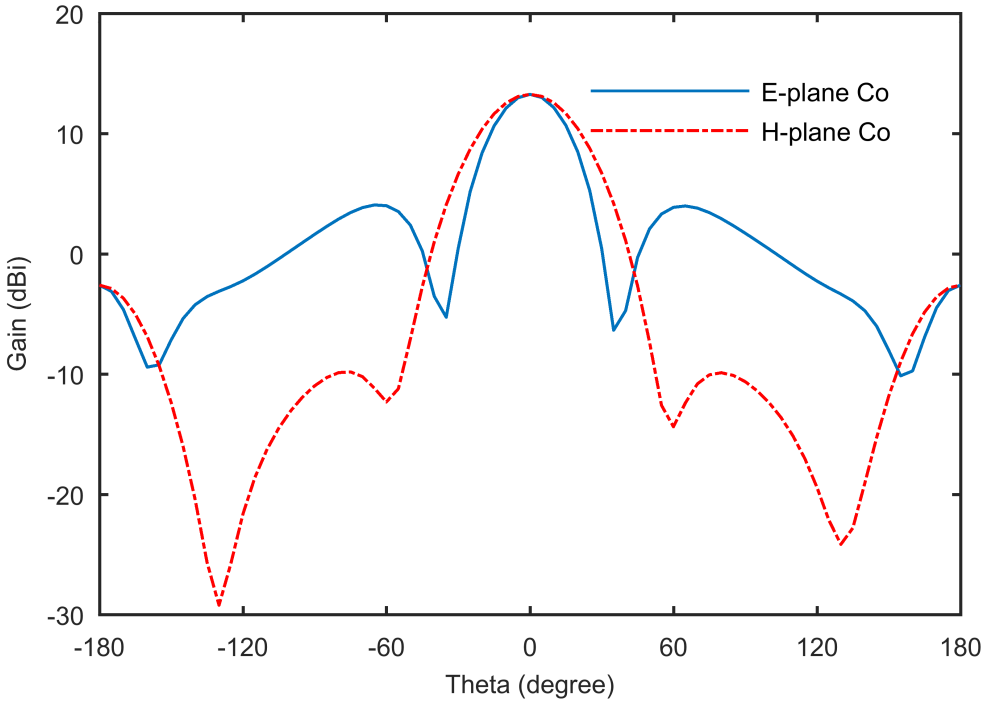

(a)

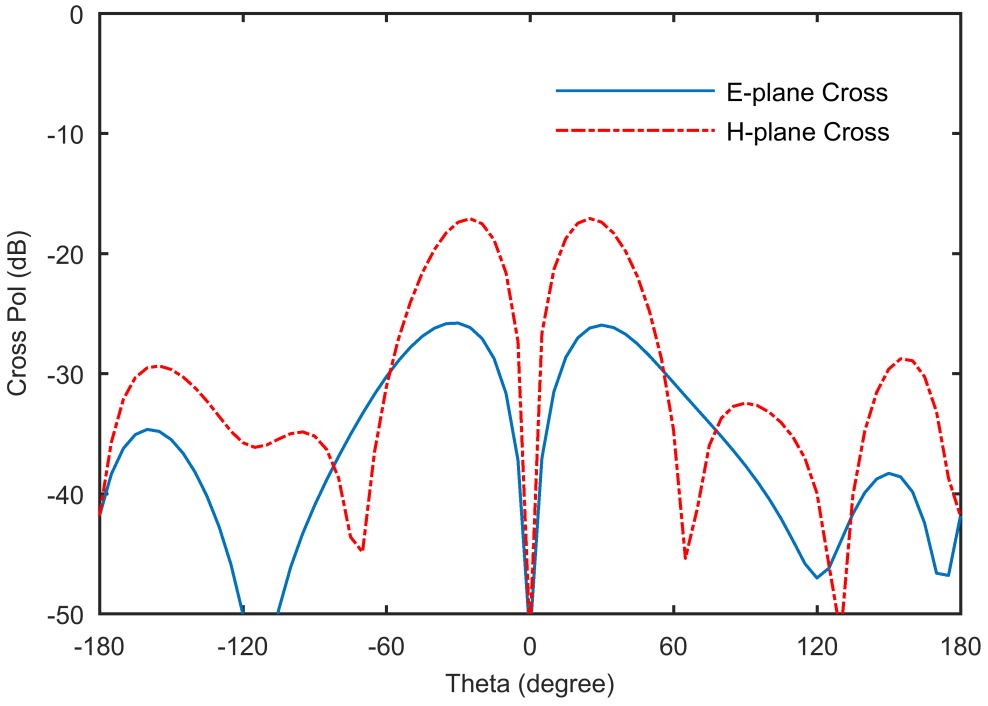

(b)

FIGURE 5.8: Simulated E and H-plane radiation patterns for 2×2 slot loaded TM_{30} mode patch (a) Co, (b) Cross.

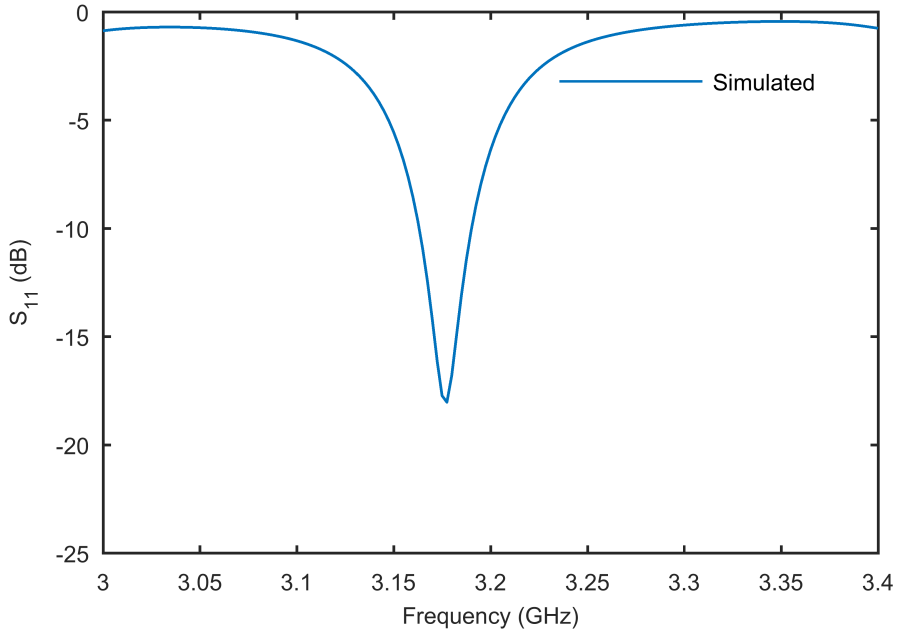

FIGURE 5.9: Simulated S_{11} of 2×2 slot loaded TM_{30} mode patch.

TABLE 5.2: Differential and single-fed slot loaded TM_{30} mode patch antennas.

Antenna	Frequency (GHz)	Gain (dBi)	SLL (dB)	Bandwidth (MHz)
Differential fed slot loaded TM_{30}	3	13.2	-12.7	21
Single-fed slot loaded TM_{30}	3.18	13.3	-9.2	30

5.4 Summary

In this chapter, two methods for improving the radiation characteristics of TM_{30} mode patch antennas are presented. In first method, it is shown that by combining the fractal and notch loading technique SLL reduction and return loss improvement can be realized. It is demonstrated that fractal and notch loaded TM_{30} mode patch can achieve more than 5 dB in reduction in E-plane SLL and 7 dB improvement in return loss. In second method, a solution for asymmetric radiation pattern in single-fed 1×2 slot loaded TM_{30} mode patch is proposed. In this method, a planar 2×2 slot array is etched in the center of TM_{30} mode patch. It is demonstrated that single-fed 2×2 slot loaded TM_{30} mode patch can achieve high gain and symmetric radiation pattern without the need of differential feeding used

earlier. The proposed 2×2 slot loaded TM_{30} mode patch has better bandwidth compared to 1×2 slot loaded patch. However, the SLL of 2×2 slot loaded patch are higher than the 1×2 slot loaded patch. One possible reason can be that optimized antenna dimensions were found using maximum directivity criteria which ignores the SLL. In future, antenna optimization based on SLL performance can be explored.

Chapter 6

Dual Band CRLH Transmission Line Coupled Patch Antenna

6.1 Introduction

Multiband planar antennas are an integral part of many wireless communication systems. Microstrip antennas are widely used due to their low profile and ease of fabrication. In the past, different techniques have been reported to realize dual band microstrip patch antennas, which usually employ stacked patch configuration [52], or reactive loading in the form of slots [43, 57, 84].

Metamaterials due to their unique properties provide new ways of antenna design [3, 4, 20]. In particular, composite right/left handed transmission line (CRLH TL) metamaterials are attractive due to their ease of fabrication. They can be used to achieve antenna size miniaturization using zeroth order resonance (ZOR) mode and mutifrequency operation [4, 16, 59–61, 85, 86]. A dual band CRLH TL antenna using $\pm 1^{st}$ order resonance is reported in [16]. However, only fixed large frequency ratio is possible using this method. A linearly polarized multiband patch antenna, partially filled with mushroom type CRLH structure is presented in [59], wherein it is shown that two antenna configurations are possible: a dual mode tri band antenna having broadside pattern at $\pm 1^{st}$ order resonances and omnidirectional

(monopolar) pattern at ZOR mode; or a dual band antenna having broadside pattern employing $\pm 1^{st}$ order resonances. Although, arbitrary frequency ratio can be obtained using this technique but it suffers from low radiation efficiency at -1 resonance. A dual band circularly polarized antenna loaded with mushroom type CRLH structure is reported in [60]. Circular polarization is achieved by exciting two orthogonal -1 resonances with 90^0 phase difference. Recently, a dual band pattern diversity patch antenna using CRLH TL is presented in [61]. It employs an annular ring with circular patch antenna placed at the center, both loaded with CRLH TL. The annular ring provides broadside pattern using $\pm 1^{st}$ order modes while circular patch provides monopolar pattern. Although, the reported antenna has good radiation efficiency but broadside radiation patterns are not identical at upper and lower frequency bands. Moreover, fabrication complexity increases due to multilayer structure.

In general, most of the metamaterial loaded antennas reported in the literature are based on the mushroom type CRLH structure wherein dual band operation with broadside pattern is achieved using symmetric ± 1 modes. ZOR mode is primarily used for antenna size reduction or to achieve omnidirectional pattern in the horizontal plane [59, 85, 86]. However, as per our knowledge no work has been reported where ZOR mode is used for dual band frequency reconfigurable applications, with broadside radiation pattern and arbitrary non-integer frequency ratio.

In this chapter, we propose a novel dual band CRLH TL coupled patch antenna. In the proposed configuration, a CRLH TL unit cell is gap-coupled with the radiating edge of the patch. The dual band operation is achieved by resonant coupling the ZOR mode of CRLH TL and TM_{10} mode of patch antenna. The proposed antenna is distinct in the sense that dual resonance is not obtained using symmetric ± 1 modes but ZOR mode and TM_{10} mode coupling. Good radiation efficiency and almost identical broadside radiation patterns are achieved at both resonance frequencies. Another advantage of the proposed configuration is that by changing the inductance of CRLH TL unit cell resonance frequency can be changed. This feature can be used to realize frequency reconfigurable dual band patch antenna.

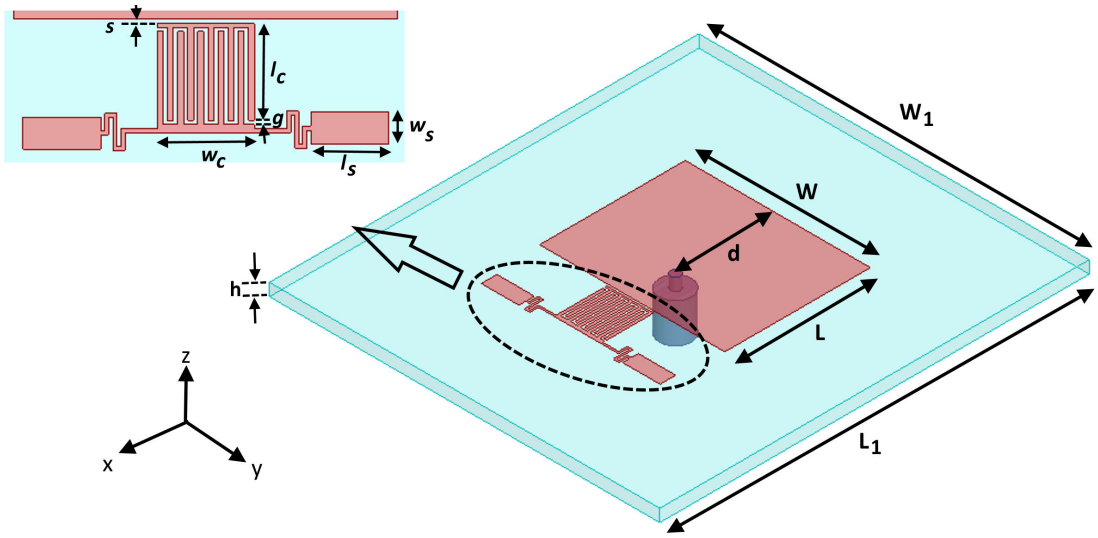

FIGURE 6.1: Geometry of the proposed antenna ($W = 23.72$, $L = 18.65$, $W_1 = 50$, $L_1 = 55$, $d = 13.12$, $s = 0.25$, $l_c = 5.75$, $w_c = 6$, $l_s = 4.8$, $w_s = 2$, $g = 0.25$, all dimensions in mm).

In addition, proposed antenna is simple to fabricate and suitable for single layer dual band array applications.

6.2 Dual Band CRLH TL Coupled Patch Antenna

6.2.1 Antenna Configuration and Working Principle

The proposed antenna geometry is shown in Fig. 6.1. It consists of a rectangular patch antenna, which is gap-coupled to a symmetrical CRLH TL unit cell along the radiating edge of the patch using a coupling gap s. The CRLH TL cell is composed of an interdigital capacitor and a meander line inductor. A virtual ground capacitor is employed to achieve via less design. Antenna is designed using Rogers RT/Duroid 5880 substrate having $\epsilon_r = 2.2$ and thickness $h = 1.58\,mm$. A single coaxial probe is used to feed the patch antenna.

An approximate equivalent circuit model of the proposed CRLH TL coupled patch antenna is shown in Fig. 6.2. A T-type equivalent circuit is used to represent

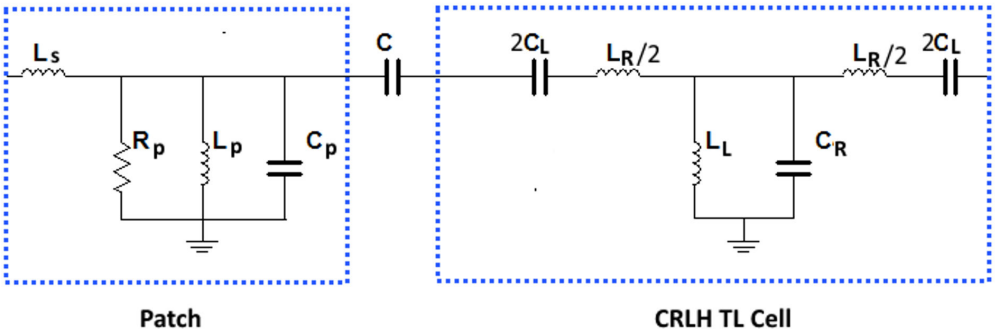

FIGURE 6.2: Equivalent circuit model of the proposed antenna ($L_S = 0.84\,nH$, $R_P = 180\ \Omega$, $L_P = 0.29\ nH$, $C_P = 3.56\ pF$, $C = 0.7\ pF$, $C_L = 0.62\ pF$, $L_R = 1.63\,nH$, $L_L = 0.23\,nH$, $C_R = 4.32\,pF$).

the symmetric CRLH unit cell [4] and a parallel RLC resonator with series probe inductance L_s is used to model the patch antenna. The patch antenna is capacitive coupled to the CRLH TL unit cell by a capacitance C. A brief explanation for the parameters of CRLH TL unit cell is as follows, L_L and L_R represent the left hand shunt and right hand series inductances whereas C_L and C_R represent the left hand series and right hand shunt capacitances as explained in Section 1.3. The equivalent circuit parameters of CRLH TL unit cell are extracted using an off resonance technique given in [87].

One of the advantages of the proposed antenna is that the CRLH TL unit cell and patch antenna can be designed separately thus providing design simplicity. The design of antenna can be carried out in three steps: a) patch antenna design, b) CRLH TL unit cell design and c) coupling design. First, a coaxial fed rectangular patch antenna is designed operating in the fundamental TM_{10} at resonance frequency of 5 GHz. Next, a symmetrical CRLH TL unit cell is designed operating in ZOR mode. The phase constant β for CRLH TL unit cell is given by [20].

$$\beta = z(\omega)\sqrt{\omega^2 L_R C_R + \frac{1}{\omega^2 L_L C_L} - \left(\frac{L_R}{L_L} + \frac{C_R}{C_L}\right)} \tag{6.1}$$

where ω is the frequency in radian and $z(\omega)$ can be calculated by using below mentioned expression.

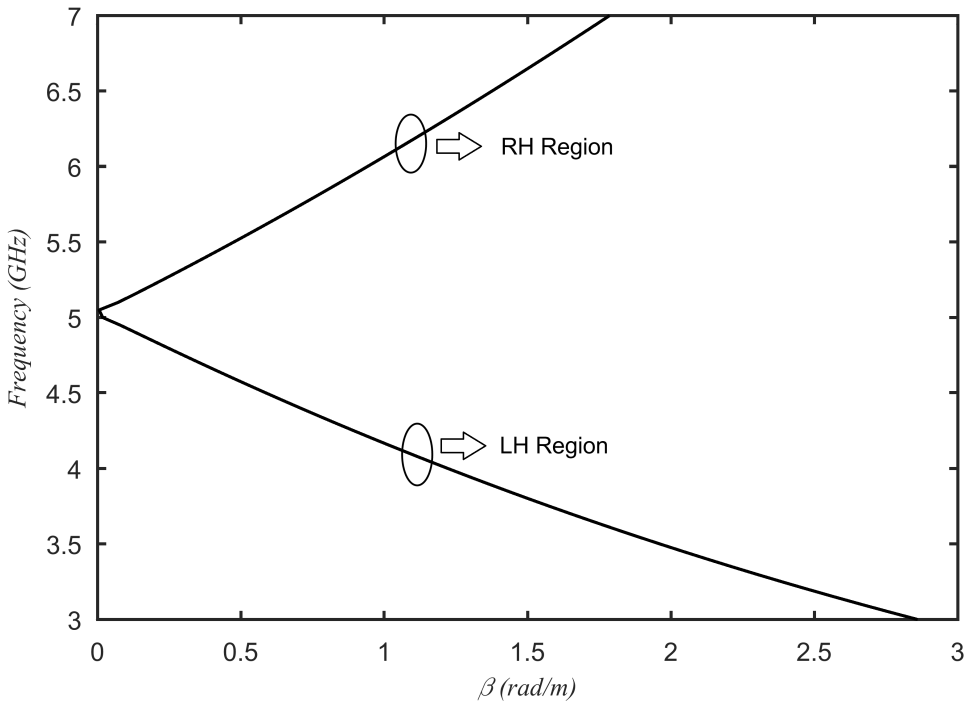

FIGURE 6.3: Dispersion diagram of CRLH TL unit cell.

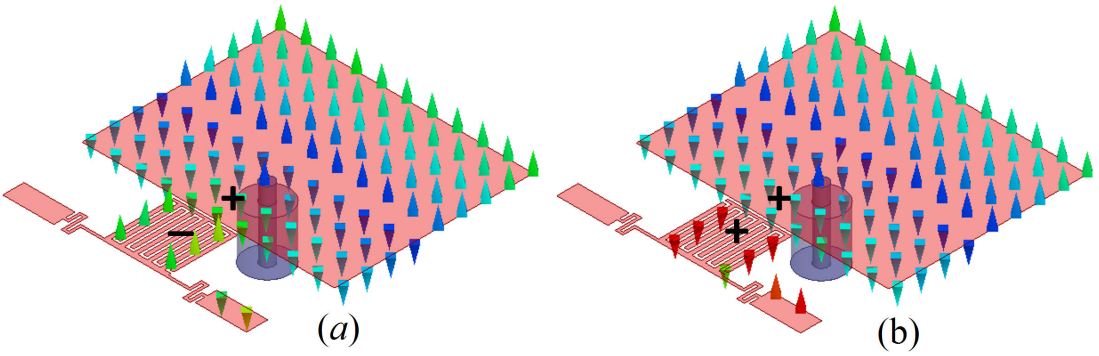

FIGURE 6.4: Electric field distributions of the proposed dual band patch antenna (a) lower resonance frequency f_1 and (b) upper resonance frequency f_2.

$$z(\omega) = \begin{cases} -1 \quad if\ \omega < \omega_{\Gamma 1} = min\left(\dfrac{1}{\sqrt{L_R C_L}}, \dfrac{1}{\sqrt{L_L C_R}}\right) \\ \\ +1 \quad if\ \omega > \omega_{\Gamma 2} = max\left(\dfrac{1}{\sqrt{L_R C_L}}, \dfrac{1}{\sqrt{L_L C_R}}\right) \end{cases}$$

Figure 6.3 shows the dispersion diagram of the CRLH TL. Two separate regions, i.e. left hand (LH) region and right hand (RH) region can be observed. The ZOR mode is obtained at 5.06 GHz which corresponds to $\beta = 0$ in the dispersion

diagram. Finally, the dual mode behavior is realized by coupling the TM_{10} mode patch and ZOR mode CRLH TL unit cell. The spacing between the patch and CRLH TL unit cell affects the coupling. It will be shown in Section 5.2.2 that this can be used to vary the frequency ratio of the proposed dual band patch antenna. In fact, it is possible to initially design the patch antenna and CRLH TL unit cell operating at the same resonance frequency and to control the frequency ratio later by changing the spacing between them. Since the resonance frequencies of coupled resonators (synchronously or asynchronously tuned) are different from the uncoupled single resonators. As an example, a frequency ratio of $f_2/f_1 = 1.08$ is demonstrated in the proposed design which corresponds to $s = 0.25\,mm$.

Further insight into the working of the proposed CRLH TL coupled dual band patch antenna can be gained by examining the electric field (E-field) distribution. Figure 6.4 shows the E-field distributions of antenna at lower and upper resonance frequencies. It can be seen that the coupling mechanism at both resonance frequencies is different. At lower resonance frequency, the E-field of TM_{10} mode and ZOR mode is out of phase. By contrast, the E-field of both modes is in phase at upper resonance frequency. This behavior is similar to odd and even mode coupling in coupled resonators [88].

6.2.2 Parametric Study

A parametric study was conducted to investigate the effects of different parameters on the performance of the proposed CRLH TL coupled patch antenna. All the simulations were performed using full wave EM simulator HFSS by changing only one parameter at a time. Figure 6.5 shows the simulated reflection coefficient (S_{11}) of the proposed antenna for different values of coupling gap s . It can be observed that by changing the value of s , lower resonance frequency f_1 is effected more as compared to upper resonance frequency f_2 . Thus, it can be used to control the frequency ratio f_2/f_1 . The smaller coupling gap results in larger frequency ratio. The effect of interdigital capacitor length l_c on the S_{11} is shown in Fig. 6.6. By increasing l_c , upper and lower resonance frequencies decrease and both peaks

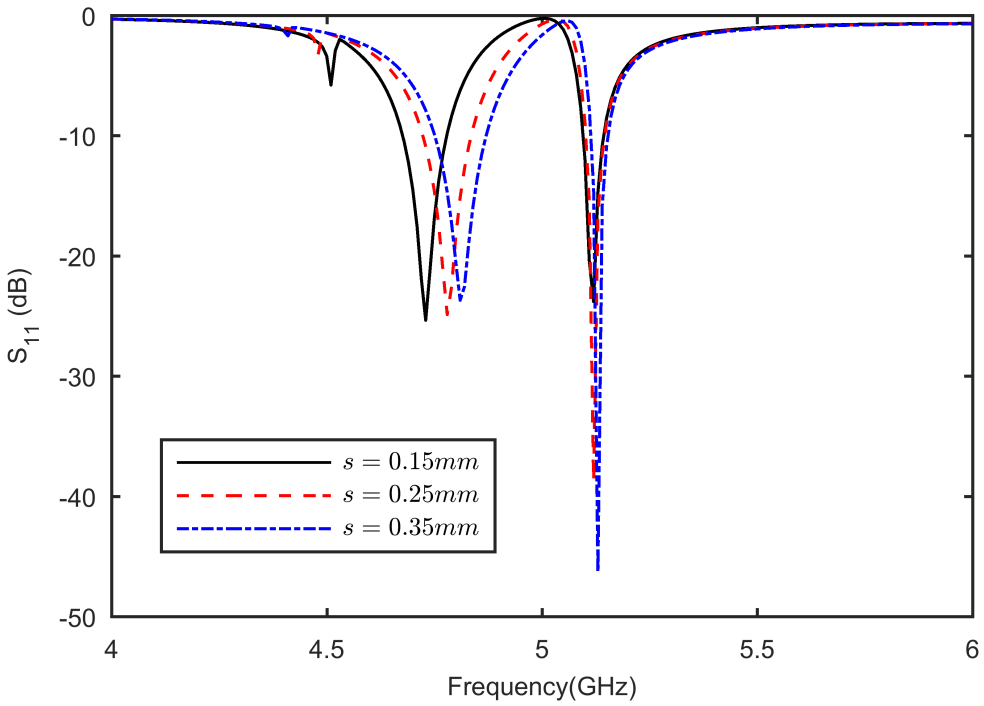

FIGURE 6.5: Effect of coupling gap s on the S_{11} of the proposed antenna.

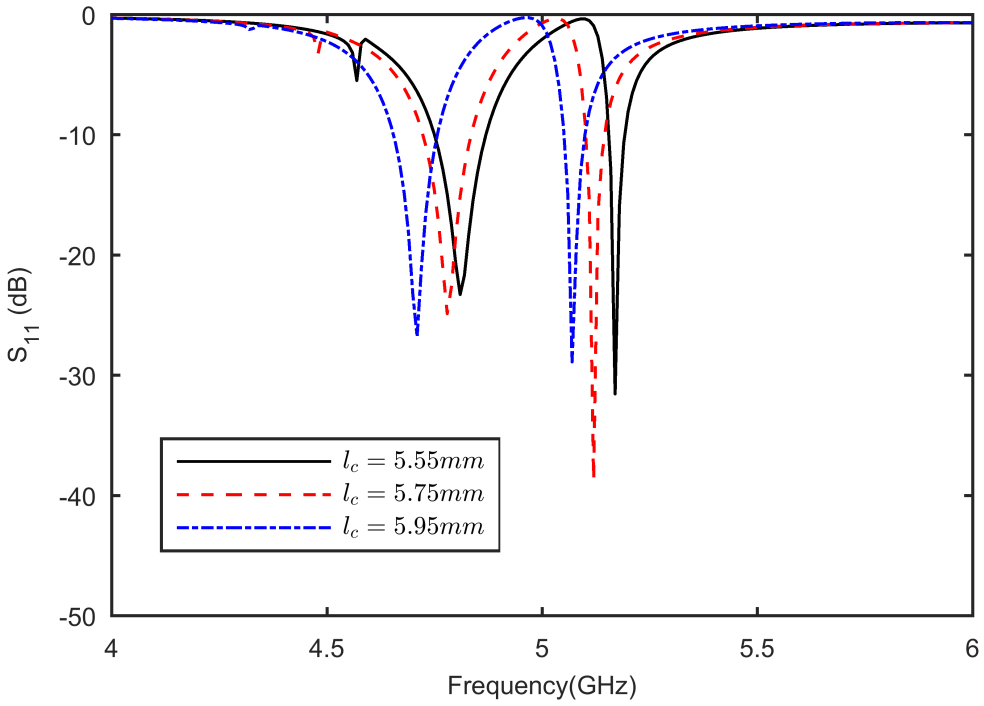

FIGURE 6.6: Effect of interdigital capacitor length l_c on the S_{11} of the proposed antenna.

shift downward. Thus, frequency ratio is not affected by changing interdigital capacitor length l_c but it can be used to set the desired dual band resonance frequencies. Figure 6.7 shows the effect of patch length L on the S_{11}. Its behavior is similar to interdigital capacitor length l_c . As the patch length L increases from $L = 18.3\,mm$ to $L = 19\,mm$, both resonance peaks move down towards a lower resonance frequency.

6.2.3 Frequency Reconfigurable Patch Antenna

Reconfigurable antennas are crucial to cater the ever increasing demand of high data rates in modern wireless communication applications [5, 6]. The proposed CRLH TL coupled patch antenna can achieve frequency reconfigurablity by changing the CRLH TL unit cell. This can be realized practically by switching on and off, one of the two meander line arm of symmetric CRLH TL unit cell. This essentially reduces the left hand inductance by half and affects the resonance frequencies of dual band structure. Figure 6.8 shows the simulated S_{11} plot of the proposed antenna as a function of frequency with two positions of switch S. Switching is implemented by simulating the switch S as open and short circuit, representing the off and on state respectively. It can be observed from Fig. 6.8 that by switching off one meander line arm of CRLH unit cell, first resonance frequency peak moves up from 4.75 GHz to 4.95 GHz, whereas second resonance frequency peak move down from 5.12 GHz to 4.41GHz. Thus beside change in resonance frequencies, frequency ratio is also affected by the switch position. The frequency ratio f_2/f_1 before and after switching is 1.08 and 1.12 respectively. Although not shown, switching off both the meander line arms (using two switches) will result in a single band patch antenna.

6.3 Results and Discussions

A prototype of the proposed CRLH TL coupled patch antenna was fabricated. LPKF PCB milling machine was used to fabricate the antenna. A snapshot of

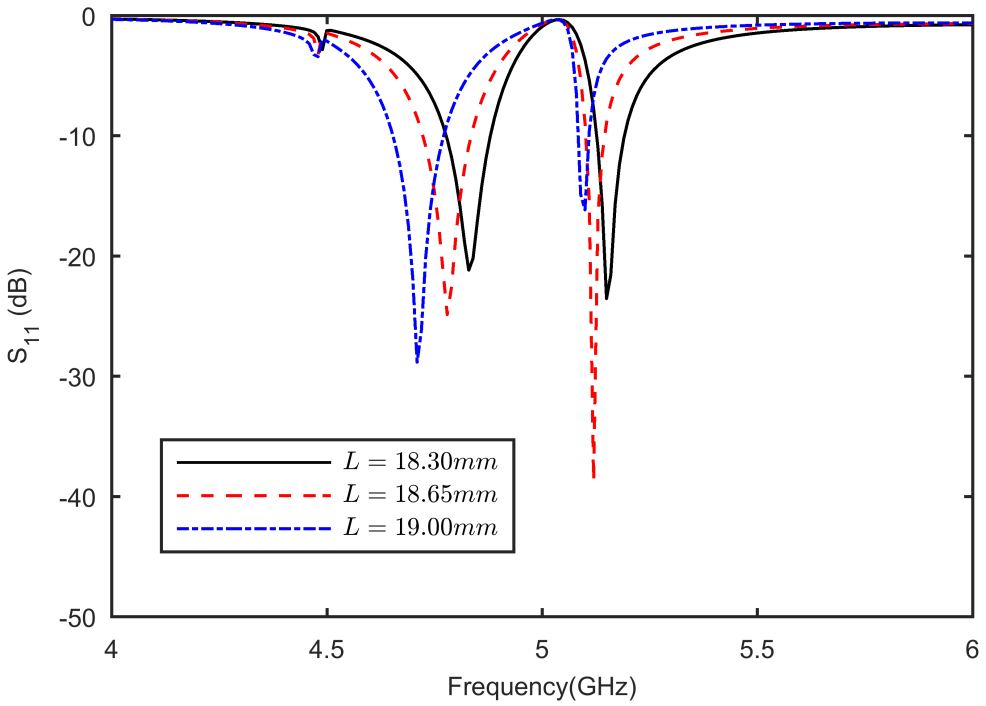

FIGURE 6.7: Effect of patch length L on S_{11} of the proposed antenna.

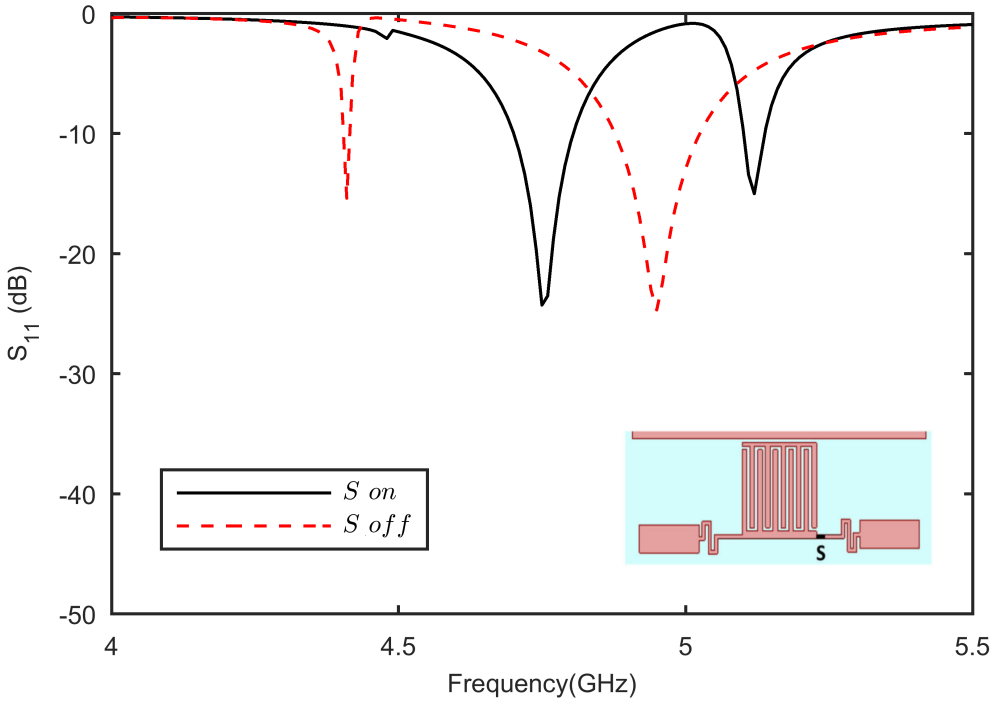

FIGURE 6.8: S_{11} of frequency reconfigurable dual band patch antenna.

the fabricated antenna is shown in Fig. 6.9. The simulated and the measured S_{11} are shown in Fig. 6.10. Agilent PNA network analyzer E8362B was used to measure the S_{11}. Measurement result (Fig. 6.10) shows a dual impedance bandwidth ($S_{11} \leq -10$ dB) of 100 MHz (from 4.78-4.88 GHz) and 50 MHz (from 5.2-5.25 GHz). The relative bandwidths of dual band antenna are 2.07 % and 0.96 % , respectively. Simulated and measured results are in reasonable agreement. Slight shift in the measured S_{11} may be attributed to the fabrication tolerances.

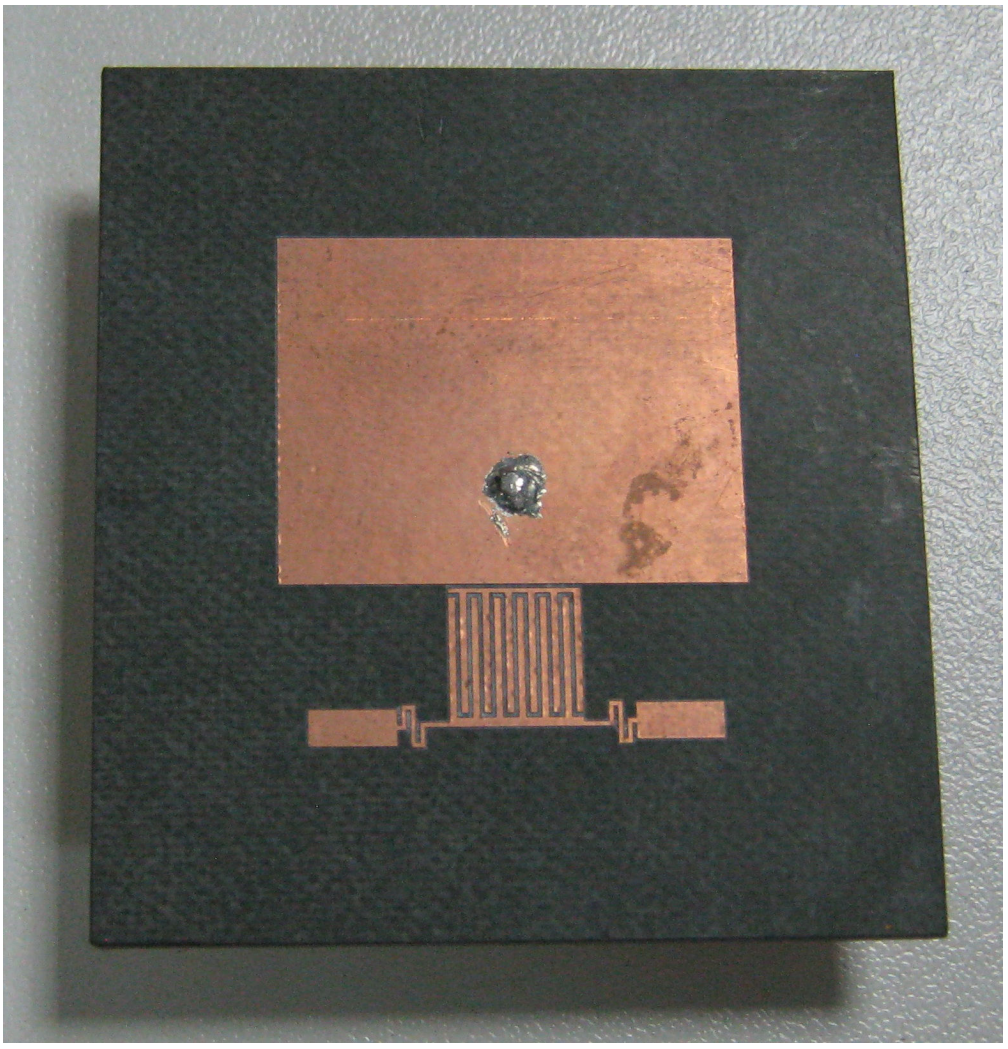

FIGURE 6.9: Fabricated dual band CRLH TL coupled patch antenna.

Simulated and measured E and H-planes normalized radiation patterns of the proposed antenna at resonance frequencies of 4.84 GHz and 5.22 GHz are shown in Figs. 6.11 and 6.12, respectively. Antenna shows broadside almost identical radiation patterns at both resonance frequencies. The measured cross polarization

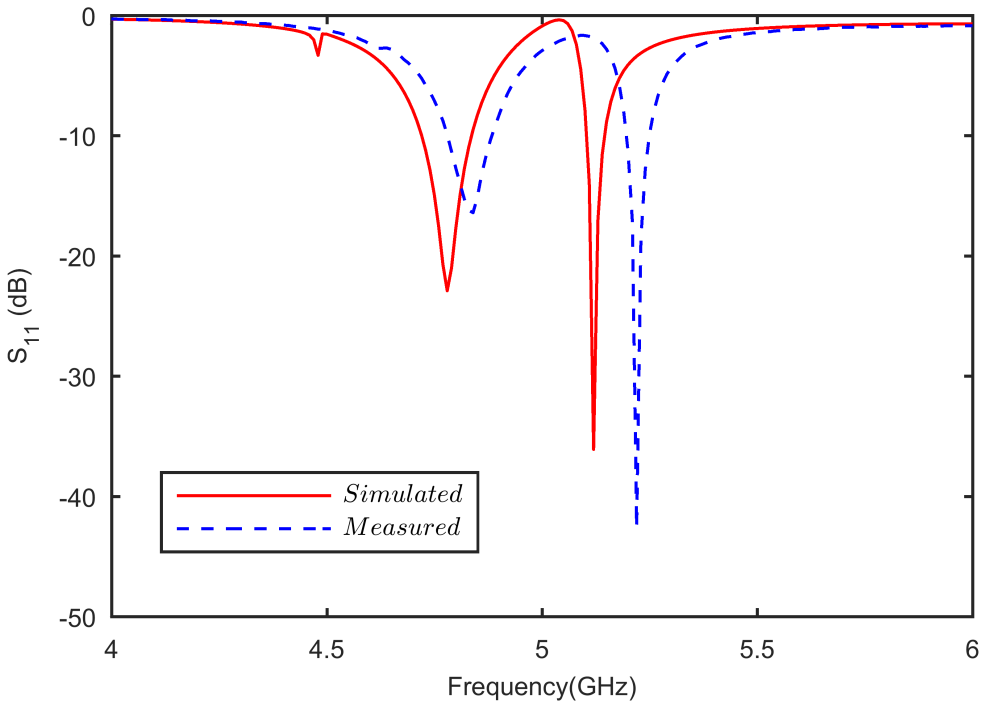

FIGURE 6.10: Simulated and measured S_{11} of dual band CRLH TL coupled patch antenna.

levels are less than -16 dB at both frequencies. The measured antenna gain is 7.4 dBi and 5.8 dBi at lower and upper resonance frequencies.

Table 6.1 shows a comparison of different CRLH TL based dual band patch antennas found in the literature. In contrast to previously reported works which use symmetric ± 1 modes for dual band operation, the proposed antenna uses ZOR and TM_{10} modes coupling to achieve dual band behaviour. Another advantage of the proposed configuration is that it allows frequency reconfigurablity. Moreover, proposed antenna has good radiation efficiency and similar gain at both upper and lower resonance frequencies bands. In addition, due to single layer structure and via less design, it provides ease of fabrication.

6.4 Dual Band CRLH TL Coupled Patch Array

The proposed antenna can be used to design dual band high gain patch arrays. As an example, a 2×2 corporate fed dual band CRLH TL coupled patch array

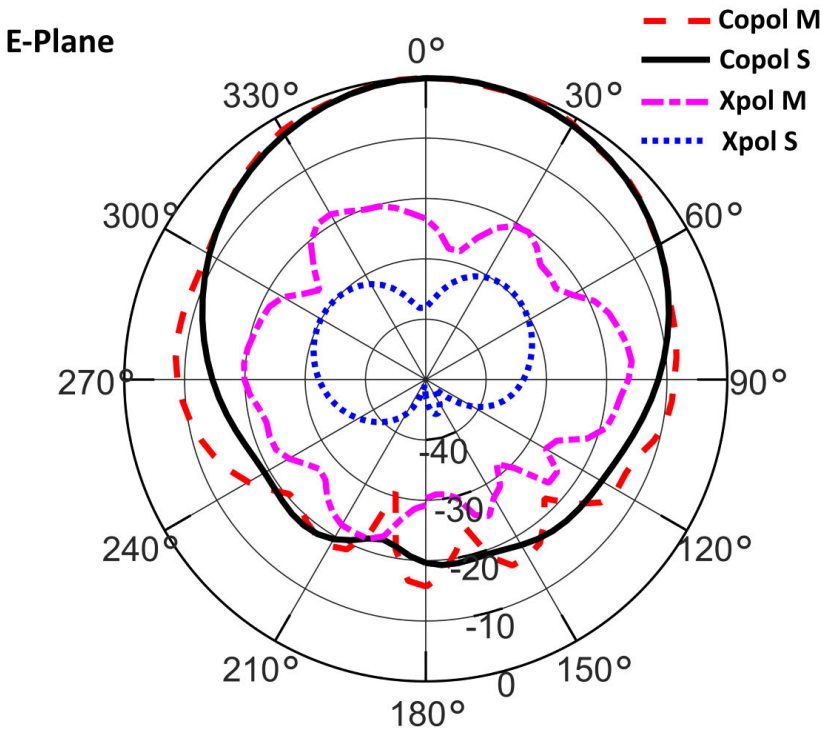

(a)

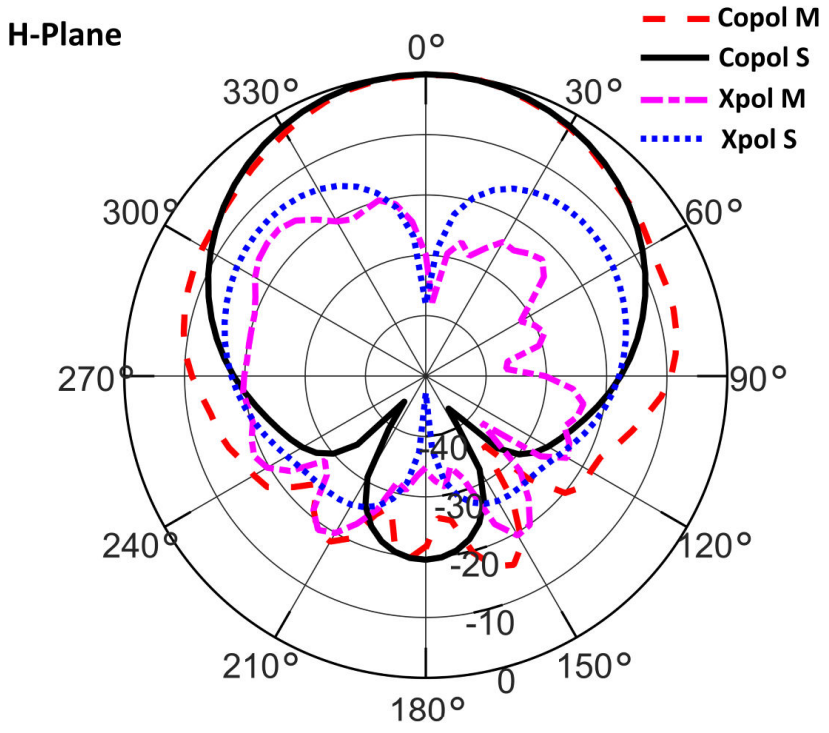

(b)

FIGURE 6.11: Simulated and measured normaized radiation patterns of dual band CRLH TL coupled patch antenna at $f_1 = 4.84$ GHz (a) E-plane and (b) H-plane.

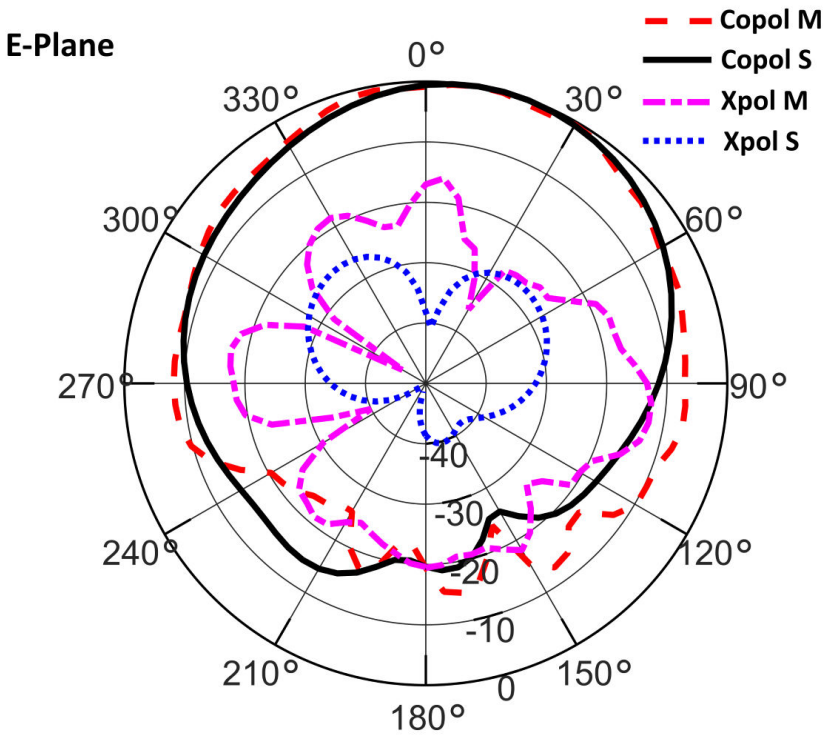

(a)

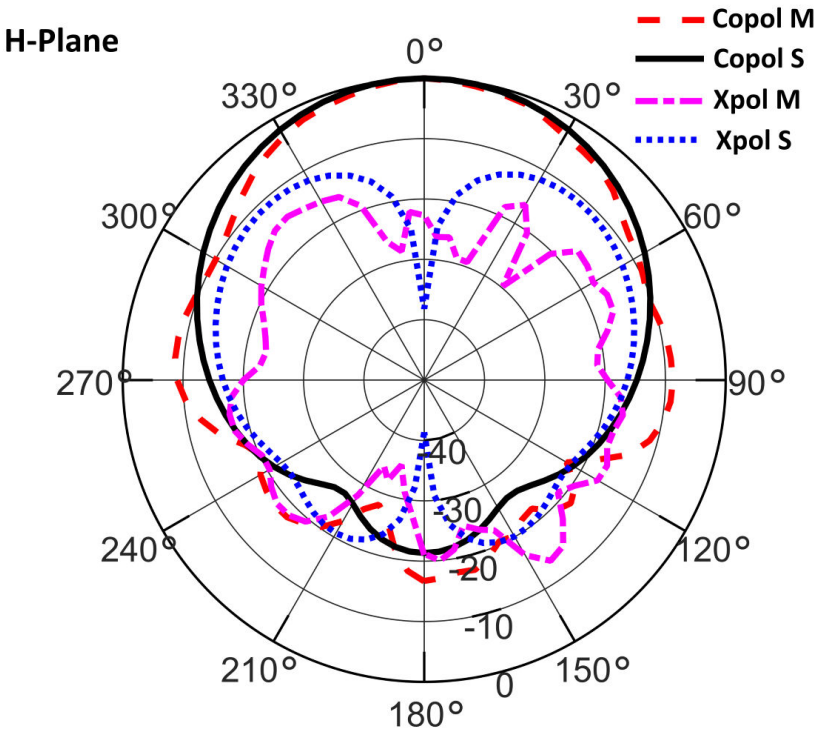

(b)

FIGURE 6.12: Simulated and measured normalized radiation patterns of dual band CRLH TL coupled patch antenna at $f_2 = 5.22$ GHz (a) E-plane and (b) H-plane.

TABLE 6.1: Comparison of different CRLH TL based dual band antennas.

Ref.	f_1/f_2 (GHz)	Gain (dBi)	Structure	Resonance Modes	Efficiency	Reconfig.
[59]	1.8/2.2	4.5/6.8	Single layer	$n = \mp 1$	60/83	No
[61]	2.45/3.5	10.3/5.1	Multilayer	$n = \mp 1$	80/88	No
This work	4.84/5.22	7.4/5.8	Single layer	TM_{10}, $n = 0$	89/72	Yes

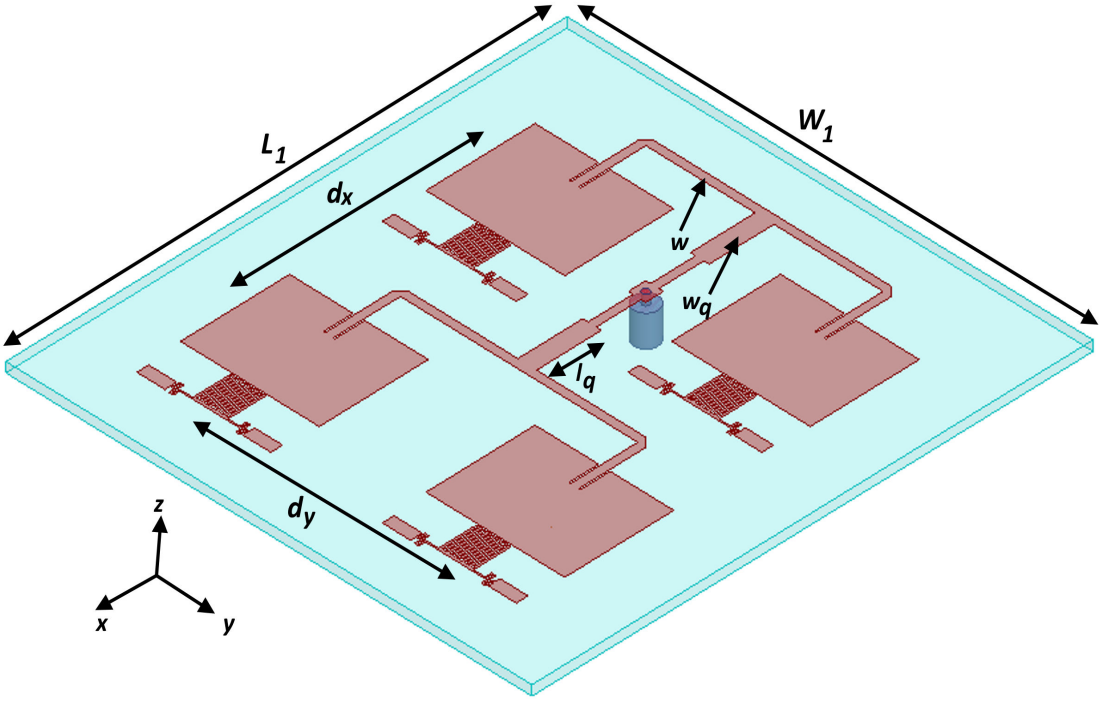

FIGURE 6.13: Geometry of dual band CRLH TL coupled patch array ($W_1 = 96, L_1 = 90, d_x = 42, d_y = 42, l_q = 11.1, w_q = 3.2, w = 1.4$, all dimensions in mm).

is demonstrated. The array geometry is shown in Fig. 6.13. Since microstrip feeding is more suitable for a patch array design, an inset fed dual band CRLH TL coupled patch antenna was optimized with an input impedance of 100 Ω and used as an array element. A corporate feed network was used to uniformly excite the individual elements. The interelement spacing between the center of patches is 42 mm, which is equal to 0.67 λ_0 at lower frequency of 4.82 GHz and 0.72λ_0 at upper frequency of 5.15 GHz, respectively. The array is fed by means of a coaxial probe at the center as illustrated in Fig. 6.13.

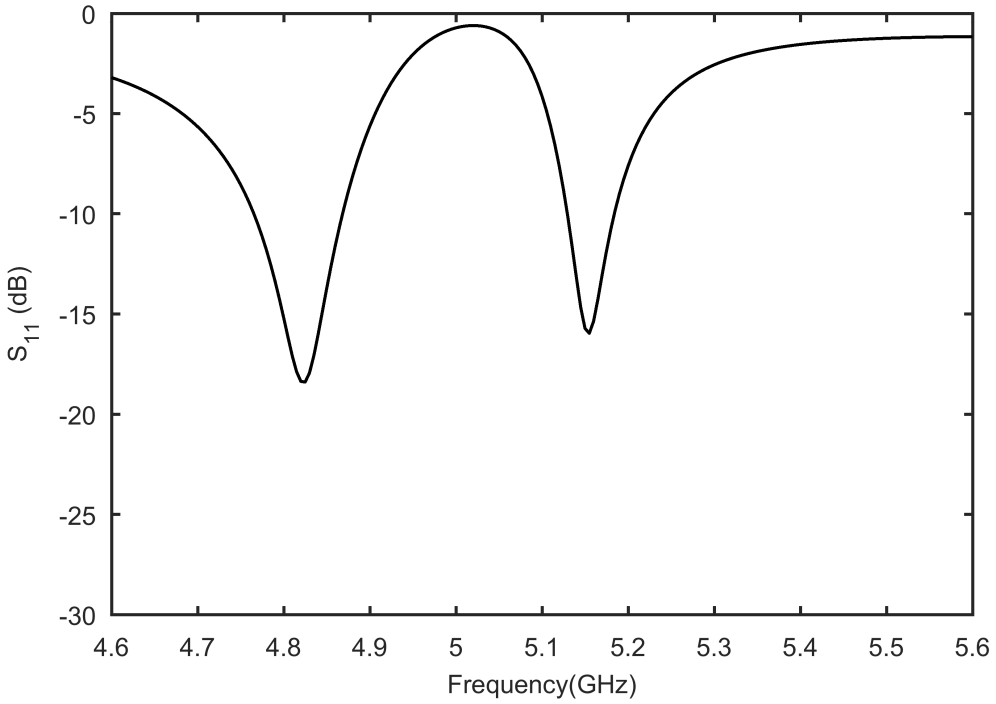

FIGURE 6.14: Simulated S_{11} of dual band CRLH TL coupled patch array.

The simulated S_{11} of the dual band patch array is shown in Fig. 6.14. The antenna shows dual impedance bandwidth ($\mathbf{S}_{11} \leq -10$ dB) of 100 MHz (from 4.77-4.87 GHz) and 50 MHz (from 5.13-5.18 GHz). The relative bandwidths of dual band antenna are 2.07 % and 0.97 % , respectively. Figure 6.15 shows the simulated E and H-planes radiation patterns of the proposed antenna at resonance frequencies of 4.82 GHz and 5.15 GHz. It can be observed that the simulated gain of the antenna is 13.1 dBi and 12.7 dBi at lower and upper resonance frequencies.

6.5 Summary

A new technique for designing frequency reconfigurable dual band patch antennas is presented. In this technique, a CRLH TL unit cell is gap-coupled with the radiating edge of patch antenna. The working principle is based on resonance frequency coupling of CRLH TL unit cell operating in ZOR mode and patch antenna operating in TM_{10} mode. ZOR mode, which has been used in the past typically for antenna miniaturization and monopolar pattern, has been used here

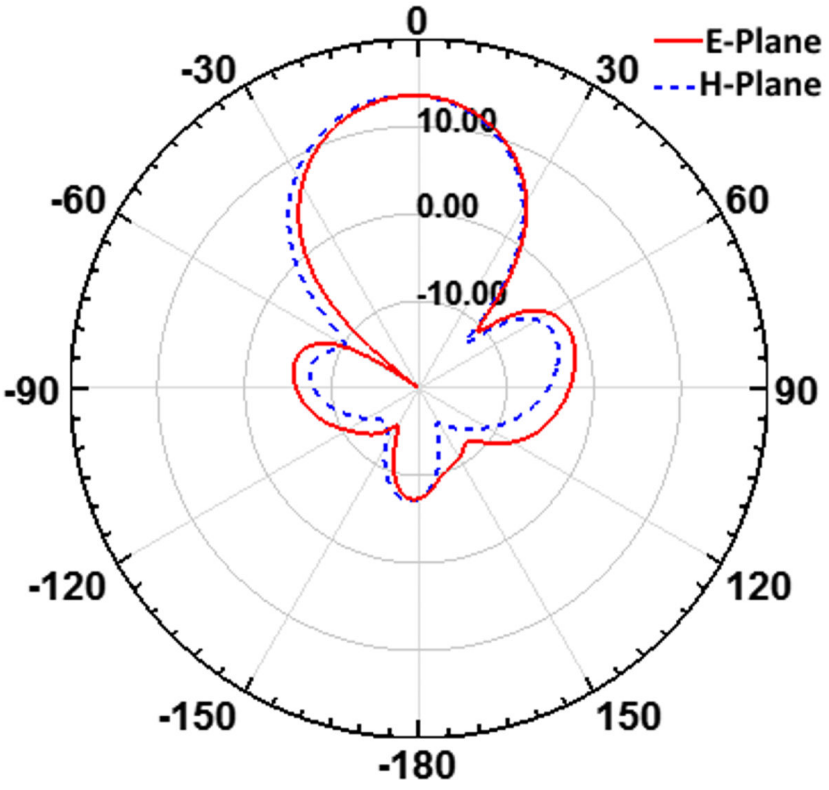

(a)

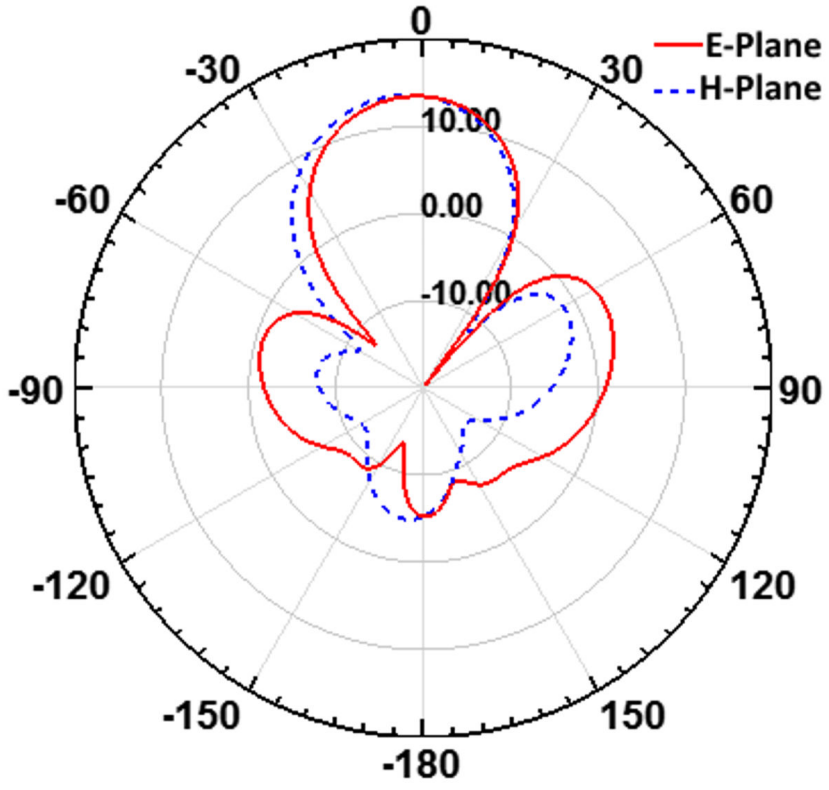

(b)

FIGURE 6.15: Simulated radiation patterns of dual band CRLH TL coupled patch array (a) $f_1 = 4.82$ GHz and (b) $f_2 = 5.15$ GHz.

to achieve dual band operation with broadside pattern. It is shown that the proposed antenna has almost identical broadside radiation patterns at both resonance frequencies with reasonable radiation efficiencies. A prototype of antenna having frequency ratio $f_2/f_1 = 1.08$ is designed and fabricated. The proposed antenna shows measured $S_{11} \leq -10$ dB bandwidth of 100 MHz and 50 MHz at resonance frequencies of $f_1 = 4.84$ GHz and $f_2 = 5.22$ GHz, respectively. A 2×2 dual band CRLH TL coupled patch array is also presented, showing more than 12.7 dBi gain at both resonance frequencies.

One of the benefits of proposed scheme is that it can be used to realize frequency reconfigurable dual band patch antenna by changing the ZOR mode frequency of CRLH TL unit cell. Moreover, it can also be used to design tri-band patch antennas by gap coupling CRLH TL cell along both radiating edges of the patch. The proposed CRLH TL gap coupling technique can be employed to design single layer, multiband band frequency reconfigurable patch antennas and arrays.

Chapter 7

Conclusion and Future Work

7.1 Conclusion

One of the objectives of this thesis was to develop broadside medium gain (10- 16 dBi) planar antennas based on higher order TM_{m0} (with odd m)mode rectangular patch antennas. Large inter element spacing between the radiating edges of TM_{m0} mode rectangular patch antenna was identified as the main cause of high E-plane SLL. To overcome this issue, two techniques namely slot-loading and partial notch-loading were proposed. Both these techniques employ superposition principle and provide ease of fabrication due to single layer configuration. A number of TM_{m0} mode patch antennas having low SLL and improved gain compared to conventional design were developed. A summary of these designs is given below.

High E-plane SLL and low directivity problem of higher order TM_{30} mode patch antenna was resolved by employing resonant slot-loading technique and differential feeding. This scheme was discussed in Chapter 3. The basic idea of this scheme was to achieve superposition of radiated fields in single layer configuration. This was achieved practically by placing in-phase slot radiators, operating in fundamental mode, in the out-of-phase current distribution region of TM_{30} mode patch antenna. A novel low profile, single layer high gain patch antenna having dimensions of $0.9\lambda_0 \times 1\lambda_0 \times 0.015\lambda_0$ is demonstrated. The proposed differential fed slot loaded higher

order mode patch antenna exhibits a 2.4 dB increase in directivity and a reduction of about 10 dB in SLL compared to conventional TM_{30} mode patch antenna. The proposed technique can be utilized to improve the radiation characteristics of higher order mode rectangular patch antennas operating in TM_{m0} (m = 3,5,..) mode.

A new notch-loading technique for gain enhancement and E-plane SLL suppression in higher order TM_{30} and TM_{70} mode rectangular patch antennas was presented in Chapter 4. In this technique, out-of-phase surface current distribution regions of TM_{m0} (m = 3, 7) mode patch antennas were partially removed to create new in-phase radiators between the two radiating edges of conventional higher mode patch antennas. In this way, problem of large inter element spacing between the radiating edges of higher order mode patch was resolved. Due to superposition of radiated far fields, a high directivity patch antenna with reduced SLL was realized. Notch loading technique, which has been used previously for size reduction in patch antenna operating in fundamental mode, is used here to achieve E-plane SLL reduction and gain enhancement in higher order mode patch antennas. Two novel probe fed single layer notch loaded patch antennas operating in higher order TM_{30} and TM_{70} modes were presented. It was demonstrated that the proposed notch loaded TM_{30} mode patch can achieve about 8 dB reduction in SLL and 3 dB improvement in gain compared to conventional TM_{30} mode patch, whereas the proposed notch loaded TM_{70} mode patch antenna showed about 15 dB reduction in SLL and greater than 5 dB improvement in gain compared to its conventional counterpart.

The proposed TM_{70} mode patch has the highest reported measured gain in single-layer higher order mode patch antennas. It showed a measured gain of 16 dBi along with good SLL of about -13 dB. In addition, it has reasonable impedance bandwidth of 3.8%. Due to its high gain, large bandwidth and good SLL proposed antenna is attractive for many wireless communication applications such as Wi-Fi directional antennas working in 900 MHz (902- 928 MHz), 2.4 GHz (2.4-2.4835 GHz), 3.6 GHz (3.655–3.695 GHz), 4.9 GHz (4.94-4.99 GHz) or 5 GHz (5.15-5.25 GHz, 5.25-5.35 GHz, 5.725-5.825 GHz) bands. The proposed notch loading scheme

can also be used to improve the radiation properties of higher order mode patch antennas with circular and triangular geometries.

The possibility of achieving low SLL notch loaded, and single fed slot loaded TM_{30} mode patch antennas were explored in Chapter 5. First, it is shown that by combining the fractal and notch loading techniques, SLL reduction and return loss improvement in TM_{30} mode notch loaded patch can be realized. It was demonstrated that fractal and notch loaded TM_{30} mode patch can achieve 5 dB reduction in SLL and 7 dB improvement in return loss compared to notch loaded TM_{30} mode patch. Another method which can be used to realize single-feeding in slot loaded TM_{30} mode patch, instead of employing differential feeding used previously, was also presented. It was demonstrated that asymmetric current distribution can be circumvented by using a planar 2×2 slot array etched at the center of TM_{30} mode patch. The proposed antennas showed symmetric radiation pattern, high gain, and improved impedance bandwidth.

The second objective of this thesis was to develop reconfigurable high gain patch antennas. A new technique for designing frequency reconfigurable dual band patch antennas was presented in Chapter 5. In this technique, a CRLH TL unit cell was gap-coupled with the radiating edge of the patch antenna. The working principle was based on resonance frequency coupling of CRLH TL unit cell operating in ZOR mode and patch antenna operating in TM_{10} mode. ZOR mode, which has been used in the past typically for antenna miniaturization and monopolar pattern, has been used here to achieve dual band operation with broadside pattern. It was shown that the proposed antenna has almost identical broadside radiation patterns at both resonance frequencies with reasonable radiation efficiencies. One of the benefits of the proposed scheme was that it can be used to realize frequency reconfigurable dual band patch antenna by changing the ZOR mode frequency of CRLH TL unit cell. Moreover, it can also be used to design tri-band patch antennas by gap coupling CRLH TL cell along both radiating edges of the patch. The proposed CRLH TL gap coupling technique can be employed to design single layer, multiband band frequency reconfigurable patch antennas and arrays.

7.2 Future Work

A number of possible future extension of present work are posible. Some of them are listed below:

1. The current work mainly focus on the gain enhancement and SLL reduction technique of TM_{m0} mode patch antennas for linearly polarization. Thus a natural extension of present work is to explore high gain, dual linear or circular polarized higher order TM_{m0} mode patch antennas. Dual linear polarized antennas are useful for polarization diversity applications whereas circular polariztion is required for communication between moving platforms.

2. Another possible frontier is to investigate multiband operation of proposed slot loaded and notch loaded TM_{mo} patch antennas. As an example fundamental TM_{10} mode and TM_{30} mode can be employed for dual band applications. Different aspects such as impedance matching, control of frequency ratio can be studied.

3. In contrary to conventional patch antennas operating in fundamental mode, higher order mode patch antennas have large size in terms of wavelength. This can be useful in high frequency applications where large antenna dimensions results in ease of fabrication. In future, the higher order mode patch antennas can be investigated for 5G millimeter-wave applications.

4. Beside SLL reduction and gain enhancement, the work on notch loaded TM_{70} mode shows an interesting possibility for improving the gain bandwidth i.e. by coupling the close in mode (TM_{36}). This method can be employed to improve the gain bandwidth of other TM_{m0} modes. Mode excitation, controlling the frequency of each mode and radiation pattern shaping of close in mode are some of the issue which need to be investigated.

5. The application of fractal slot loading on notch loaded TM_{30} mode patch shows very promising result and it was demonstrated that SLL reduction and return loss improvement can be achieved by combining the fractal and

notch loading. In future, fractal and notch loaded TM_{70} rectangular patch can be studied. In addition, effect of fractal slot on 2x2 slot loaded patch can also be investigated.

6. The proposed slot loading and notch loading techniques can be combined with other gain enhancement techniques such as superstrate or PRS loading to further increase the gain. Similarly, bandwidth enhancement technique like stacking or increase substrate height can be employed to improve the impedance bandwidth of the TM_{m0} mode rectangular patch antennas.

7. Gain enhancement and SLL reduction of higher order modes in other Euclidean geometries such as circular or triangular patch can be explored in future based on the proposed slot loading and notch loading techniques.

8. Tri-band patch antenna can be designed by gap coupling CRLH TL cell along both radiating edges of the TM_{10} mode patch. Other geometries, such as triangular or circular patch can also be investigated.

9. Present work focuses on CRLH TL coupling with fundamental TM_{10} mode of rectangular patch. In future, CRLH TL coupled higher order multiband TM_{m0} mode patch antennas can be investigated.

Bibliography

[1] J. R. James, P. S. Hall, *et al.*, *Handbook of microstrip antennas*, vol. 1. IET, 1989.

[2] S. Maci, G. B. Gentili, and G. Avitabile, "Single layer dual frequency patch antenna," *Electronics Letters*, vol. 29, no. 16, pp. 1441–1443, 1993.

[3] C. Caloz, T. Itoh, and A. Rennings, "CRLH metamaterial leaky-wave and resonant antennas," *IEEE Antennas and Propagation Magazine*, vol. 50, no. 5, 2008.

[4] Y. Dong and T. Itoh, "Metamaterial-based antennas," *Proceedings of the IEEE*, vol. 100, no. 7, pp. 2271–2285, 2012.

[5] R. L. Haupt and M. Lanagan, "Reconfigurable antennas," *IEEE Antennas and Propagation Magazine*, vol. 55, no. 1, pp. 49–61, 2013.

[6] J. Costantine, Y. Tawk, S. E. Barbin, and C. G. Christodoulou, "Reconfigurable antennas: Design and applications," *Proceedings of the IEEE*, vol. 103, no. 3, pp. 424–437, 2015.

[7] C. A. Balanis, *Antenna theory: Analysis and design*. John Wiley & Sons, 2016.

[8] D. M. Pozar, "Microstrip antennas," *Proceedings of the IEEE*, vol. 80, no. 1, pp. 79–91, 1992.

[9] E. Nishiyama, M. Aikawa, and S. Egashira, "Stacked microstrip antenna for wideband and high gain," *IEE Proceedings-Microwaves, Antennas and Propagation*, vol. 151, no. 2, pp. 143–148, 2004.

[10] G. Kumar and K. Gupta, "Nonradiating edges and four edges gap-coupled multiple resonator broad-band microstrip antennas," *IEEE Transactions on Antennas and Propagation*, vol. 33, no. 2, pp. 173–178, 1985.

[11] R. Mailloux, J. McIlvenna, and N. Kernweis, "Microstrip array technology," *IEEE Transactions on Antennas and Propagation*, vol. 29, no. 1, pp. 25–37, 1981.

[12] E. Levine, G. Malamud, S. Shtrikman, and D. Treves, "A study of microstrip array antennas with the feed network," *IEEE Transactions on Antennas and Propagation*, vol. 37, no. 4, pp. 426–434, 1989.

[13] K. F. Lee, Luk, and K. Man, *Microstrip patch antennas*. World Scientific, 2011.

[14] V. Veselago, "The electrodynamics of substances with simultaneously negative values of and μ," *Soviet Physics Uspekhi*, vol. 92, p. 517, 1967.

[15] D. R. Smith, W. J. Padilla, D. Vier, S. C. Nemat-Nasser, and S. Schultz, "Composite medium with simultaneously negative permeability and permittivity," *Physical Review Letters*, vol. 84, no. 18, p. 4184, 2000.

[16] C. Caloz and T. Itoh, *Electromagnetic metamaterials: Transmission line theory and microwave applications*. John Wiley & Sons, 2005.

[17] S. Ramo, J. R. Whinnery, and T. Van Duzer, *Fields and waves in communication electronics*. John Wiley & Sons, 2008.

[18] C. Caloz and T. Itoh, "Application of the transmission line theory of left-handed (lh) materials to the realization of a microstrip "LH line"," in *IEEE-APS International Symposium*, vol. 2, pp. 412–415, IEEE, 2002.

[19] A. A. Oliner, "A periodic-structure negative-refractive-index medium without resonant elements," in *IEEE-APS/URSI International Symposium Digest, 2002*, vol. 41, 2002.

[20] A. Lai, T. Itoh, and C. Caloz, "Composite right/left-handed transmission line metamaterials," *IEEE Microwave Magazine*, vol. 5, no. 3, pp. 34–50, 2004.

[21] R. Q. Lee and K.-F. Lee, "Experimental study of the two layer electromagnetically coupled rectangular patch antenna," *IEEE Transactions on Antennas and Propagation*, vol. 38, no. 8, pp. 1298–1302, 1990.

[22] N. Alexopoulos and D. Jackson, "Fundamental superstrate (cover) effects on printed circuit antennas," *IEEE Transactions on Antennas and Propagation*, vol. 32, no. 8, pp. 807–816, 1984.

[23] D. Jackson and N. Alexopoulos, "Gain enhancement methods for printed circuit antennas," *IEEE Transactions on Antennas and Propagation*, vol. 33, no. 9, pp. 976–987, 1985.

[24] A. Foroozesh and L. Shafai, "Investigation into the effects of the patch type FSS superstrate on the high-gain cavity resonance antenna design," *IEEE Transactions on Antennas and Propagation*, vol. 58, no. 2, pp. 258–270, 2010.

[25] A. Foroozesh and L. Shafai, "On the characteristics of the highly directive resonant cavity antenna having metal strip grating superstrate," *IEEE Transactions on Antennas and Propagation*, vol. 60, no. 1, pp. 78–91, 2011.

[26] H. Zhu, S. W. Cheung, and T. I. Yuk, "Enhancing antenna boresight gain using a small metasurface lens: Reduction in half-power beamwidth," *IEEE Antennas and Propagation Magazine*, vol. 58, no. 1, pp. 35–44, 2016.

[27] A. P. Feresidis, G. Goussetis, S. Wang, and J. C. Vardaxoglou, "Artificial magnetic conductor surfaces and their application to low-profile high-gain planar antennas," *IEEE Transactions on Antennas and Propagation*, vol. 53, no. 1, pp. 209–215, 2005.

[28] L. Zhou, H. Li, Y. Qin, Z. Wei, and C. Chan, "Directive emissions from subwavelength metamaterial-based cavities," *Applied Physics Letters*, vol. 86, no. 10, p. 101101, 2005.

[29] C. Borja, G. Font, S. Blanch, and J. Romeu, "High directivity fractal boundary microstrip patch antenna," *Electronics Letters*, vol. 36, no. 9, pp. 778–779, 2000.

[30] J. Anguera, C. Puente, C. Borja, R. Montero, and J. Soler, "Small and high-directivity bow-tie patch antenna based on the Sierpinski fractal," *Microwave and Optical Technology Letters*, vol. 31, no. 3, pp. 239–241, 2001.

[31] A. B. Younas, Z. Ahmed, and M. B. Ihsan, "A new high-directivity fractal antenna based on the modified koch snowflake geometry," in *2010 Asia-Pacific Microwave Conference*, pp. 191–194, IEEE, 2010.

[32] W. L. Stutzman and G. A. Thiele, *Antenna theory and design*. John Wiley & Sons, 2013.

[33] R. Munson, "Conformal microstrip antennas and microstrip phased arrays," *IEEE Transactions on Antennas and propagation*, vol. 22, no. 1, pp. 74–78, 1974.

[34] L. Chiu and Q. Xue, "Oversize rectangular microstrip patch with higher-order mode suppression using multifeed network," *Microwave and Optical Technology Letters*, vol. 50, no. 11, pp. 2749–2751, 2008.

[35] J. W. Jayasinghe, J. Anguera, and D. N. Uduwawala, "A high-directivity microstrip patch antenna design by using genetic algorithm optimization," *Progress In Electromagnetics Research*, vol. 37, pp. 131–144, 2013.

[36] D. Wang, K. B. Ng, C. H. Chan, and H. Wong, "A novel wideband differentially-fed higher-order mode millimeter-wave patch antenna," *IEEE Transactions on Antennas and Propagation*, vol. 63, no. 2, pp. 466–473, 2014.

[37] P. Juyal and L. Shafai, "A novel high gain printed antenna configuration based on TM_{12} mode of circular disc," *IEEE Transactions on Antennas and Propagation*, vol. 64, no. 2, pp. 790–796, 2016.

[38] P. Juyal and L. Shafai, "A high gain single feed dual mode microstrip disc radiator," *IEEE Transactions on Antennas and Propagation*, vol. 64, no. 6, pp. 2115–2126, 2016.

[39] P. Juyal and L. Shafai, "Sidelobe reduction of TM_{12} mode of circular patch via nonresonant narrow slot," *IEEE Transactions on Antennas and Propagation*, vol. 64, no. 8, pp. 3361–3369, 2016.

[40] K.-F. Tong, K.-M. Luk, K.-F. Lee, and R. Q. Lee, "A broad-band U-slot rectangular patch antenna on a microwave substrate," *IEEE Transactions on Antennas and Propagation*, vol. 48, no. 6, pp. 954–960, 2000.

[41] F. Yang, X.-X. Zhang, X. Ye, and Y. Rahmat-Samii, "Wide-band E-shaped patch antennas for wireless communications," *IEEE Transactions on Antennas and Propagation*, vol. 49, no. 7, pp. 1094–1100, 2001.

[42] G. Dubost and A. Rabbaa, "Analysis of a slot microstrip antenna," *IEEE Transactions on Antennas and Propagation*, vol. 34, no. 2, pp. 155–163, 1986.

[43] S. Maci, G. B. Gentili, and G. Avitabile, "Single-layer dual frequency patch antenna," *Electronics Letters*, vol. 29, no. 16, pp. 1441–1443, 1993.

[44] M. Polivka, M. Drahovzal, and M. Mazanek, "Synthesis of dual band broadside radiated microstrip patch antenna operating with TM/sub 10/and TM/-sub 21/modes," in *IEEE Antennas and Propagation Society Symposium, 2004*, vol. 1, pp. 245–248, IEEE, 2004.

[45] G. Kossiavas, A. Papiernik, J. Boisset, and M. Sauvan, "The C patch: A small microstrip element," *Electronics letters*, vol. 25, no. 4, pp. 253–254, 1989.

[46] M. Sanad, "Double c-patch antennas having different aperture shapes," in *IEEE Antennas and Propagation Society International Symposium. 1995 Digest*, vol. 4, pp. 2116–2119, IEEE, 1995.

[47] V. Palanisamy and R. Garg, "Rectangular ring and H-shaped microstrip antennas—alternatives to rectangular patch antenna," *Electronics Letters*, vol. 21, no. 19, pp. 874–876, 1985.

[48] D. Singh, C. Kalialakis, P. Gardner, and P. S. Hall, "Small H-shaped antennas for MMIC applications," *IEEE Transactions on Antennas and Propagation*, vol. 48, no. 7, pp. 1134–1141, 2000.

[49] K. L. Chung, "A wideband circularly polarized H-shaped patch antenna," *IEEE Transactions on Antennas and Propagation*, vol. 58, no. 10, pp. 3379–3383, 2010.

[50] J. George, M. Deepukumar, C. Aanandan, P. Mohanan, and K. Nair, "New compact microstrip antenna," *Electronics Letters*, vol. 32, no. 6, pp. 508–509, 1996.

[51] P. M. Bafrooei and L. Shafai, "Characteristics of single-and double-layer microstrip square-ring antennas," *IEEE Transactions on Antennas and Propagation*, vol. 47, no. 10, pp. 1633–1639, 1999.

[52] S. Long and M. Walton, "A dual-frequency stacked circular-disc antenna," *IEEE Transactions on Antennas and propagation*, vol. 27, no. 2, pp. 270–273, 1979.

[53] J. Dahele, K.-F. Lee, and D. Wong, "Dual-frequency stacked annular-ring microstrip antenna," *IEEE Transactions on Antennas and Propagation*, vol. 35, no. 11, pp. 1281–1285, 1987.

[54] J. Anguera, G. Font, C. Puente, C. Borja, and J. Soler, "Multifrequency microstrip patch antenna using multiple stacked elements," *IEEE Microwave and Wireless Components Letters*, vol. 13, no. 3, pp. 123–124, 2003.

[55] S. Zhong and Y. Lo, "Single-element rectangular microstrip antenna for dual-frequency operation," *Electronics Letters*, vol. 19, pp. 298–300, 1983.

[56] K.-F. Lee, K.-M. Luk, and J. S. Dahele, "Characteristics of the equilateral triangular patch antenna," *IEEE Transactions on Antennas and Propagation*, vol. 36, no. 11, pp. 1510–1518, 1988.

[57] K.-F. Lee, S. L. S. Yang, and A. A. Kishk, "Dual-and multiband U-slot patch antennas," *IEEE Antennas and Wireless Propagation Letters*, vol. 7, pp. 645–647, 2008.

[58] A. Boukarkar, X. Q. Lin, Y. Jiang, and Y. Q. Yu, "Miniaturized single-feed multiband patch antennas," *IEEE Transactions on Antennas and Propagation*, vol. 65, no. 2, pp. 850–854, 2016.

[59] F. J. Herraiz-Martinez, V. Gonzalez-Posadas, L. E. Garcia-Munoz, and D. Segovia-Vargas, "Multifrequency and dual-mode patch antennas partially filled with left-handed structures," *IEEE Transactions on Antennas and Propagation*, vol. 56, no. 8, pp. 2527–2539, 2008.

[60] Y. Dong, H. Toyao, and T. Itoh, "Compact circularly-polarized patch antenna loaded with metamaterial structures," *IEEE Transactions on Antennas and Propagation*, vol. 59, no. 11, pp. 4329–4333, 2011.

[61] S. Yan and G. A. Vandenbosch, "Low-profile dual-band pattern diversity patch antenna based on composite right/left-handed transmission line," *IEEE Transactions on Antennas and Propagation*, vol. 65, no. 6, pp. 2808–2815, 2017.

[62] Q. U. Khan, M. B. Ihsan, D. Fazal, F. M. Malik, S. A. Sheikh, and M. Salman, "Higher order modes: A solution for high gain, wide band patch antennas for different vehicular applications," *IEEE Transactions on Vehicular Technology*, vol. 66, no. 5, pp. 3548–3554, 2016.

[63] R. Waterhouse, "Small printed antennas with low cross-polarised fields," *Electronics Letters*, vol. 33, no. 15, pp. 1280–1281, 1997.

[64] R. S. Elliot, *Antenna theory and design.* John Wiley & Sons, 2003.

[65] P. Hammer, D. Van Bouchaute, D. Verschraeven, and A. Van de Capelle, "A model for calculating the radiation field of microstrip antennas," *IEEE Transactions on Antennas and Propagation*, vol. 27, no. 2, pp. 267–270, 1979.

[66] X. Zhang and L. Zhu, "Gain-enhanced patch antenna without enlarged size via loading of slot and shorting pins," *IEEE Transactions on Antennas and Propagation*, vol. 65, no. 11, pp. 5702–5709, 2017.

[67] R. E. Collin, *Antennas and radiowave propagation.* McGraw-Hill, 1985.

[68] D. M. Pozar and D. H. Schaubert, *Microstrip antennas: The analysis and design of microstrip antennas and arrays*. John Wiley & Sons, 1995.

[69] H. Yang and N. Alexopoulos, "Gain enhancement methods for printed circuit antennas through multiple superstrates," *IEEE Transactions on Antennas and Propagation*, vol. 35, no. 7, pp. 860–863, 1987.

[70] A. P. Feresidis, G. Goussetis, S. Wang, and J. C. Vardaxoglou, "Artificial magnetic conductor surfaces and their application to low-profile high-gain planar antennas," *IEEE Transactions on Antennas and Propagation*, vol. 53, no. 1, pp. 209–215, 2005.

[71] A. Pirhadi, H. Bahrami, and J. Nasri, "Wideband high directive aperture coupled microstrip antenna design by using a FSS superstrate layer," *IEEE Transactions on Antennas and Propagation*, vol. 60, no. 4, pp. 2101–2106, 2012.

[72] X. Zhang and L. Zhu, "Gain enhanced patch antennas with loading of shorting pins," *IEEE Transactions on Antennas and Propagation*, vol. 64, no. 8, pp. 3310–3318, 2016.

[73] X. Zhang and L. Zhu, "High gain circularly polarized microstrip patch antenna with loading of shorting pins," *IEEE Transactions on Antennas and Propagation*, vol. 64, no. 6, pp. 2172–2178, 2016.

[74] P. Juyal and L. Shafai, "Gain enhancement in circular microstrip antenna via linear superposition of higher zeros," *IEEE Antennas and Wireless Propagation Letters*, vol. 16, pp. 896–899, 2017.

[75] P. Squadrito, S. Zhang, and G. F. Pedersen, "Wideband or dual-band low profile circular patch antenna with high gain and sidelobe suppression," *IEEE Transactions on Antennas and Propagation*, vol. 66, no. 6, pp. 3166–3171, 2018.

[76] Z. Ahmed, M. M. Ahmed, and M. B. Ihsan, "A novel differential fed high gain patch antenna using resonant slot loading," *Radioengineering*, vol. 27, pp. 662–670, 09 2018.

[77] Q. U. Khan, D. Fazal, and M. bin Ihsan, "Use of slots to improve performance of patch in terms of gain and sidelobes reduction," *IEEE Antennas and Wireless Propagation Letters*, vol. 14, pp. 422–425, 2015.

[78] X. Zhang and L. Zhu, "Dual band high gain differentially fed circular patch antenna working in TM_{11} and TM_{12} modes," *IEEE Transactions on Antennas and Propagation*, vol. 66, no. 6, pp. 3160–3165, 2018.

[79] N.-W. Liu, L. Zhu, W.-W. Choi, and X. Zhang, "A low profile differential fed patch antenna with bandwidth enhancement and sidelobe reduction under operation of TM_{10} and TM_{12} modes," *IEEE Transactions on Antennas and Propagation*, vol. 66, no. 9, pp. 4854–4859, 2018.

[80] X. Zhang, L. Zhu, and Q.-S. Wu, "Sidelobe reduced and gain enhanced square patch antennas with adjustable beamwidth under TM_{03} mode operation," *IEEE Transactions on Antennas and Propagation*, vol. 66, no. 4, pp. 1704–1713, 2018.

[81] Y. He, Y. Li, W. Sun, and Z. Zhang, "Dual polarized, high gain, and low profile magnetic current antenna," *IEEE Transactions on Antennas and Propagation*, vol. 67, no. 2, pp. 1312–1317, 2019.

[82] M. Sanad, "Double C patch antennas having different aperture shapes," in *Antennas and Propagation Society International Symposium, 1995. AP-S. Digest*, vol. 4, pp. 2116–2119, IEEE, 1995.

[83] D. Singh, C. Kalialakis, P. Gardner, and P. S. Hall, "Small H shaped antennas for MMIC applications," *IEEE Transactions on Antennas and Propagation*, vol. 48, no. 7, pp. 1134–1141, 2000.

[84] K. Lee, K. Luk, K.-F. Tong, S. Shum, T. Huynh, and R. Lee, "Experimental and simulation studies of the coaxially fed U-slot rectangular patch antenna," *IEE Proceedings-Microwaves, Antennas and Propagation*, vol. 144, no. 5, pp. 354–358, 1997.

[85] A. Lai, K. M. Leong, and T. Itoh, "Infinite wavelength resonant antennas with monopolar radiation pattern based on periodic structures," *IEEE Transactions on Antennas and Propagation*, vol. 55, no. 3, pp. 868–876, 2007.

[86] S. Yan and G. A. Vandenbosch, "Zeroth-order resonant circular patch antenna based on periodic structures," *IET Microwaves, Antennas & Propagation*, vol. 8, no. 15, pp. 1432–1439, 2014.

[87] A. A. Chaudhry, J. K. Arif, Z. Ahmed, M. A. Chaudhary, and M. B. Ihsan, "Parameter extraction of composite right/left handed (CRLH) transmission line unit cell using off resonance method," in *2017 14th International Bhurban Conference on Applied Sciences and Technology (IBCAST)*, pp. 779–781, IEEE, 2017.

[88] D. M. Pozar, "Microwave engineering," *Tramsmission Lines and Waveguides*, pp. 143–149, 2005.